(12) LEVEL III (19) CR-00380, AD-E430 132

(18) CONTRACT REPORT ARBRL-CR-00380

SBIE

(6)

INCORPORATION OF THE NAG-FRAG MODEL FOR DUCTILE AND BRITTLE FRACTURE INTO HELP, A 2D MULTIMATERIAL EULERIAN PROGRAM.

(9) Final rept. 19 Apr 76 - 18 Jun 77,

Prepared by

(14) SSS-R-77-3389

(10) L. J. Hageman
R. G. Herrmann

Systems, Science and Software
P. O. Box 1620
La Jolla, California 92038

(12) 128 p.

(11) September 1978

US ARMY ARMAMENT RESEARCH AND DEVELOPMENT COMMAND
BALLISTIC RESEARCH LABORATORY
ABERDEEN PROVING GROUND, MARYLAND

(15) DAAD05-76-C-0760

Approved for public release; distribution unlimited.

388 507

78 11 08 081

BLANK PAGES
IN THIS
DOCUMENT
WERE NOT
FILMED

Destroy this report when it is no longer needed.
Do not return it to the originator.

Secondary distribution of this report by originating or sponsoring activity is prohibited.

Additional copies of this report may be obtained from the National Technical Information Service, U.S. Department of Commerce, Springfield, Virginia 22161.

The findings in this report are not to be construed as an official Department of the Army position, unless so designated by other authorized documents.

The use of trade names or manufacturers' names in this report does not constitute indorsement of any commercial product.

UNCLASSIFIED

SECURITY CLASSIFICATION OF THIS PAGE (When Data Entered)

REPORT DOCUMENTATION PAGE

READ INSTRUCTIONS BEFORE COMPLETING FORM

1. REPORT NUMBER: CONTRACT REPORT ARBRL-CR-00380	2. GOVT ACCESSION NO. / 3. RECIPIENT'S CATALOG NUMBER
4. TITLE (and Subtitle): INCORPORATION OF THE NAG-FRAG MODEL FOR DUCTILE AND BRITTLE FRACTURE INTO HELP, A 2D MULTIMATERIAL EULERIAN PROGRAM	5. TYPE OF REPORT & PERIOD COVERED: Final Report 4/19/76 - 6/18/77
	6. PERFORMING ORG. REPORT NUMBER: SSS-R-77-3389
7. AUTHOR(s): L. J. Hageman and R. G. Herrmann	8. CONTRACT OR GRANT NUMBER(s): DAAD05-76-C-0760
9. PERFORMING ORGANIZATION NAME AND ADDRESS: Systems, Science and Software, P.O. Box 1620, La Jolla, California 92038	10. PROGRAM ELEMENT, PROJECT, TASK AREA & WORK UNIT NUMBERS
11. CONTROLLING OFFICE NAME AND ADDRESS: US Army Armament Research & Development Command, US Army Ballistic Research Laboratory (DRDAR-BL), Aberdeen Proving Ground, MD 21005	12. REPORT DATE: SEPTEMBER 1978
	13. NUMBER OF PAGES: 135
14. MONITORING AGENCY NAME & ADDRESS (if different from Controlling Office)	15. SECURITY CLASS. (of this report): UNCLASSIFIED
	15a. DECLASSIFICATION/DOWNGRADING SCHEDULE

16. DISTRIBUTION STATEMENT (of this Report)

Approved for public release; distribution unlimited.

17. DISTRIBUTION STATEMENT (of the abstract entered in Block 20, if different from Report)

18. SUPPLEMENTARY NOTES

19. KEY WORDS (Continue on reverse side if necessary and identify by block number)

NAG-FRAG	α-ε Phase Change in Iron	Fragmenting Round
Material Failure Models	Lagrangian Codes	Iron
Ductile Material	HELP	Aluminum
Brittle Material	HEMP	
Eulerian Codes	PUFF	
	Tapered Flyer Plate Impact	

20. ABSTRACT (Continue on reverse side if necessary and identify by block number)

The method of incorporating the NAG-FRAG failure models for ductile and brittle materials into the Eulerian HELP code and the associated modifications to the code are described in this report. Results from three HELP calculations employing either the ductile or brittle failure model are presented and compared with results obtained from Lagrangian codes which also employed the NAG-FRAG models. Several auxiliary improvements to HELP, including the

DD FORM 1 JAN 73 1473 EDITION OF 1 NOV 65 IS OBSOLETE

UNCLASSIFIED

SECURITY CLASSIFICATION OF THIS PAGE (When Data Entered)

20. ABSTRACT (continued)

incorporation of the α-ε phase change in the iron equation of state, are described and documented.

alpha - epsilon

TABLE OF CONTENTS

TABLE OF CONTENTS (continued)

LIST OF ILLUSTRATIONS

LIST OF ILLUSTRATIONS (continued)

LIST OF ILLUSTRATIONS (Continued)

LIST OF TABLES

1. INTRODUCTION

Continuum mechanics codes have been applied to a wide variety of impact situations, including those in which severe material damage occurs to both the penetrator and the target material. It is important to include in such calculations an appropriate description of the material damage generation process.

Recently, rather detailed material failure models have been developed at SRI International[1] which relate material failure to the nucleation and growth of microscopic holes or cracks. These models, known collectively as NAG-FRAG (Nucleation And Growth-FRAGmentation), were developed for both ductile materials (the DFRACT model) and brittle materials (the BFRACT model). These models have been incorporated into the 1975 documented version of HELP[2] to produce the present NAG-FRAG version of the code which gives a much more detailed description of material failure.

The major modification to the HELP code for the incorporation of these models involves the establishment and subsequent manipulation of "Lagrangian damage regions." These damage regions encompass pockets of failed material and move across the Eulerian mesh with the local velocity field. A damage region is formed when material in an Eulerian cell first satisfies the failure criterion.

The two NAG-FRAG subroutines, BFRACT and DFRACT, communicate with the external HELP code by calculating the stress state of the material in the damage regions. In turn, the external code provides BFRACT and DFRACT with such quantities as material density, internal energy and the strain increments to be used in the calculation of the damage region stresses. Furthermore, unlike the properties of neighboring Eulerian cells, the characteristics of contiguous damage regions are not diffused because there is no material convected from one to the other.

This report documents the changes that were necessary to incorporate the SRI NAG-FRAG models into the HELP code. In Section 2, these models are briefly described, and in Section 3 the modifications that were made to the HELP code for their incorporation are discussed. Section 4 discusses several auxiliary improvements that were made to the HELP code concurrently with the incorporation of the NAG-FRAG models. In Section 5 results from several calculations performed using the version of HELP that contains the NAG-FRAG models are presented. These results are compared with Lagrangian calculations performed by SRI. Appendices A and B are, respectively, a user's guide to the revised code which supplements the 1975 documentation, and a new set of input forms.

By incorporating the NAG-FRAG failure models into the Eulerian HELP code, an improved numerical tool has been developed for the simulation of the armor penetration process which involves both large material deformations and extensive material failure. This numerical tool can be used by designers of both penetrator and armor systems and can provide detailed data to vulnerability and survivability analysts.

2. A DESCRIPTION OF THE NAG-FRAG MODELS

The NAG-FRAG (Nucleation And Growth-FRAGmentation) models incorporated into the HELP code were developed by SRI for predicting the damage incurred by ductile and brittle materials when subjected to tensile stresses. The damage is assumed to result from the generation of small spherical voids (ductile failure) or disc shaped cracks (brittle failure) and is reflected by a degradation of material strength properties.

Reference [1] describes these models (DFRACT for ductile materials and BFRACT for brittle materials) in detail. The following is a brief description of those aspects of the models for which an understanding was necessary in the development of the NAG-FRAG version of HELP. In the course of this description, reference will be made to the TSR array which contains those material properties unique to the NAG-FRAG models.

2.1 VOID NUCLEATION AND GROWTH IN DUCTILE MATERIALS

The spherical voids responsible for damage in ductile materials are assumed to (1) be generated at a prescribed rate if the tensile pressure exceeds a nucleation threshold and (2) grow in size at a prescribed rate if the tensile pressure is above a growth threshold. During nucleation, the voids are assumed to be generated according to a given size distribution.

More specifically, the nucleation rate $\dot{N}$ (number of voids generated per unit volume per unit time) is given by the following relations wherein pressure is defined to be negative in tension:

$$\dot{N} = \begin{cases} \dot{N}_o \, e^{\frac{P-P_{no}}{P_1}} & \text{if } P < P_{no} \\ 0 & \text{if } P \geq P_{no} \end{cases} .$$

where

P = tensile pressure

P_{no} = TSR(m,5) = nucleation threshold pressure

P_1 = TSR(m,6) = nucleation sensitivity factor

$\dot{N}_o$ = TSR(m,4) = nucleation rate at threshold pressure.

The first index of the TSR array, m, identifies the particular material being modeled.

The void radii at the time of nucleation are assumed distributed according to

$$f(R) = 1 - e^{-R/R_n}$$

where f(R) is the fraction of voids having a radius less than R and

$R_n \equiv TSR(m,3)$ = nucleation void radius distribution parameter.

Thus, the volume of voids nucleated per unit volume of material during a time step Δt is (assuming P remains constant during the time step)

$$\Delta V_n = \Delta t \frac{4\pi \dot{N}}{3} \int_0^\infty R^3 \frac{df(R)}{dR} dR$$

$$= 8\pi \dot{N} R_n^3 \Delta t \quad .$$

The void radii are assumed to grow according to the law

$$\dot{R} = \begin{cases} \frac{P-P_{go}}{4\eta} R & \text{if } P < P_{go} \\ 0 & \text{if } P \geq P_{go} \end{cases}$$

where

η = material viscosity

$P_{go} = TSR(m,2)$ = growth threshold pressure .

Thus, if a particular void has a radius R_o at the beginning of the time step, its radius at the end of the time step will be

$$R = \begin{cases} R_o \, e^{\frac{P-P_{go}}{4\eta} \Delta t} & \text{if } P < P_{go} \\ R_o & \text{if } P \geq P_{go} \end{cases} .$$

As a consequence of this growth law, the void content of a mass of damaged material remains unchanged during recompression. Given a void volume, $V_o = 4/3\ \pi\ R_o^3$, at the beginning of the time step, the void volume at the end of the time step will be

$$V = V_o\ e^{\frac{3}{4\eta}\ (P-P_{go})\Delta t}\ .$$

The factor $3/4\eta$ is input to the model as TSR(m,1).

2.2 CRACK NUCLEATION AND GROWTH IN BRITTLE MATERIALS

The nucleation and growth of cracks in brittle materials is treated in a fashion much like, but more complex than, the voids in ductile materials. The number of cracks nucleated with a particular angular orientation $\phi\psi$ is assumed governed by a nucleation rate

$$\dot{N} = \begin{cases} \dot{N}_o e^{\frac{\sigma_{\phi\psi} - \sigma_{no}}{\sigma_1}} & \text{if } \sigma_{\phi\psi} < \sigma_{no} \\ \dot{N}_o & \text{if } \sigma_{\phi\psi} \geq \sigma_{no} \end{cases}$$

where

$\sigma_{\phi\psi}$ = stress normal to the plane of the crack

σ_{no} = TSR(m,5) = nucleation threshold stress

σ_1 = TSR(m,6) = nucleation sensitivity factor

$\dot{N}_o$ = TSR(m,4) = nucleation rate at threshold stress.

In this section of the report and in the NAG-FRAG subroutines, both the pressure and the total and deviatoric stresses are defined to be positive in compression. So as not to consider every possible angular orientation, five bin angles are constructed as shown in Figure 2.1. For example, all cracks whose faces are normal to the direction given by

$$45° \leq \psi \leq 135° \text{ and } -22.5° \leq \phi \leq 22.5°$$

or

$$0° \leq \psi \leq 45° \text{ and } 0° \leq \phi \leq 360°$$

are included in bins 1 and 5, respectively.

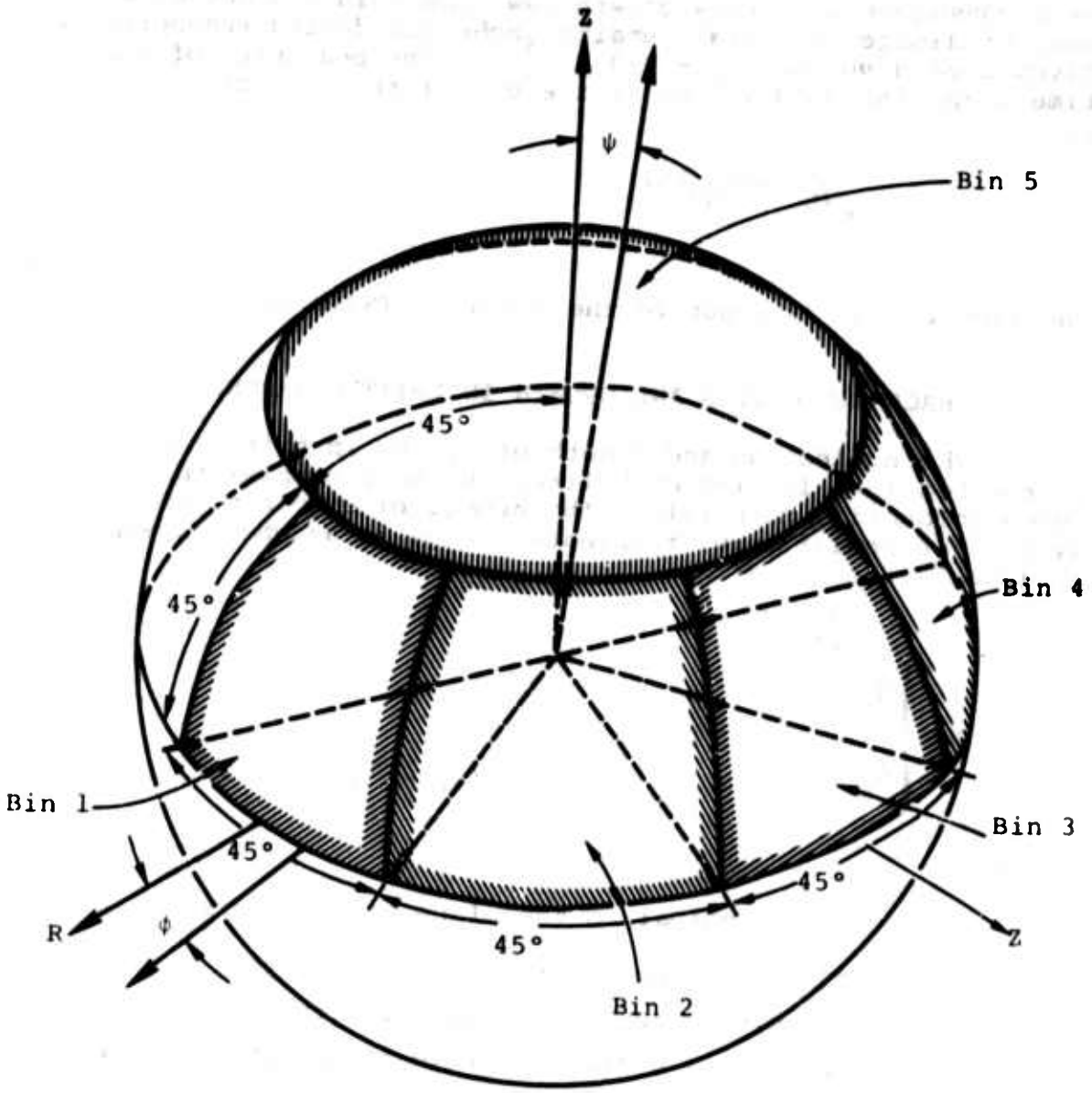

Figure 2.1. Crack orientation bins. (Upper hemisphere only is shown.)

Crack radii growth is assumed governed by the equation

$$\dot{R} = \begin{cases} \frac{\sigma_{\phi\psi} - \sigma_{go}}{4\eta} R & \text{if } \sigma_{\phi\psi} < \sigma_{go} \\ 0 & \text{if } \sigma_{\phi\psi} \geq \sigma_{go} \end{cases}$$

or, analogous to void growth,

$$R = \begin{cases} R_o \, e^{\frac{\sigma_{\phi\psi} - \sigma_{go}}{4\eta} \Delta t} & \text{if } \sigma_{\phi\psi} < \sigma_{go} \\ R_o & \text{if } \sigma_{\phi\psi} \geq \sigma_{go} \end{cases}$$

where

σ_{go} = TSR(m,2) = growth threshold stress.

The cracks are assumed to open elastically to form ellipsoids having a thickness 2δ where δ is given by

$$\delta \equiv \frac{4(1-\nu^2)}{\pi E} R \, \sigma^*_{\phi\psi}$$

and

E = Young's modulus

ν = Poisson's ratio

$\sigma^*_{\phi\psi} = \max(-\sigma_{\phi\psi}, 0)$.

The volume of a crack is therefore

$$V = \frac{4}{3}\pi R^2 \delta = \frac{16}{3} \left(\frac{1-\nu^2}{E}\right) R^3 \sigma^*_{\phi\psi}$$

and the crack volume associated with bin i is

$$\int_0^\infty V \frac{df(R)}{dR} dR = \frac{32 (1-\nu^2)}{E} N_o^i (R^i)^3 \sigma^{i*}_{\phi\psi} ,$$

where as before

$$f(R) = 1 - e^{-R/R_n} .$$

Thus it is assumed that a crack radius R remains constant during recompression but that the thickness 2δ and therefore the volume become zero.

2.3 DEGRADATION OF MATERIAL PROPERTIES, FRAGMENTATION

The nucleation and growth laws provide an estimate of a void volume fraction V_v. The shear modulus G and the yield strength Y are assumed related to the values G_o and Y_o for undamaged material by the relation

$$G = G_o \left| 1 - V_v \rho F \right|$$

$$Y = Y_o \left| 1 - 4 V_v \rho \right|$$

where the factor

$$F = 15 \left(\frac{1-\nu}{7-5\nu} \right)$$

is defined by a data statement in the models to have the value 1.88 corresponding to a Poisson's ratio, ν, of 1/3.

In the brittle failure model, the density of cracks together with a consideration of their orientation leads to an estimate of the extent to which fragmentation occurs. This estimate includes both the number of fragments formed and their size. As fragmentation becomes complete (the quantity FU2D goes to zero), the material can no longer sustain tensile pressures. Fragmentation is governed by the input values read into TSR(m,10) through TSR(m,13).

2.4 EQUATION OF STATE

It is assumed that the equation of state can be adequately represented during fracture (because of the small solid strains) by

$$P_s = A\mu + \Gamma \rho_s E$$

where

P_s = pressure of the solid material (i.e., exclusive of voids)

A = material bulk modulus

Γ = Grunεisen's ratio

$\mu = \rho_s/\rho_o - 1$, ρ_s being the density of the solid material and ρ_o the initial density.

Both of the NAG-FRAG models determine simultaneously, during a time step, the damage quantities (number of voids or cracks and the void volume fraction) and the stresses. This is done in a complex iteration procedure in which the new pressure estimate must be carefully initialized. A detailed discussion of this procedure is given in Reference [1].

3. INCORPORATION OF THE NAG-FRAG FAILURE MODELS INTO THE EULERIAN HELP CODE

As described in the foregoing section, the NAG-FRAG failure models provide considerable detail as to the extent and type of damage experienced by a given volume of material over a given period of time. In a Lagrangian code, where the computational cells are associated with the same mass throughout the calculation, the time-dependent damage characteristics (e.g., void (or crack) number and volume) of each cell are easily computed. On the other hand, in an Eulerian code, such as HELP, where the grid remains fixed and the mass is transported from one computational cell to another, these time-dependent damage characteristics become severely diffused if they are transported as the momentum and energy quantities are transported.

To avoid this diffusion, damage regions, which deform with the mass in the manner of a Lagrangian cell, have been incorporated into the HELP code. The stresses and damage characteristics of these damage regions are computed by the NAG-FRAG subroutines, DFRACT and BFRACT. The Eulerian cells that are completely contained within the boundaries of a single damage region assume the stress state of that region; whereas, those cells completely outside the damage region retain the stress state assigned to them by the equation of state for the undamaged material. A cell intersected by a damage region boundary is assigned a stress which is a volume weighted average of the stresses associated with damaged and undamaged portions of the cell.

Once the stresses of the Eulerian cells are so determined, the equations of motion and energy and the transport of mass, momentum and energy are executed as before.

To insure the success of this approach, several refinements were made to the computations of transport volumes and of deviatoric strain and stress increments in HELP. These refinements along with a description of the algorithms for generating and updating the damage regions are discussed in the sections that follow. Additional information of the type required by a user of the code is given in Appendix A.

3.1 CREATION AND PROPAGATION OF DAMAGE REGIONS

A damage region is created when material in an Eulerian cell first fails, i.e., the cell's pressure (DFRACT) or stresses normal to bin angles (BFRACT) are sufficiently

tensile to nucleate voids or cracks. Special damage region tracer particles are placed around the newly failed material and thereafter move with the local velocity field. These particles, in so far as they represent the boundary of this failed material, provide a means of tracking the material as well as measuring its volumetric and shearing strains as it continues to deform.

3.1.1 Movement of Damage Region Tracer Particles

The local velocity field of a damage region tracer particle is defined in the same manner as that for a material interface tracer particle. The velocity components of those Eulerian cells overlayed by a rectangle of cell dimensions that is centered about a given tracer particle are averaged to give the velocity components of the given tracer particle. At most, four Eulerian cells are overlayed. The components of the i^{th} cell are weighted by the area common to it and the rectangle

$$u = \frac{\Sigma u_i A_i}{\Sigma A_i}$$

$$v = \frac{\Sigma v_i A_i}{\Sigma A_i}$$

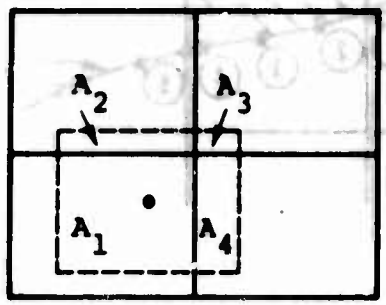

This procedure gives a spatially continuous velocity field for tracer particle motion.

3.1.2 Creation of Damage Regions for Pure Eulerian Cells

If the Eulerian cell which has just failed is pure, i.e., contains only one, undamaged material, the boundary of the new damage region coincides with the boundary of the entire cell. Five damage region tracer particles are placed at the corners of the cell in a counter-clockwise order with the fifth particle being a repeat of the first.

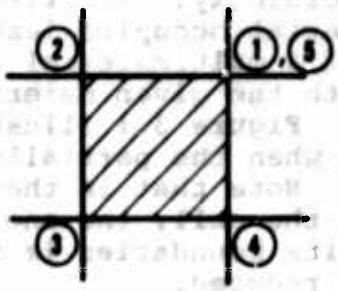

3.1.3 Creation of Damage Regions from Multimaterial Eulerian Cells

When one of the materials in a multimaterial Eulerian cell first satisfies the failure condition, the boundary of the new damage region coincides with the boundary of that material in the cell. Damage region tracer particles are placed at the intercepts of the material interface with the cell boundary, at the included corners of the cell, if any, and along the material interface, coinciding with the material interface tracer particles. The last particle closes off the region by being a repeat of the first.

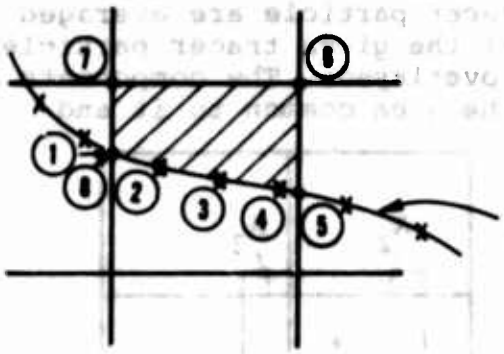

• Damage region tracer particles

x Material interface tracer particles

Material Interface

3.1.4 Enlargement and Reduction of Existing Damage Regions

A partially damaged cell is one which contains the boundary of one or more damage regions and therefore contains both damaged and undamaged materials. During each time step the stress state of the undamaged material is independently assessed and the appropriate failure criteria is applied to it. When the failure criterion is satisfied, one of two courses is taken: either the newly damaged material is included in an existing damage region, or a new damage region is created to include the previously as well as the newly failed material; the damage regions associated with the previously damaged material are reduced accordingly. The first option is chosen if the newly damaged material occupies less than half the cell volume, or in the case of a multimaterial cell, less than half the volume associated with the given material; otherwise, the second option is chosen. Figure 3.1 illustrates these two occurrences for the case when the partially damaged cell contains only one material. Note that in the case where an existing damage region intersects the cell, the one which has the largest part of the cell within its boundaries is the one which is enlarged; the others are reduced.

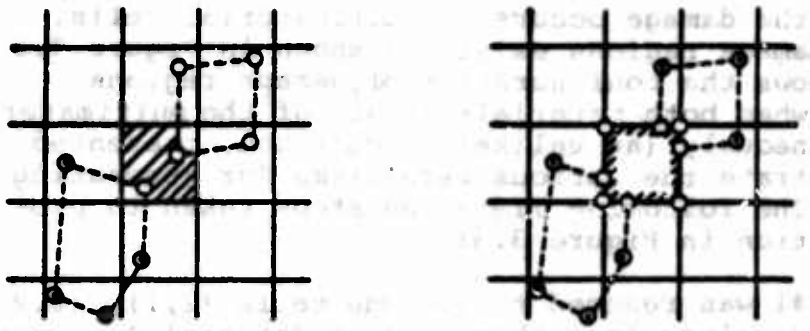

Case 1: A pure Eulerian cell with less than one-half of its material previously damaged - a new damage region is created, and the overlapping damaged regions are reduced.

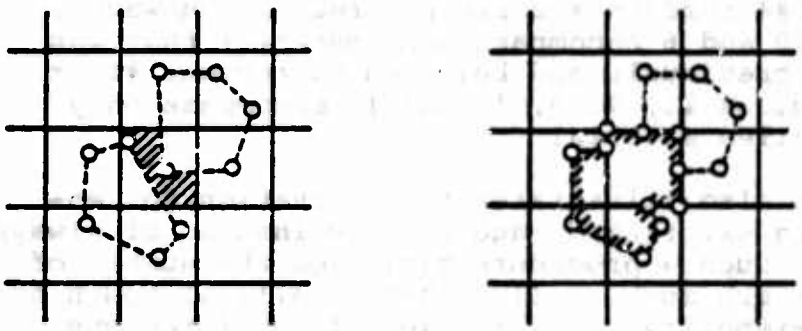

Case 2: A pure Eulerian cell with more than one-half of its material previously damaged - one of the existing damage regions is enlarged, and the other(s) are reduced.

Figure 3.1. The creation or enlargement of Lagrangian damage regions.

To further illustrate the way in which damage regions are created, enlarged and reduced, Figures 3.2 and 3.3 represent a portion of an Eulerian grid in which all of these options are exercised and the damage occurs in multimaterial cells. Initially, three damage regions exist, as shown in Figure 3.2. The next figure shows the configuration of damage regions which is produced when both materials in all of the multimaterial cells fail simultaneously (an unlikely occurrence, presented here only to illustrate the various mechanisms for generating damage regions). The following lists the steps taken to produce the configuration in Figure 3.3:

1. Region #1 was reduced to exclude cells (2,1), (2,2) and (1,2) since less than half of Material A in any of those cells was previously damaged.

2. Region #2 was enlarged to include all of material B in cell (2,2) since it had already encompassed more than half of material B in that cell.

3. Region #3 was eliminated altogether when it was reduced twice; once when region #4 was created and again when region #6 was created.

4. Regions #4 through #12 are new regions; however, #4, 8, 10 and 6 encompass some material that was damaged previously and belonged to regions #1 or #3. Regions #5, 7, 9, 11 and 12 encompass only newly failed material.

This example also illustrates the motivation for enlarging and reducing existing damage regions instead of always creating new ones. Such a procedure minimizes the number of damage regions that are much smaller than a cell; although as regions #5 and #9 exemplify, the creation of small regions is not always avoided. In addition, this procedure minimizes the formation of damage regions having very irregular shapes, such as the undamaged portion of material A in cells (1,2) and (2,2) in Figure 3.2.

The boundary of an existing damage region is enlarged or reduced by removing tracer particles interior to the newly failed material as well as by adding tracer particles at appropriate cell corners and at intercepts of the damage region and the cell boundaries.

When a region is reduced, its mass is adjusted as follows:

$$M_i^{n+1} = M_i^n - \rho_i \, \Delta V$$

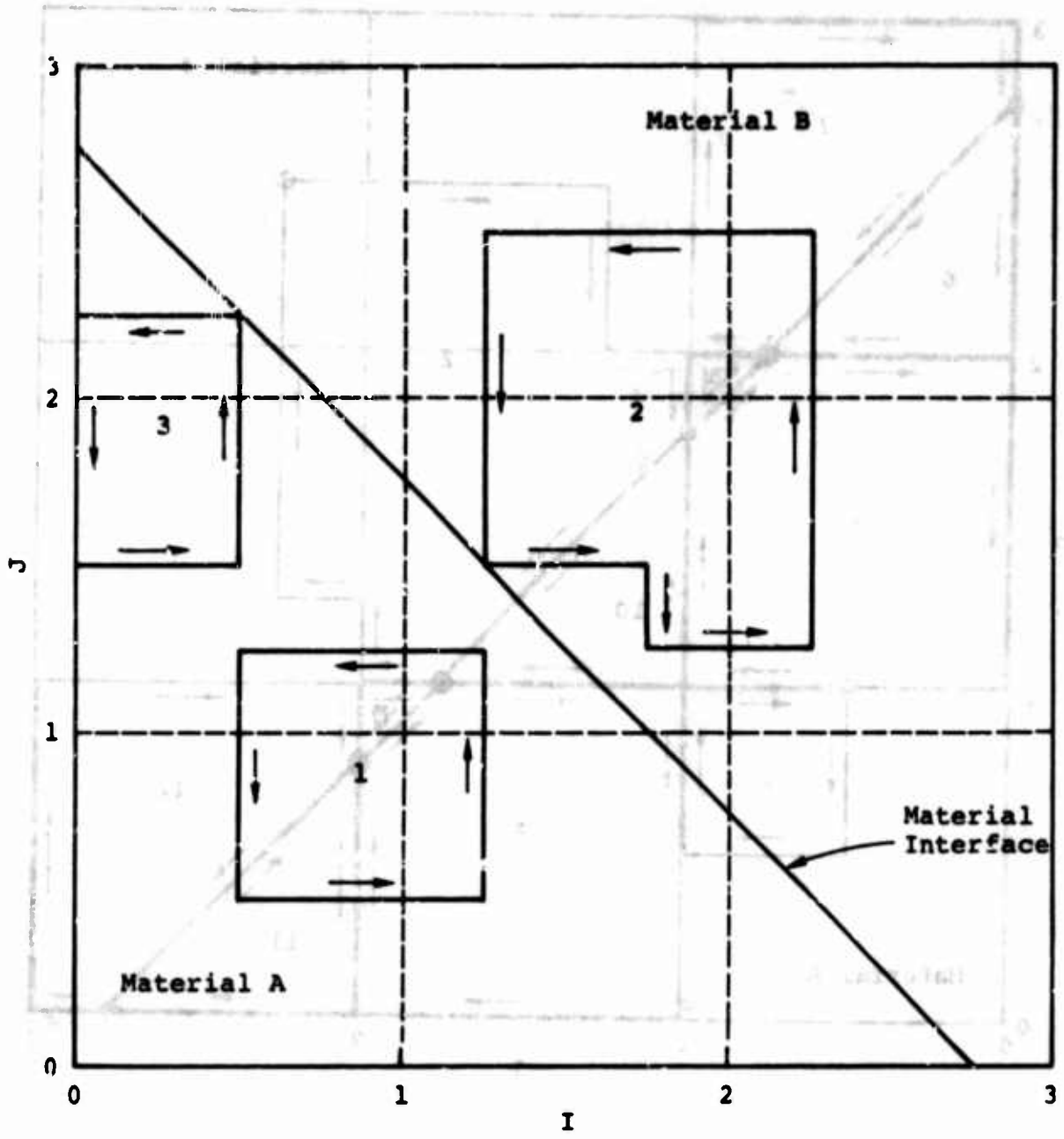

Figure 3.2. Three damage regions superimposed on an Eulerian grid near a material interface.

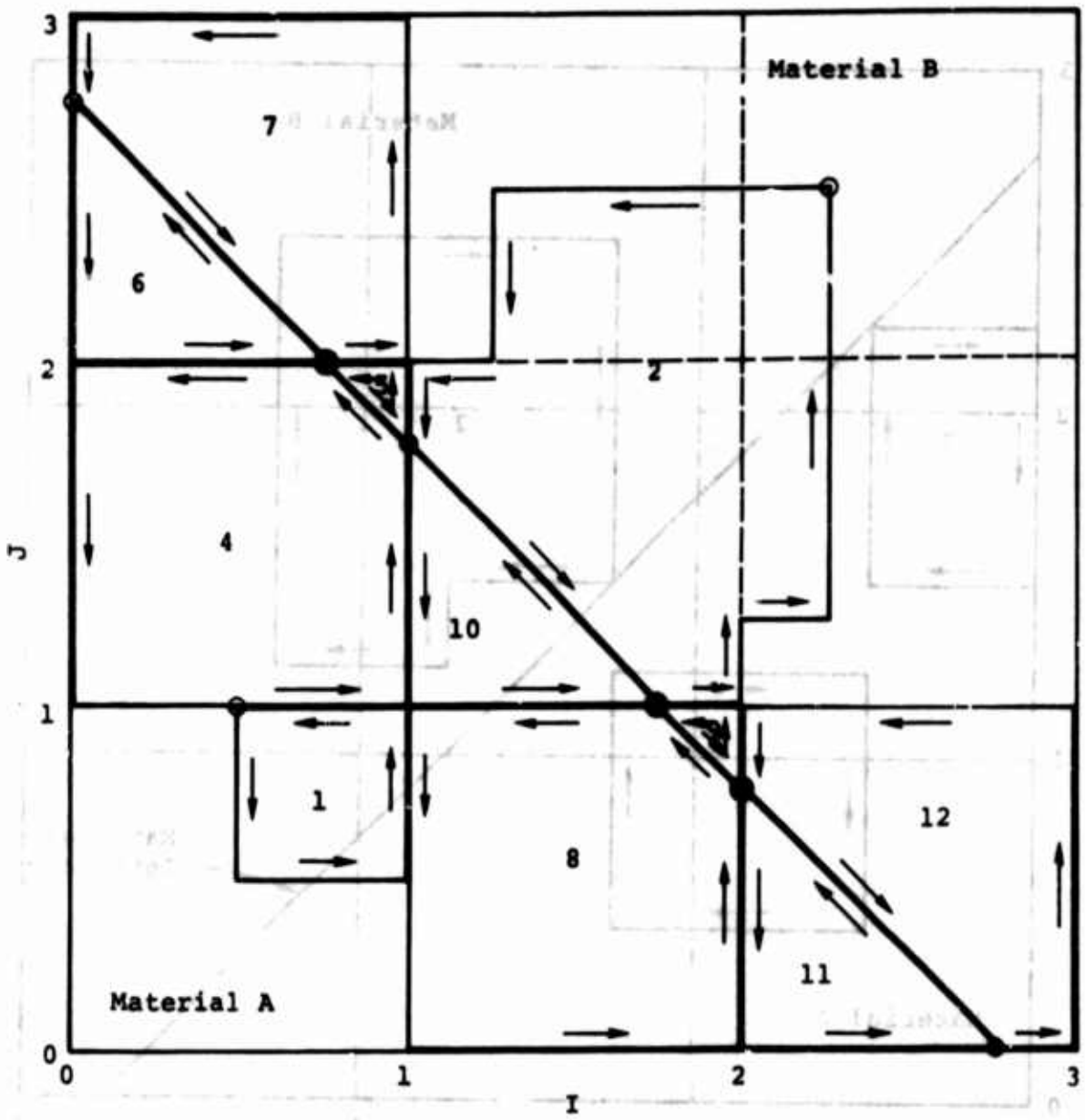

Figure 3.3. Configuration of damage regions after both materials fail simultaneously in all of the multimaterial cells.

where ρ_j is the current mass density of the region and ΔV is the volume by which it is being reduced. Likewise, when a region is enlarged, its mass becomes

$$M_i^{n+1} = M_i^n + \rho_j \Delta V \quad .$$

where ρ_j is the current mass density of the newly failed material and ΔV is its volume.

Enlarging a damage region requires all of the material properties, not just the mass, to be redefined. The damage parameters and the stress components of the enlarged region are redefined to be a volume weighted average of those quantities associated with the region before it was enlarged and those quantities associated with the material that has just failed and just been added to the region. For example, the pressure of the enlarged region becomes

$$p_i^{n+1} = (P_i^n V_i + P_j^n \Delta V)/(V_i + \Delta V)$$

where i and j subscripts refer to the existing and newly damaged materials, respectively. On the other hand, the specific internal energy of the enlarged region is a mass weighted average of the previously and newly damaged materials:

$$E_j^{n+1} = [E_i^n M_i^n + E_j^n (\Delta V \rho_j)]/M_i^{n+1} \quad .$$

3.2 SYNCHRONIZATION OF MASS TRANSPORT AND THE MOVEMENT OF DAMAGE REGION BOUNDARIES

Previously the HELP code employed two different transport algorithms: one for the tracer particles, which define the material interfaces and the damage region boundaries and another for the mass. As described in Section 3.1.1 and illustrated by Figure 3.4a, the velocity of each tracer particle is determined by an interpolation procedure which area weights the velocities of at most four cells in the vicinity of the particle, and which thereby define a spatially continuous velocity field.

The original HELP algorithm for transporting mass, on the other hand, presumed a discontinuous velocity field, i.e.,

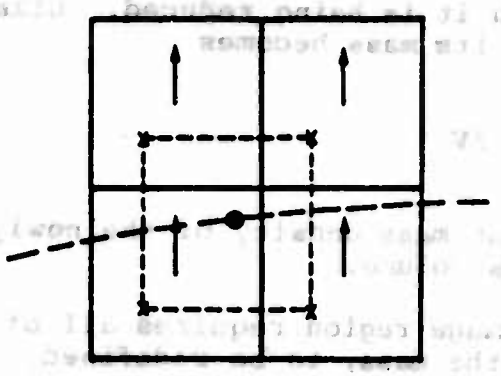

a. The tracer particle velocity is based on values at locations denoted by x, which were interpolated from neighboring cell centered values.

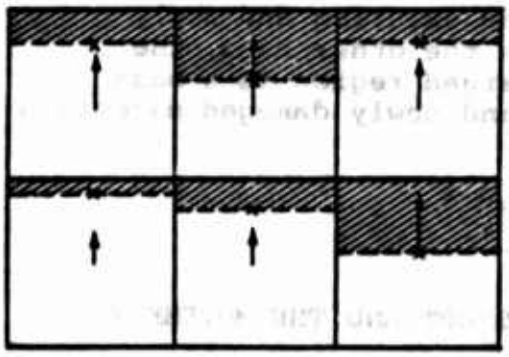

b. In the original HELP treatment, a single transport velocity (at x) computed at each cell boundary.

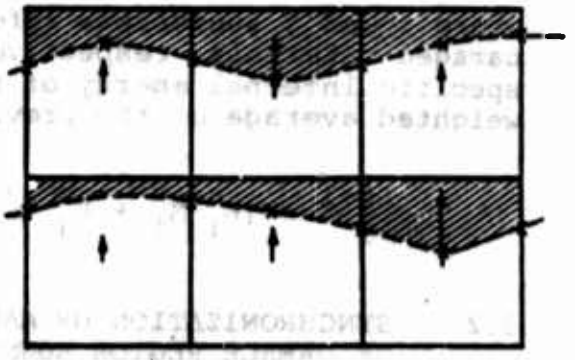

c. In the modified transport treatment, transport velocities (at x) are computed at three points for each cell boundary.

Figure 3.4. A comparison of the velocity interpolations used in moving the tracer particles and in computing the transport quantities.

it was based on the assumption that all of the mass in each cell had the velocity of the cell center. As illustrated by Figure 3.4b, the volume of material transported from one cell to another was based only on the cell-centered velocities of the two cells.

3.2.1 Use of Continuous Velocity Field in Mass Transport

To synchronize the movement of the tracer particles and the mass, the calculation of the transport volumes for transporting mass was rewritten so as to be based on a spatially continuous velocity field. Consider the mass transport in the axial direction as illustrated in Figure 3.4c. The "map line" is the locus of points such that each point exactly reaches the cell interface when transported through the time step Δt with its locally interpolated axial velocity component. If every material point in the grid (together with its associated momentum and energy) is moved through the time step Δt with its local (interpolated) axial velocity, and if each tracer point is moved likewise, then axial mass transport is consistent with axial tracer motion. The same argument applies to the radial transport and tracer motion.

If a material interface intersects a cell boundary, the transport volume determined by the map line is apportioned among the constituents on the basis of the fractional areas subtended by each material.

3.2.2 Division of Transport Phase Into Axial and Radial Subphases

To simplify the logic of the new transport scheme, the transport phase of the computational cycle has been divided into two subphases with only axial (or radial) transport taking place in the first subphase and radial (or axial) transport in the second. To prevent bias, the order, radial-axial or axial-radial, is reversed each computational cycle. The tracer particles as well as the mass are moved in these two subphases.

3.3 REVISED COMPUTATION OF PRESSURES AND DEVIATORIC STRESSES

The computation of the deviatoric stresses and the calculation of the effects of both the pressure and the deviatoric stresses has been modified in the NAG-FRAG version of the HELP code as described in the sections that follow.

3.3.1 Computing Separate Stress States for Materials in Mixed Cells

In order to apply the NAG-FRAG failure model to each material in mixed or free surface cells, an accurate account of the stress state of each material is necessary. Previously, tensile pressures in all interface cells and the deviatoric stresses of free surfaces cells were set to zero, thus making it impossible to apply a failure criterion to these cells. Table 3.1 summarizes the changes made to the calculation of the pressures and deviatoric stresses in mixed and free surface cells so that the NAG-FRAG failure model could be applied individually to the materials in these cells.

3.3.2 Combining the Hydrodynamic and Strength Phases of HELP

Previously the HELP computational cycle was divided into three phases, the hydrodynamic phase (HPHASE) the strength phase (SPHASE), and the transport phase (TPHASE). In the hydrodynamic phase the cell pressures were computed and the effects of these pressures on the cell velocities and internal energies were determined; an intermediate set of cell velocities and energies were stored. In the strength phase the strain increments were computed (using the post-HPHASE intermediate velocities) and the deviatoric stresses of the cells were updated accordingly. These updated stress deviators were then applied in the momentum and energy equations and another intermediate set of cell velocities and internal energies were defined.

The first two phases, HPHASE and SPHASE have been combined to conform with the requirements of the BFRACT failure criterion, which considers the total stress components normal to the bin angles, and to facilitate the mapping of the damage region stress states into the Eulerian grid. Thus, the effects of the pressure and deviatoric stresses are now computed in the same phase (SPHASE for stress phase), and only one set of intermediate velocities and internal energies are generated prior to the transport phase (still TPHASE).

3.3.3 Mapping the Damage Region Stresses into the Eulerian Grid

On each computational cycle the Eulerian cell stresses are defined by the following procedure. First the stresses of each damage region are computed by the NAG-FRAG subroutines DFRACT and/or BFRACT. Next the HELP subroutines determine the stress state of the material in all of the Eulerian cells.

TABLE 3.1. MODIFICATIONS TO THE COMPUTATION OF STRESSES IN FREE SURFACE AND MULTIMATERIAL CELLS

ORIGINAL HELP MODEL	REVISED HELP MODEL FOR INCLUSION OF THE MAG-FRAG FAILURE CRITERION
A. Pressure	A. Pressure
The pressure of a multimaterial cell is computed by equilibrating the pressures of its constituents in an iteration on mass density (the specific internal energy of each material is held constant). This iteration therefore defines the mass densities as well as the pressures of the constituents.	The tracer particle positions are used in conjunction with the boundaries of a cell to compute the volume occupied by each material. By dividing the mass of each material by this volume, its density is determined.
The pressure of a free surface cell is computed by assuming the mass occupies the entire cell. Therefore, the material density used in the equation of state is simply the cell mass divided by the total cell volume.	A pressure for each material in a multimaterial or free surface cell is t computed using the density that is computed from the tracer particle positions and the specific internal energy of each material.
In either a multimaterial cell or a free surface cell, if the computed pressure is negative (tensile), the cell pressure is set to zero, i.e., tensile states are not allowed in multimaterial or free surface cells. Tensile failure criterion are therefore not applied to multimaterial or free surface cells.	To arrive at an average cell-centered pressure in a multimaterial or a free surface cell the pressures of the constituents are volume weighted $\bar{P} = \frac{\Sigma P_i V_i}{\Sigma V_i}$. To account for the void in a free surface cell, a zero pressure is associated with the void volume. The average cell centered stresses are used only in the equations of motion and energy. The failure criterion is based on the individual material stresses.
B. Deviatoric Stresses	B. Deviatoric Stresses
The deviatoric stresses of a multimaterial cell are derived from strain increments that are based on the velocities of its eight contiguous neighbor cells, and from a volume weighted average of the strength parameters of the cell's constituents.	The deviatoric stresses of each material in a multimaterial cell are updated using strain increments that are derived solely from a velocity field that lies within the boundaries of each material. The shear yield strength applied to the deviatoric stresses of a material is, likewise, a function of the strength parameters associated with that material.
Material in free surface cells is assumed to have no strength; therefore, the deviatoric stresses of all free surface cells are zero.	The deviatoric stresses of a multimaterial or free surface cell are defined to be a volume weighted average of the deviatoric stresses of its constituents $\bar{S}_{ij} = \frac{\Sigma (S_{ij})_k V_k}{\Sigma V_k}$. In defining the deviator stresses to be associated with the cell center of a free surface cell the void is included in the weighted average unless the void volume is more than 9/10 of the cell volume, in which case the deviatoric stresses of the cell are set to zero.

Next, if the stress state of undamaged material in an Eulerian cell satisfies the NAG-FRAG failure condition, a new damage region is created to redefine the stress state of this newly formed damage region. Finally, the stresses of all the damage regions (old and new) are mapped into the Eulerian grid, thus altering the stress state of those cells containing damaged material. For example, the final cell pressure, P^f, of a single material, pure cell is defined as follows:

$$P^f = \begin{cases} P^e & \text{if the cell contains only undamaged material} \\ \dfrac{\Sigma\, V_n^{\ell} P_n^{\ell}}{\Sigma\, V_n^{\ell}} & \text{if the cell contains only damaged material} \\ \dfrac{V^e P^e + \Sigma V_n^{\ell} P_n^{\ell}}{V_{cell}} & \text{if the cell contains both damaged and undamaged material} \end{cases}$$

where

V_n^{ℓ} = the volume common to the n^{th} damage region and to the cell

V^e = the volume of undamaged material in the cell

P_n^{ℓ} = the pressure in the n^{th} damage region

P^e = the pressure of the undamaged material in the cell.

The volume, V_n^{ℓ}, common to a given damage region and a given cell is computed using the current positions of the damage region tracer particles (which define the boundary of the region) and the fixed boundaries of the cell. These partial volumes are computed every computational cycle for every cell which contains the boundary of one or more damage regions.

4. AUXILIARY IMPROVEMENTS TO THE HELP CODE

Three auxiliary improvements were made to the HELP code as the NAG-FRAG failure models were incorporated and tested. Options were added for making the top and right grid boundaries either transmittive or reflective, and for adding either, or both, a linear and a quadratic artificial viscosity term to cell boundary stresses. Further, the α-ε phase transition in the Hugoniot of iron in compression was implemented into the iron equation of state. These improvements will be described in the sections that follow.

4.1 ADDITIONAL REFLECTIVE GRID BOUNDARY OPTIONS

In the 1975 documented version of HELP, the left grid boundary, which is an axis of symmetry when cylindrical coordinates are used, is always reflective, the bottom grid boundary can be either transmittive or reflective, and the right and top grid boundaries are always transmittive. (The transmittive and reflective grid boundary conditions are described in detail in Chapter III of the 1975 documentation of HELP [Reference 2].) The tapered flyer plate plane-strain calculations, which were performed in order to test out the implementation of the NAG-FRAG failure models, required that the right as well as the left grid boundary be reflective. Thus the option to have the right and top grid boundaries be reflective was implemented, even though the reflective boundary condition was required only on the right.

In the new version of HELP, therefore, the user dictates the condition of the bottom, right and top grid boundaries when defining the Z-block variables CVIS, CVISR, and CVIST, respectively, in the input deck. A zero value (which is the default value) indicates a transmittive condition; whereas, -1. indicates a reflective condition. (Note: The opposite convention is used in the other versions of HELP, wherein -1. indicates a transmittive boundary condition. Also, the location of CVIS in the Z-block has been changed from 27 to 125.)

4.2 LINEAR AND QUADRATIC ARTIFICIAL VISCOSITY

The form of the artificial viscosity added to cell boundary stresses in the NAG-FRAG version of HELP is more accurate than that used in the standard 1975 version of the code.

The expression for linear artificial viscosity when applied, for example, to the right cell boundary is of the form

$$Q_L = QLIN*c*\rho*\sqrt{A}*\dot{\varepsilon}_{RR}$$

where

QLIN = linear artificial viscosity coefficient

c = sound speed

ρ = material density

A = cell area = $\Delta R*\Delta Z$

$\dot{\varepsilon}_{RR}$ = normal strain rate in R direction.

In the 1975 documented version of HELP, this expression was simplified by assuming $\Delta R = \Delta Z$, $Q_{LIN} = 1$ and $c = \sqrt{P/\rho}$ which led to

$$Q_L = \sqrt{P_\rho} * [u(K+1) - u(K)] \quad .$$

Such a sound speed calculation is suitable for an ideal gas (in which $c = \sqrt{\gamma P/\rho}$) but a poor approximation for materials represented by a Tillotson equation of state.

The linear artificial viscosity used in the NAG-FRAG version (1) does not require square zoning, (2) applies a user defined coefficient QLIN ≡ Z(93) and (3) uses a more accurately calculated sound speed:

$$c = \begin{cases} c_o & \text{for a Tillotson equation of state (materials 1-19)} \\ \sqrt{\dfrac{\gamma P}{\rho}} & \text{for an ideal gas or JWL equation of state (materials 20-25)} \end{cases}$$

In addition, a quadratic artificial viscosity term, Q_Q, may be added in compressing regions:

$$Q_Q = QQUAD*\rho*A*(\dot{\varepsilon}_{RR})^2 \quad ,$$

where QQUAD = Z(94) is defined by the user. (NOTE: since the use of artificial viscosity is now governed by the input variables QLIN and QQUAD, the formerly used input flag LVISC has been deleted from the Z-array.)

4.3 IMPLEMENTATION OF THE α-ε PHASE CHANGE IN IRON

In addition to the specific work involving the fragmentation models, the equation of state for iron has been

modified to account for the α-ε phase change that occurs at pressures in the vicinity of 130 kbars. This modification was made since any failure model depends on dynamic quantities calculated from the constitutive relation, and the accuracy with which BFRACT and DFRACT predict fragmentation in rolled homogeneous armor and penetrator steels is therefore highly dependent upon the accuracy of the constitutive model over the entire range of stresses and pressures expected.

The usual form for the equation of state employed in the HELP code is that due to Tillotson[3] modified to give a smooth transition between condensed and expanded states. For the condensed states, i.e., when $\rho/\rho_o > 1$, or for any cold states, $E < E_s$ the equation of state has the form

$$p = p_c = \left[a + \frac{b}{\frac{E}{E_o\eta^2} + 1}\right] E\rho + A\mu + B\mu^2 \quad . \tag{1}$$

For expanded hot states, i.e., when $\rho/\rho_o < 1$ and $E < E_s'$, the equation of state has the form

$$p = p_E = aE\rho + \left[\frac{bE\rho}{\frac{E}{E_o\eta^2} + 1} + A\mu e^{-\beta(v/v_o - 1)}\right] e^{-\alpha(v/v_o - 1)^2} \quad . \tag{2}$$

A smooth transition between the condensed and expanded states is insured by a transition equation for the intermediate region defined by $E_s < E < E_s'$ and $\rho/\rho_o < 1$. This blended portion of the equation of state has the form

$$p = \frac{(E - E_s)p_E + (E_s' - E)p_c}{E_s' - E_s} \quad . \tag{3}$$

In Equations (1) through (3) p, E and ρ are pressure, specific internal energy, and mass density, respectively, $\eta = \rho/\rho_o = \mu + 1 = v_o/v$, and ρ_o, a, b, E_o, E_s, E_s', A, B, α and β are constants for the particular material.

The material parameters employed in the Tillotson equation of state for iron are given in Table 4.1.

The Tillotson equation of state for compressed states of iron may also be written as

TABLE 4.1. MATERIAL PARAMETERS FOR IRON

PROPERTY \ MATERIAL	STEEL
ρ_o (g/cm^3)	7.856
A (dynes/cm^2)	See Text
B (dynes/cm^2)	See Text
a	0.5
b	1.5
α	5.0
β	5.0
E_o (ergs/g)	9.5×10^{10}
E_s (ergs/g)	2.44×10^{10}
E_s' (ergs/g)	1.02×10^{11}
G (dynes/cm^2)	8.0×10^{11}
Y_o (dynes/cm^2)	6.0×10^{9}
Y_1 (dynes/cm^2)	0
Y_2 (dynes/cm^2)	0
E_m (ergs/g)	1.3×10^{10}
S* (dynes/cm^2)	3.8×10^{10}

*S = Spall strength

$$P = f(\rho) + \left[a + \frac{b}{1 + \frac{E}{E_o \eta^2}}\right] \rho E \qquad (4)$$

where the appropriate form of $f(\rho)$, for $\eta \geq 1.0$ is

$$f(\rho) = P_H - \left[a + \frac{b}{1 + \frac{E_H}{E_o \eta^2}}\right] \rho E_H \quad . \qquad (5)$$

The second term in the expression for $f(\rho)$ insures that the pressure P will be equal to the Hugoniot pressure, P_H, when the energy E is equal to the Hugoniot energy, E_H.

The analytic fit to the Hugoniot of iron in compression as given by Mader[4] was modified for use in the HELP code. The α-ε phase transition is bridged by a two-piece analytic fit which maintains continuity of the pressure and its first derivative along the Hugoniot curve. The resulting approximate equation of state assumes that the phase change is instantaneous.

For low pressure states ($0 \leq P_H < 125$ kbar) the analytic fit to the Hugoniot is

$$P_H = \rho_o C_{o\ell}^2 \frac{\varepsilon}{(1 - S_\ell \varepsilon)^2} \quad , \qquad (6)$$

where

$$\rho_o = 7.856 \text{ gm/cm}^3$$

$$C_{o\ell} = 4.63 \times 10^5 \text{ cm/sec}$$

$$S_\ell = 1.275$$

and

$$\varepsilon \equiv 1 - \rho_o/\rho \quad .$$

Equation (6) for the pressure in dyne/cm^2 is valid for the range of specific volumes

$$0.11929584 \leq V \leq 0.12729124 = 1/\rho_o \quad .$$

For the pressure range from 125 kbar to 140 kbar, the Hugoniot pressure is fitted as

$$P_H = A + B\,(\Delta V) + C_\ell\,(\Delta V)^2 + D_\ell\,(\Delta V)^{10} \qquad (7)$$

where

$$A = 140 \times 10^9$$
$$B = -\,4.0 \times 10^{12}$$
$$C_\ell = 2.383828348 \times 10^{14}$$
$$D_\ell = -\,6.060826938 \times 10^{34}$$
$$\Delta V \equiv V - 0.1162$$

and the range of specific volumes is

$$0.1162 \leq V \leq 0.11929584 \quad .$$

For the pressure range from 140 kbar to 155 kbar, the Hugoniot pressure is given by

$$P_H = A + B\,(\Delta V) + C_h\,(\Delta V)^2 + D_h\,(\Delta V)^{10} \qquad (8)$$

with A and B as before and

$$C_h = -\,7.090650579 \times 10^{13}$$
$$D_h = 1.224016343 \times 10^{35} \quad .$$
$$\Delta V \equiv V - 0.1162$$

The range of specific volumes is

$$0.11335815 \leq V \leq 0.1162$$

For the pressure range 155 to 364 kbar, the analytical fit to the Hugoniot is

$$P_H = \rho_o C_{oh}^2 \frac{\varepsilon}{(1 - S_h \varepsilon)^2} \quad , \tag{9}$$

with

$$\rho_o = 7.856 \text{ gm/cm}^3$$

$$C_{oh} = 3.20 \times 10^5 \text{ cm/sec}$$

$$S_h = 2.25$$

$$\varepsilon \equiv 1 - \rho_o/\rho \quad ,$$

and the range of specific volumes is

$$0.1055 < V \leq 0.11335815 \quad .$$

For pressures from 364 kbar to 457 kbar the following equations are suggested.

For volumes in the range

$$0.1030 \leq V \leq 0.1055$$

the Hugoniot pressure in (dyne/cm^2) is

$$P_H = A + B\,(\Delta V) + C\,(\Delta V)^2 + D\,(\Delta V)^3 \tag{10}$$

with

$$A = 3.6432733 \times 10^{11}$$

$$B = -3.7667780 \times 10^{13}$$

$$C = -1.712352 \times 10^{}$$

$$D = 3.6615110 \times 10^{16}$$

$$\Delta V \equiv V - 0.1055 \quad .$$

For specific volumes

$V < 0.1030$

the Hugoniot pressure is

$$P_H = \rho_o C_o^2 \frac{\varepsilon}{(1 - S\varepsilon)^2} \qquad (11)$$

with

$\rho_o = 7.856$ gm/cm^3

$C_o = 3.78 \times 10^5$ cm/sec

$S = 1.652$

$\varepsilon \equiv 1 - \rho_o/\rho$.

For pressures in the range $0 \geq P \leq 125$ kbar, or equivalently, for volumes in the range

$$0.11929584 \leq V \leq 0.12729124$$

the Hugoniot energy is computed with

$$E_H = \frac{1}{2} P_H (V_o - V) \quad , \qquad (12)$$

where

$V_o = 0.12729124$.

For the volume range

$$0.1066867 \leq V \leq 0.11929584$$

the energy is computed from

$$E_H = \frac{1}{2} P_1 (V_o - V_1) + \frac{1}{2} (P_H + P_1)(V_1 - V) \qquad (13)$$

with

$$P_1 = 1.25 \times 10^{11} \text{ dyne/cm}^2$$

$$V_1 = 0.11929584 \text{ cm}^3/\text{gm} \quad .$$

For the volume less than 0.1066867, Equation (12) is used to compute the Hugoniot energy.

The modified Hugoniot for modeling the phase change in iron is plotted in Figure 4.1 for the pressure range between 0 and 400 kbar and a magnified plot of the fits to the transition region is given in Figure 4.2.

For condensed iron at pressures less than 0 kbar the form of the $f(\rho)$ equation is

$$f(\rho) = A\mu + B\mu^2 \qquad (14)$$

where

$$A = 1.28 \times 10^{12}$$

$$B = 1.05 \times 10^{12} \quad .$$

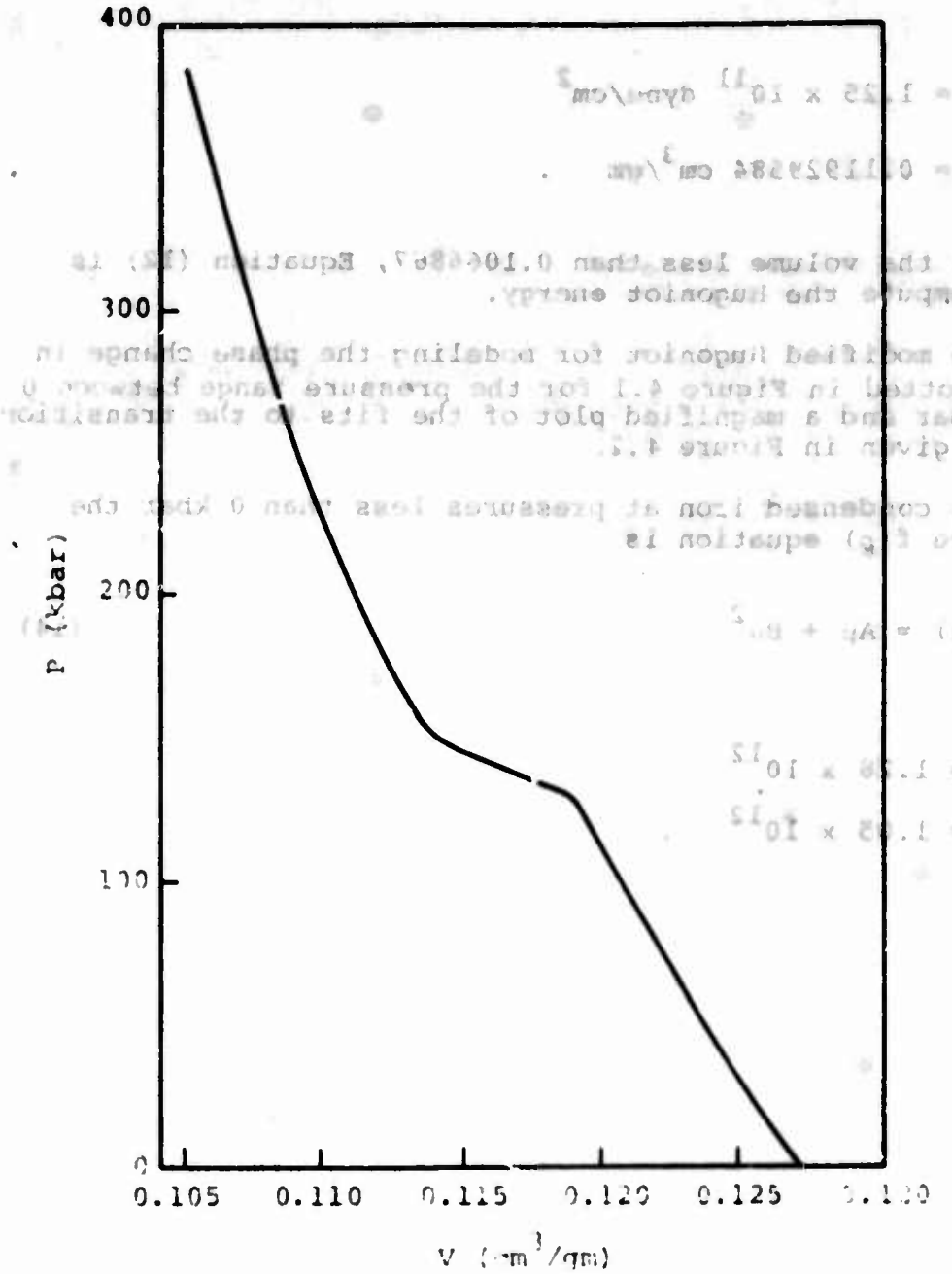

Figure 4.1. Hugoniot for iron.

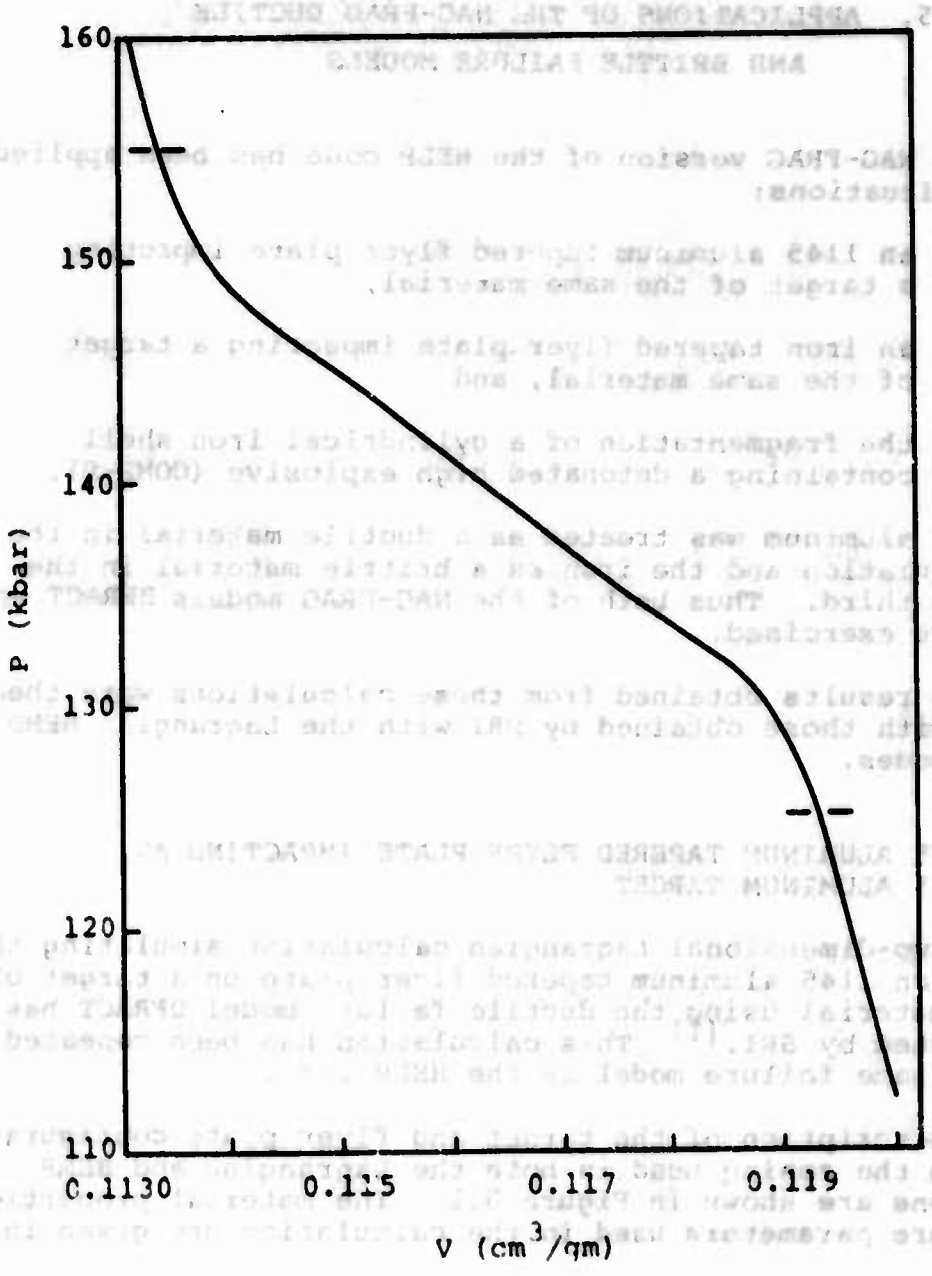

Figure 4.2. Analytic fits to the transition region.

5. APPLICATIONS OF THE NAG-FRAG DUCTILE AND BRITTLE FAILURE MODELS

The NAG-FRAG version of the HELP code has been applied to three situations:

1. an 1145 aluminum tapered flyer plate impacting a target of the same material,

2. an iron tapered flyer plate impacting a target of the same material, and

3. the fragmentation of a cylindrical iron shell containing a detonated high explosive (COMP-B).

The aluminum was treated as a ductile material in the first calculation and the iron as a brittle material in the second and third. Thus both of the NAG-FRAG models BFRACT and DFRACT were exercised.

The results obtained from these calculations were then compared with those obtained by SRI with the Lagrangian HEMP and PUFF codes.

5.1 1145 ALUMINUM TAPERED FLYER PLATE IMPACTING AN 1145 ALUMINUM TARGET

A two-dimensional Lagrangian calculation simulating the impact of an 1145 aluminum tapered flyer plate on a target of the same material using the ductile failure model DFRACT has been reported by SRI.[1] This calculation has been repeated using the same failure model in the HELP code.

A description of the target and flyer plate configuration along with the zoning used in both the Lagrangian and HEMP calculations are shown in Figure 5.1. The material properties and fracture parameters used in the calculation are given in Table 5.1.

In the HELP calculation several options were considered concerning the treatment of the target-flyer plate interface: (1) not allowing tensile pressures in interface cells, (2) allowing tensile pressures but not allowing separation at the interface and (3) removing the flyer plate when the interface first becomes tensile. It was found that the third option gave the closest agreement with the Lagrangian calculation. (In the Lagrangian calculation interface separation was permitted, hence this option appears the most appropriate.) Also, several

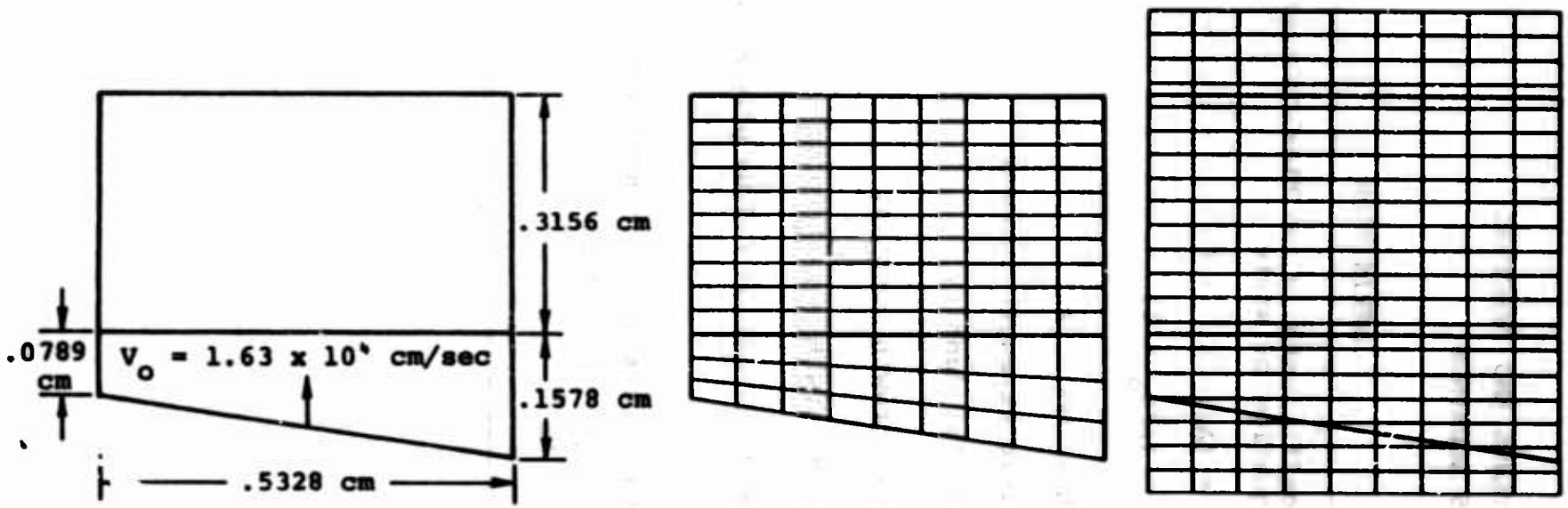

Initial Dimensions of 1145 Aluminum Target and Flyer Plate

SRI Grid Configuration (HEMP)

S³ Grid Configuration (HELP)

Figure 5.1. Dimensions and grid configurations for 1145 aluminum tapered flyer plate impact calculations.

TABLE 5.1. MATERIAL CONSTANTS AND FRACTURE PARAMETERS FOR 1145 ALUMINUM

SYMBOL	VALUE	DEFINITION
A	760 kbars	Coefficients in the Mie-Gruneisen equation of state $P = (A\mu + B\mu^2 + C\mu^3)(1 - \frac{\Gamma}{2}\mu) + \Gamma\rho E$ $\mu = (\rho/\rho_o - 1)$
B	1500 kbars	
C	0	
Γ	2.04	
G	300 kbars	Shear modulus
Y	1.1547 kbars	Yield strength in shear
ρ_o	2.70 gm/cm^3	Initial density
$\frac{3}{4\eta}$	-0.01 cm^2/dyne/sec	Void growth constant
P_{go}	-4.0 kbars	Void growth threshold
R_n	10^{-4} cm	Void nucleation radius parameter
$\dot{N}_o$	3.0 x 10^9/cm^3/sec	Parameters for void nucleation $\dot{N} = \dot{N}_o e^{(P-P_{no})/P_1}$
P_{no}	-3.0 kbars	
P_1	-0.4 kbars	

levels of linear artificial viscosity were tested in the HELP code. Although the results were generally smoother, the damage levels were significantly reduced when the artificial viscosity was added. Accordingly, in the HELP calculation whose results are presented here no artificial viscosity was added and the flyer plate was removed at about 0.71 μs.

Since the rate of both void nucleation and growth is a strong function of tensile stress, any spurious behavior in the stress field might well lead to a prediction of very high localized damage. On the other hand, while artificial viscosity is effective in damping out such behavior, it was found in the test case to significiantly alter the damage throughout the entire grid. Experience suggests a reasonable means of treating this problem might be to require the tensile stress to exceed the nucleation threshold for several cycles before allowing material to fail.

A measure of the dynamic response of the target free surface to flyer plate impact is given by Figure 5.2 in which the average velocity across this surface is plotted as a function of time for both the Lagrangian and HELP calculations.

Two measures of target damage level, the void volume fraction and the number of voids per cm^3, as computed by the HELP code are shown in Figures 5.3. and 5.4 at times 0.93, 1.17, and 1.62 μs. (Corresponding values of these quantities obtained from the HEMP calculation at 1.46 μs are shown in Figures 5.5 and 5.6). It may be noted that the areal extent of damage increases little after 0.93 μs. However, the level of damage increases due to both nucleation and growth of voids. The damage levels existing in both the SRI and S^3 calculations after target recompression, during which the damage level remains constant, is shown in the surface plots of Figures 5.7 and 5.8.

5.2 ARMCO IRON TAPERED FLYER PLATE IMPACTING ON ARMCO IRON TARGET

SRI reported [1] a second 2-D Lagrangian impact calculation simulating the impact of an Armco iron tapered flyer plate on a target of the same material using the brittle failure model BFRACT. This calculation was repeated using the same failure model in the HELP code.

A description of the target and flyer plate configuration along with the zoning used in both the Lagrangian (HEMP) and Eulerian (HELP) calculations are shown in Figure 5.9. The material properties and fracture parameters used in the calculation appear in Table 5.2.

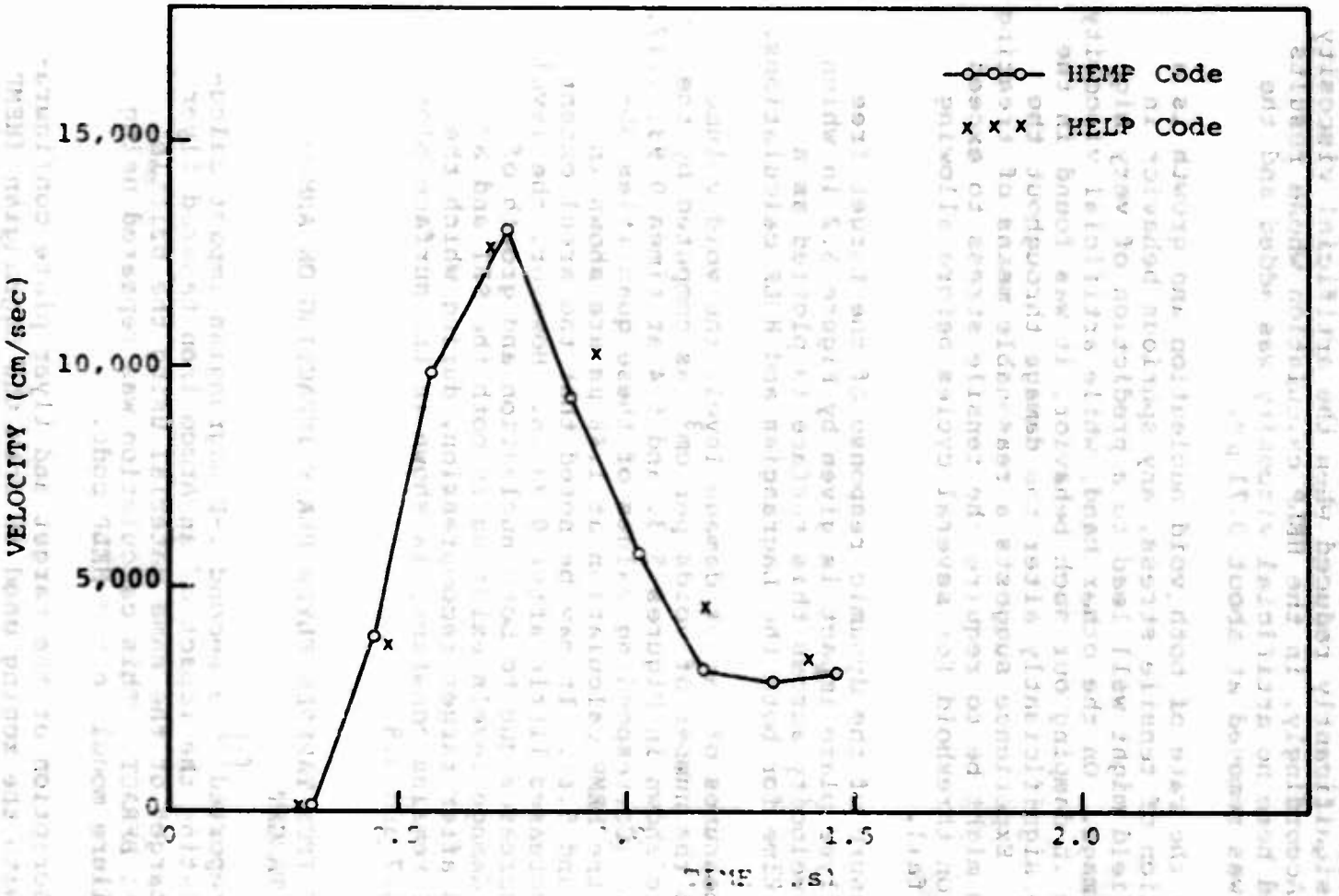

Figure 5.2. Comparison of 1145 aluminum target free surface velocities obtained by SRI with the Lagrangian (HEMP) code with those obtained by the Eulerian (HELP) code.

.03	.01	.01	.01					
.00	.00	.00	.00	.01	.01	.01	.01	.01
32.66	16.29	6.24	3.29	.44	.11	.03	.02	.01
.00	.01	.03	.10	.20	.20	.25	.14	.10
18.80	8.97	5.09	4.71	1.79	2.70	.82	.47	.32
.02	.04	.12	.45	.64	1.59	8.37	10.16	7.39
						.01	.02	.01

t = 0.93 μs

.11	.01	.01	.01					.00
.00	.01	.01	.02	.06	.10	.16	.21	.16
4718.45	4075.18	3599.62	3643.91	2685.52	2658.06	2044.40	1344.39	2523.97
421.50	1408.79	3539.81	5696.06	7664.23	9761.13	11793.92	11543.82	13187.23
2782.80	3517.29	4416.93	5728.26	8007.84	11263.42	12810.53	14000.46	17169.66
213.17	968.09	1836.95	2384.06	2496.47	3789.77	4915.27	5880.45	6521.39
16.93	10.46	12.86	8.86	13.61	4.59	2.99	9.10	5.60
.03	.03	.04	.03	.03	.03	.05	.09	.09
								.00

t = 1.17 μs

.11	.05	.03	.02					.00
.00	.01	.01	.02	.06	.10	.16	.21	.16
4741.69	4092.83	3615.91	3661.22	2697.15	2670.23	2055.07	1351.37	2534.97
422.95	1413.36	3552.20	5709.19	7689.18	9797.08	11838.47	11582.58	13243.92
2797.96	3535.37	4437.44	5752.14	8036.10	11305.03	12846.94	14043.82	17257.51
213.87	971.25	1843.53	2392.64	2505.63	3806.22	4936.69	5903.22	6548.16
16.96	10.47	12.87	8.87	13.64	4.60	3.00	9.13	5.62
.03	.03	.04	.03	.03	.03	.03	.09	.09
								.00

t = 1.62 μs

Figure 5.3. Relative void volume of damage regions at three times after impact in the 1145 aluminum flyer plate calculation. (Numbers shown are to be multiplied by 10^{-6}.) Impact plane is at bottom, and thick end of flyer plate is at right.

1.1	.6	.3	.2					
.1	.1	.1	.1	3	.3	.3	.3	.3
939.0	494.2	202.4	111.2	16.1	4.4	1.3	.6	.5
.1	.4	1.2	3.9	7.7	7.8	9.7	5.3	3.9
560.3	289.7	173.0	163.7	65.5	100.5	31.5	18.3	12.5
.7	1.4	4.6	18.3	21.7	57.3	293.9	360.5	265.3
						.4	.7	.6

t = 0.93 μs

4.4	1.9	1.1	.7					.0
.1	.2	.4	.8	2.3	4.0	6.3	7.6	6.0
11542.6	10189.2	9231.0	10303.2	8310.9	9552.7	7630.?	5370.5	9178.0
2077.8	5139.9	12663.7	21313.2	29504.4	37259.1	45120.2	46897.8	50818.6
5735.6	7419.1	9769.1	13014.1	18985.0	11069.7	14983.1	40731.9	45333.9
810.4	2394.7	4382.9	5733.3	5926.9	9254.7	13961.8	17741.1	19466.1
213.6	150.2	173.1	133.2	181.1	80.0	55.5	109.2	80.4
.6	.6	1.0	1.0	1.0	1.0	1.8	3.5	3.4
								.1

t = 1.17 μs

4.4	2.0	1.1	.7					.0
.1	.2	.4	.8	2.3	4.0	6.4	7.8	6.2
11643.5	10284.6	9325.7	10384.6	8375.4	9632.3	7694.4	5419.4	9254.0
2103.2	5385.1	12781.5	21520.7	29767.1	37612.3	45513.4	47309.5	51227.6
5796.4	7497.2	9864.8	13133.0	19149.6	31341.3	35240.7	41044.9	45629.6
827.0	2426.9	4432.4	5793.6	5987.2	9346.6	14095.0	17900.9	19627.2
220.3	158.1	180.5	139.4	187.3	83.5	58.0	114.1	83.1
1.2	1.1	1.5	1.2	1.1	1.0	1.8	3.5	3.4
								.1

t = 1.62 μs

Figure 5.4. Number of voids per cubic centimeter in damage regions at three times after impact in the 1145 aluminum flyer plate calculation. (Numbers shown are to be multiplied by 10^3.) Impact plane is at bottom, and thick end of flyer plate is at right.

.00	.00	.00	.00	.00	.00	.00	.00	.00
.00	.00	.00	.00	.00	.00	.00	.004	.008
.04	.05	.11	.21	.48	1.28	3.92	10.29	19.17
214.0	162.5	135.7	194.3	449.0	1106	2152	3342	4042
131.4	278.0	970.7	2716	5283	8273	10700	12250	13060
1319	1254	1410	2025	3518	6132	8995	10610	11100
278.7	475.3	1107	1926	1847	1185	906.2	941.8	1025
13.53	16.52	35.70	35.39	52.89	38.07	31.45	16.43	18.82
.01	.04	.07	.06	.05	.04	.03	.04	.07
.00	.00	.00	.00	.00	.00	.00	.00	.00

Figure 5.5 Relative void volume of material in the 1145 aluminum target at 1.46 μs after impact as computed by the Lagrangian (HEMP) code. (Numbers shown are to be multiplied by 10^{-6}.). Impact plane is at bottom, and thick end of flyer plate is at right.

.0	.0	.0	.0	.0	.0	.0	.0	.0
.0	.0	.0	.0	.0	.0	.0	.1	.3
1.5	21.1	4.2	8.2	15.3	29.6	65.8	134.2	216.9
1384	1018	773.9	929.1	1735	3872	7805	12690	15600
590.7	974.5	2396	6379	14300	24620	32760	36450	36960
3990	3767	4081	5335	8595	16160	25440	31090	32620
1548	2286	4627	7858	7561	4201	2424	2486	2696
217.3	256.1	476.2	455.5	612.0	483.6	417.7	251.5	280.5
.6	1.6	3.0	2.4	1.9	1.5	1.0	1.8	2.9
.0	.0	.0	.0	.0	.0	.0	.0	.0

Figure 5.6 Number of voids per cubic centimeter of material in the 1145 aluminum target at 1.46 μs after impact as computed by the Langrangian (HEMP) code. (Numbers shown are to be multiplied by 10^{3}.). Impact plane is at bottom, and thick end of flyer plate is at right.

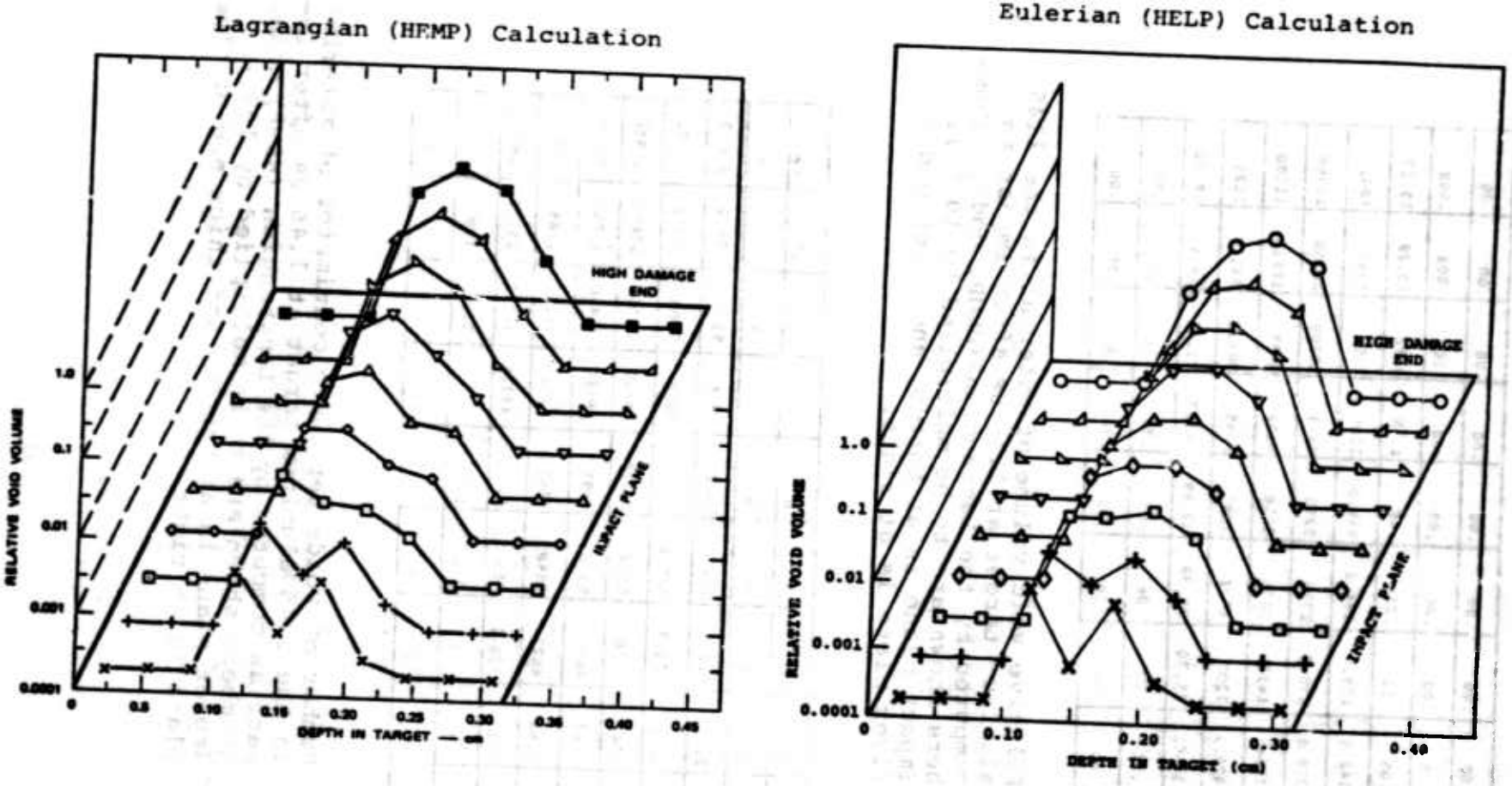

Figure 5.7. Relative void volume in the 1145 aluminum target after recompression as computed by both the Lagrangian (HEMP) code and the Eulerian (HELP) code.

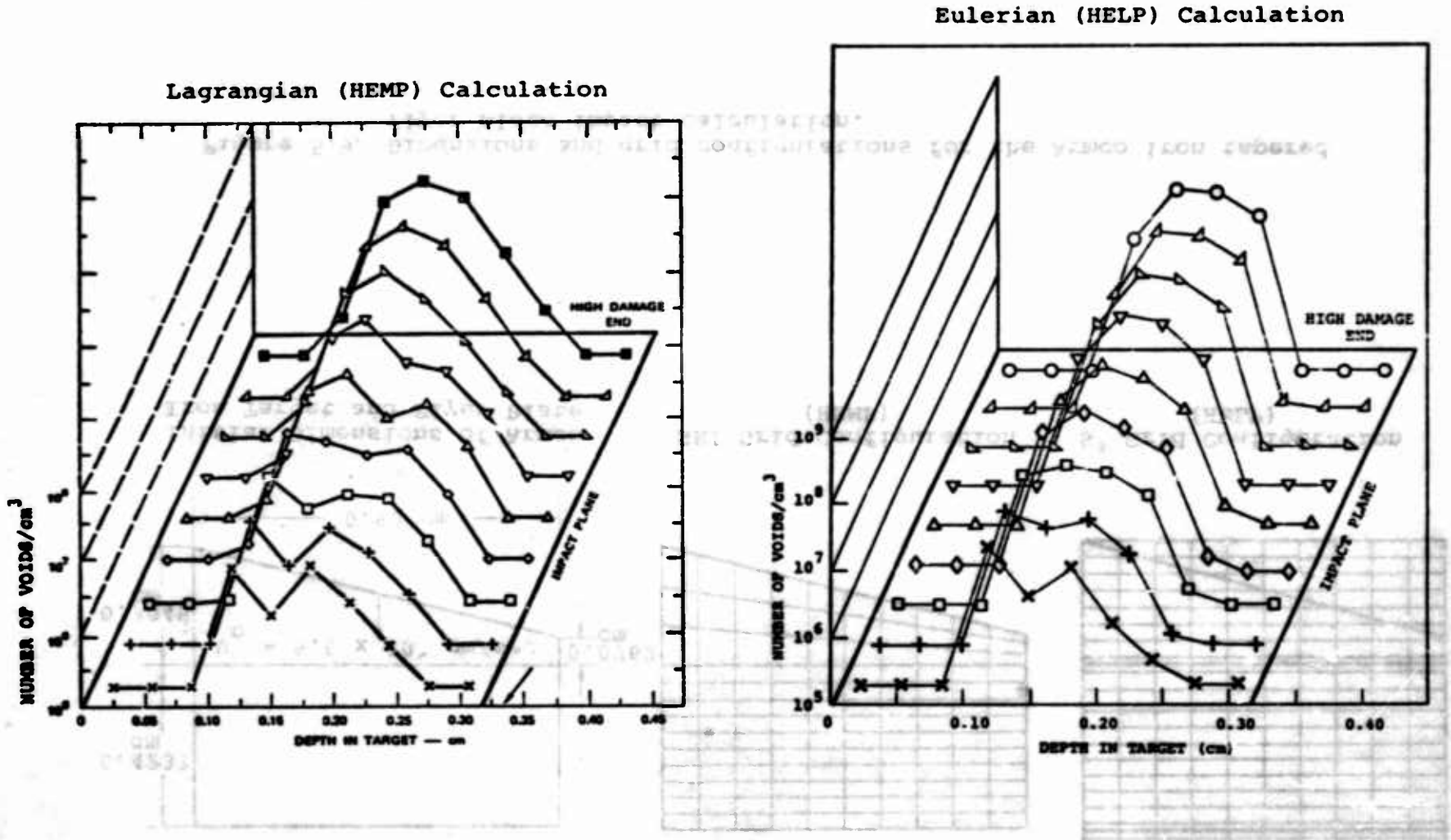

Figure 5.8. Number of voids per cubic centimeter in the 1145 aluminum target after recompression as computed by both the Lagrangian (HEMP) code and the Eulerian (HELP) code.

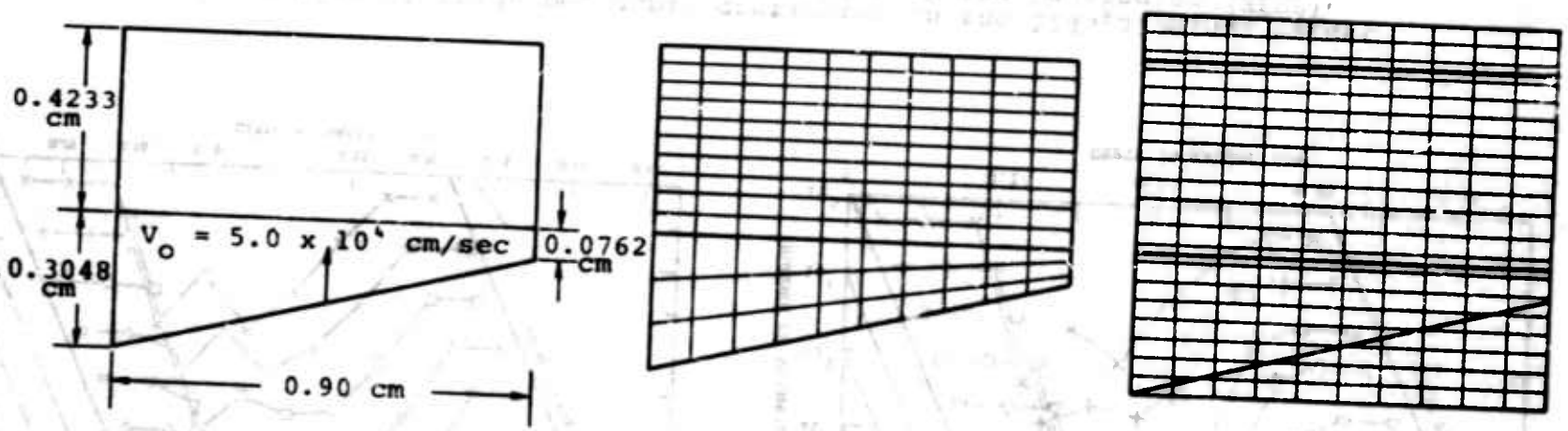

Figure 5.9. Dimensions and grid configurations for the Armco iron tapered flyer plate impact calculation.

TABLE 5.2. MATERIAL CONSTANTS AND FRACTURE PARAMETERS FOR ARMCO IRON

SYMBOL	VALUE	DEFINITION
A	1589 kbars	Coefficients in the Mie-Gruneisen equation of state $P = (A\mu + B\mu^2 + C\mu^3)(1 - \frac{\Gamma}{2}) + \Gamma\rho E$
B	5170 kbars	
C	51700 kbars	$\mu = (\rho/\rho_o - 1)$
Γ	1.69	
G	819 kbars	Shear modulus
Y	6.062 kbars	Shear yield strength
ρ_o	7.85 gm/cm^3	Initial density
$\frac{3}{4\eta}$	-0.00012 (cm^2/dyne/sec)	Void growth constant
σ_{go}	0.0	Void growth threshold
R_n	0.004	Void nucleation radius parameter
$\dot{N}_o$	5.0 x 10^8	Parameters for void nucleation $\dot{N} = \dot{N}_o e^{(\sigma_{\phi\psi} - \sigma_{no})/\sigma_1}$
σ_{no}	-11.2 kbars	
σ_1	-0.74 kbars	
TSR(10)	0.25	Fragmentation parameters provided by SRI
TSR(11)	1.0	
TSR(12)	0.2	
TSR(13)	1.0	

As in the aluminum flyer plate calculations, the iron flyer plate was removed when the projectile-target interface first became tensile in both the HEMP and HELP calculations. The separation occurred at about 1.32 μs.

To get the best agreement between the HEMP and HELP results, both linear and quadratic artificial viscosity terms were added to the cell boundary stresses in compressing regions of the HELP grid; in the expanding regions only the linear viscosity term was added. The form of the artificial viscosity in this version of HELP is described in Section 4.2. The linear and quadratic coefficients used in this calculation were 0.1 and 4.0, respectively.

Three measures of damage in the brittle target material, the number of cracks per cm^3, the void volume fraction, and the fraction of fragmented material, as computed by HELP, are shown in Figures 5.10, 5.11 and 5.12 at times 1.18, 1.46, and 2.11 μs. (Corresponding values of the number of cracks per cm^3 and the fraction of fragmented material as computed by the HEMP code are shown in Figures 5.13 and 5.14 at 1.24, 1.51 and 2.33 μs. The void volume fraction was not an edited quantity in the HEMP calculations.) It is evident from these figures that failure begins at the end of the plate impacted by the thin part of the flyer. This is expected (and actually occurs in the aluminum impact calculation as well) since the rarefaction wave from the free surface of the flyer has less far to travel at the thin end. Although the damage first appears at the so-called thin end, the greatest damage is ultimately incurred at the end impacted by the thick part of the flyer. These figures also reveal a significant increase in the damage and fragmentation of the target near the thick end of the flyer between 1.46 and 2.11 μs; whereas, the damage at the thin end, due to both nucleation and growth of cracks, does not increase significantly after 1.46 μs.

The surface plots of Figures 5.15 and 5.16 show the number of cracks and the amount of fragmentation predicted by the Lagrangian (HEMP) code and the Eulerian (HELP) code at 2.33 and 2.11 μs, respectively. Although the HELP calculation predicts a slightly larger number of cracks per cm^3 near the thin end of the flyer, and somewhat more damage near the back free surface of the target, the regions of complete fragmentation and the concentration of cracks at the high damage end, as predicted by the two codes, are in very good agreement.

5.3 FRAGMENTING MUNITIONS

A 1-D calculation was performed with the NAG-FRAG version of HELP in which the expansion and subsequent failure of an infinitely long iron cylinder filled with detonated COMP B explosive was simulated. In order to verify the HELP prediction of failure near the free surface of the cylinder, the results were compared with those obtained by SRI using the 1-D PUFF code.

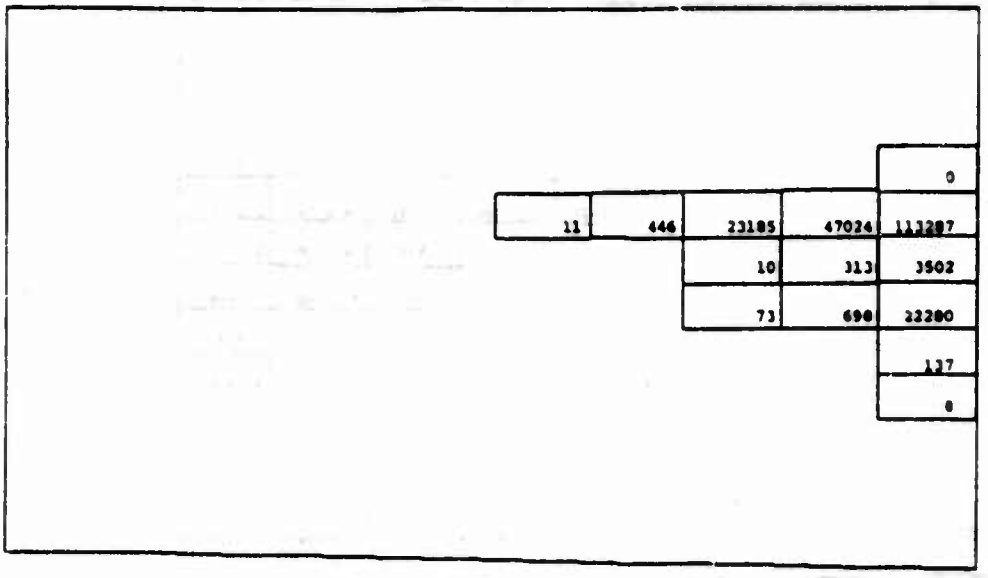

				0
11	446	23185	47024	111287
		10	313	3502
		73	698	22280
				127
				0

t = 1.18 μs

0	13986	476	25						
863999	682110	592367	513399	545688	489728	359458	261258	252346	89128
9	0	2204	80738	212353	303631	357021	382841	375806	400117
417106	425799	460400	494830	517276	537063	527732	533423	485027	327822
514761	536218	588951	645563	654063	644522	609120	572284	527739	354331
566610	592137	625083	666791	659447	633668	583337	506519	461146	194487
581814	598315	601867	632467	587607	526047	427926	343408	304188	1271
502900	529834	505887	493461	403575	341913	160619	82515	111128	7
391458	392530	311275	250193	112424	21621		74	73	9
					100	15			

t = 1.46 μs

0	343846	169075	52524	26096	1687				
867443	704782	617744	531958	562682	[illegible]516	368709	264032	253190	162405
425591	384045	303005	120036	212124	102610	358431	384974	377734	400831
503026	508262	514464	517081	515549	522880	510651	514350	468854	319492
559968	571468	604502	636586	633538	619983	585212	551044	509780	349527
667460	689346	683838	681301	653084	613375	536914	489824	449387	195157
729531	716895	682809	644565	583846	514037	423499	340956	310014	1836
605784	603372	556698	510913	424658	351387	213849	126346	169790	7
363154	355895	282972	221603	117251	22642		294	907	1514
					181	22			

t = 2.11 μs

Figure 5.10. Number of cracks per cubic centimeter in damage regions at three times after impact in the Armco iron flyer plate calculation. Impact plane is at bottom and thick end of flyer is at left.

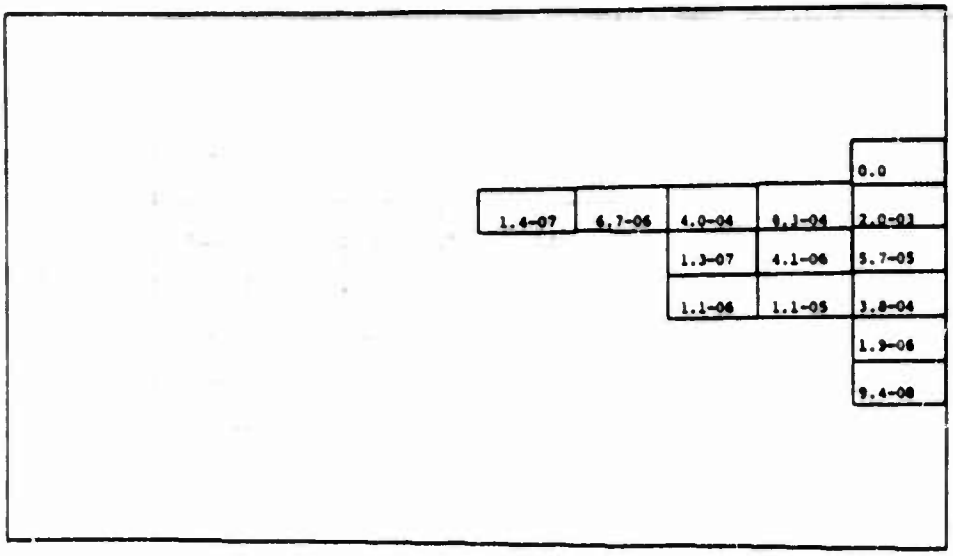

t = 1.18 μs

2.7-01	2.5-06	6.5-06	3.0-07						
2.1-02	2.1-02	1.9-02	1.6-02	1.0-03	1.7-02	1.3-02	1.0-02	9.6-03	1.5-03
9.7-08	0.0	4.1-05	2.0-03	5.5-03	9.5-03	1.3-02	1.7-02	1.7-02	2.0-02
1.0-02	1.1-02	1.2-02	1.4-02	1.7-02	2.1-02	2.2-02	2.5-02	2.4-02	1.7-02
1.4-02	1.4-02	1.7-02	2.1-02	2.4-02	2.7-02	2.7-02	2.9-02	2.8-02	1.8-02
1.4-02	1.5-02	1.7-02	2.0-02	2.2-02	2.4-02	2.1-02	2.2-02	2.0-02	7.1-03
1.4-02	1.5-02	1.6-02	2.0-02	2.0-02	2.1-02	1.7-02	1.4-02	9.9-03	2.3-05
1.2-02	1.3-02	1.3-02	1.5-02	1.2-02	1.1-02	3.3-03	1.6-03	2.3-03	1.2-08
9.9-03	1.0-02	7.2-03	6.6-03	2.4-03	4.2-04		9.7-07	9.7-07	5.2-08
					2.5-06	1.7-07			

t = 1.46 μs

2.7-01	1.3-02	7.0-03	1.1-03	5.6-04	1.3-05				
1.9-03	4.0-03	5.7-03	3.9-03	5.4-03	6.9-03	6.6-03	1.0-02	9.1-03	1.4-03
2.0-02	1.3-02	7.1-03	7.3-03	9.9-03	1.0-02	7.7-03	7.6-03	8.1-03	7.3-03
5.9-03	4.8-03	1.9-03	-2.0+00	-2.0+00	-2.0+00	-2.0+00	-2.0+00	-2.0+00	4.4-03
-2.0+00	-2.0+00	-2.0+00	-2.0+00	-2.0+00	-2.0+00	-2.0+00	-2.0+00	-2.0+00	7.4-03
-2.0+00	-2.0+00	-2.0+00	-2.0+00	-2.0+00	-2.0+00	-2.0+00	-2.0+00	-2.0+00	1.1-02
-2.0+00	-2.0+00	-2.0+00	-2.0+00	-2.0+00	-2.0+00	4.3-03	1.0-02	1.4-02	0.0
-2.0+00	-2.0+00	3.9-03	8.1-03	1.7-02	7.9-03	1.9-03	0.0	5.2-03	0.0
1.2-02	1.3-02	6. -03	9.7-04	2.1-07	0.0		0.0	6.5-05	0.0
					4.4-06	3.0-07			

t = 2.11 μs

Figure 5.11. Void volume fraction in damage regions at three times after impact in the Armco iron flyer plate calculation. Impact plane is at bottom and thick end of flyer is at left. Values of -2.0 correspond to regions that are completely fragmented.

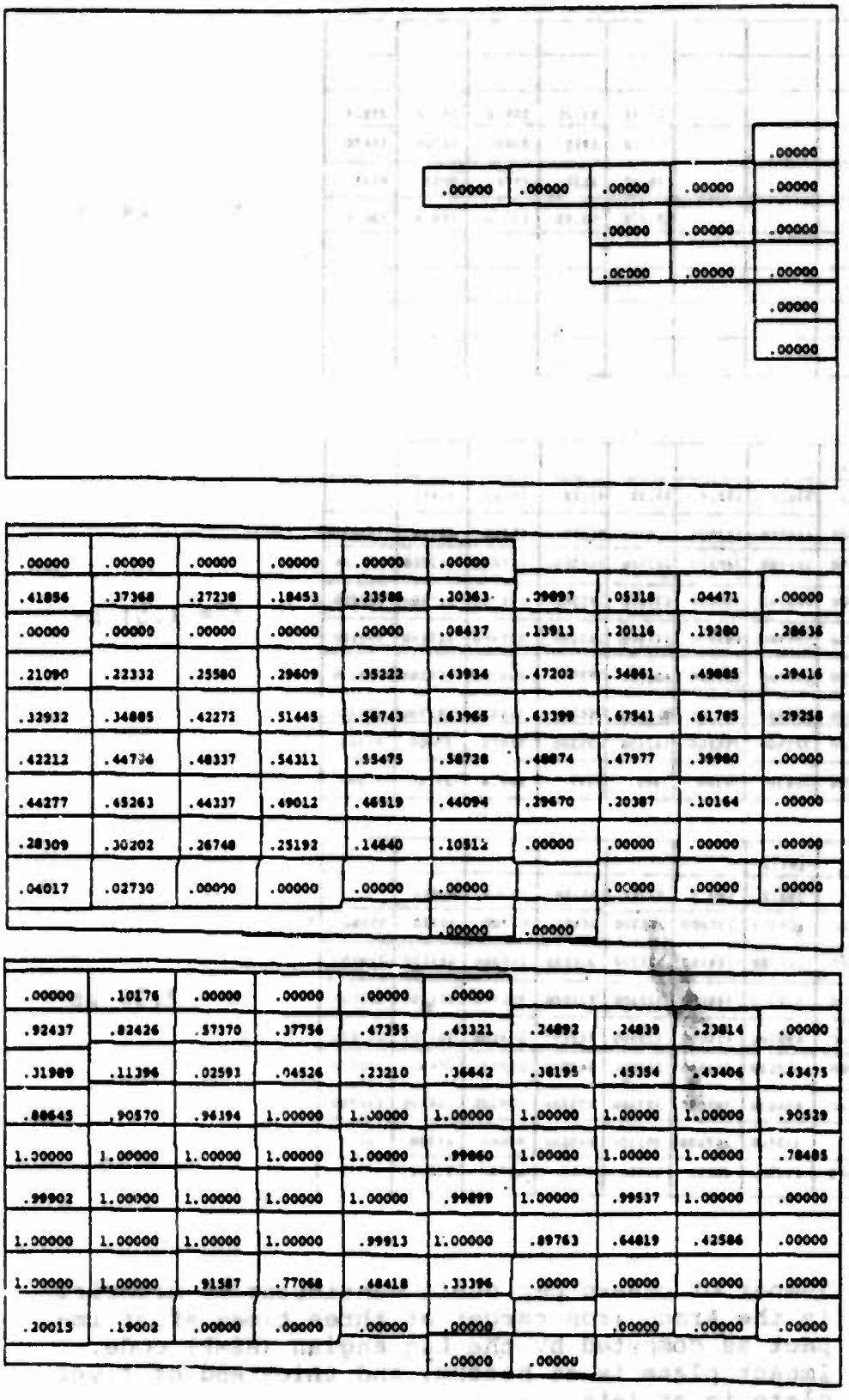

Figure 5.12. The fraction of fragmented material in damage regions at three times after impact in the Armco iron flyer plate calculation. Impact plane is at bottom, and thick end of flyer is at left.

					15.41	93.35	209.2	273.8	290.9
					12.58	1919	7363	12790	15470
					48.43	1129	4976	8057	8843
					3.318	53.82	157.0	188.4	126.8

t = 1.24 μs

1041	568.1	107.3							
1339	1021	631.2	370.6	192.4	93.32	41.82	19.46	9.413	
188500	179600	164200	146200	127800	108200	86300	65310	48710	39360
398300	393100	383200	366400	345900	323500	296300	267600	242000	226300
500600	501600	494200	485100	456000	422600	385900	349100	317300	298200
552500	550200	536700	509300	489500	441500	393200	347700	311100	290100
562500	555900	536100	503500	466000	406200	349000	299300	261300	239700
526900	513200	487800	454900	391100	326100	266100	214200	171700	146400
438900	419500	378600	320900	251100	182400	120900	71050	33630	16500
189200	175909	140700	91630	39300	7889	1299	180.4	27.69	3.908

t = 1.51 μs

19960	13740	4412	194.9						
5916	2604	718.1	383.8	193.2	93.69	41.98	19.55	9.461	
200100	190200	172400	150700	129800	109200	86990	65700	49110	39690
401300	396300	385300	366300	344100	321200	294100	266200	241600	226400
495000	494100	485100	474200	444600	412100	377000	341700	311200	293100
545600	541300	524400	495700	475000	429000	382900	339600	305300	285000
559700	549400	526800	492100	454900	396800	343000	298000	264300	245600
530100	514200	486100	451600	389000	327900	273800	229400	194700	174000
449500	428200		332100	267600	203300	145600	98660	61330	40410
219500	194500	158300	111800	60790	19660	4596	1058	275.1	62.99

t = 2.33 μs

Figure 5.13 Number of cracks per cubic centimeter of material in the Armco iron target at three times after impact as computed by the Lagrangian (HEMP) code. Impact plane is at bottom, and thick end of flyer plate is at left.

					0.0	0.0	0.0	0.0	0.0
					0.0	0.0	0.0	0.0	0.0
					0.0	0.0	0.0	0.0	0.0
					0.0	0.0	0.0	0.0	0.0

t = 1.24 μs

0.0	0.0	0.0							
0.0	0.0	0.0	0.0	0.0	0.0	0.0	0.0	0.0	
0.0	0.0	0.0	0.0	0.0	0.0	0.0	0.0	0.0	0.0
0.0	0.0	0.0	0.0	0.0	0.0	0.0	0.0	0.0	0.0
0.0	0.0	0.0	0.0	0.0	0.0	0.0	0.0	0.0	0.0
0.0	0.0	0.0	0.0	0.0	0.0	0.0	0.0	0.0	0.0
0.0	0.0	0.0	0.0	0.0	0.0	0.0	0.0	0.0	0.0
0.0	0.0	0.0	0.0	0.0	0.0	0.0	0.0	0.0	0.0
0.0	0.0	0.0	0.0	0.0	0.0	0.0	0.0	0.0	0.0
0.0	0.0	0.0	0.0	0.0	0.0	0.0	0.0	0.0	0.0

t = 1.51 μs

0.0	0.0	0.0	0.0						
0.0	0.0	0.0	0.0	0.0	0.0	0.0	0.0	0.0	
0.11	0.0662	0.0095	0.0	0.0	0.0	0.0	0.0	0.0	0.0
0.9792	0.9260	0.8578	0.8014	0.7604	0.7212	0.6579	0.5643	0.4614	0.3976
0.9956	1.0	1.0	0.999	1.0	1.0	0.9994	0.9956	0.9786	0.9035
0.9960	0.9905	1.0	1.0	1.0	0.9925	0.9994	1.0	0.9682	0.8701
0.9981	1.0	1.0	1.0	1.0	1.0	1.0	0.8344	0.6447	0.5426
1.0	1.0	1.0	1.0	1.0	0.9027	0.6314	0.3959	0.2358	0.1566
1.0	1.0		0.819	0.5649	0.3255	0.1283	0.0	0.0	0.0
0.3977	0.3142	0.1987	0.0575	0.0	0.0	0.0	0.0	0.0	0.0

t = 2.33 μs

Figure 5.14 The fraction of fragmented material in the Armco iron target at three times after impact as computed by the Lagrangian (HEMP) code. Impact plane is at bottom and thick end of flyer plate is at left.

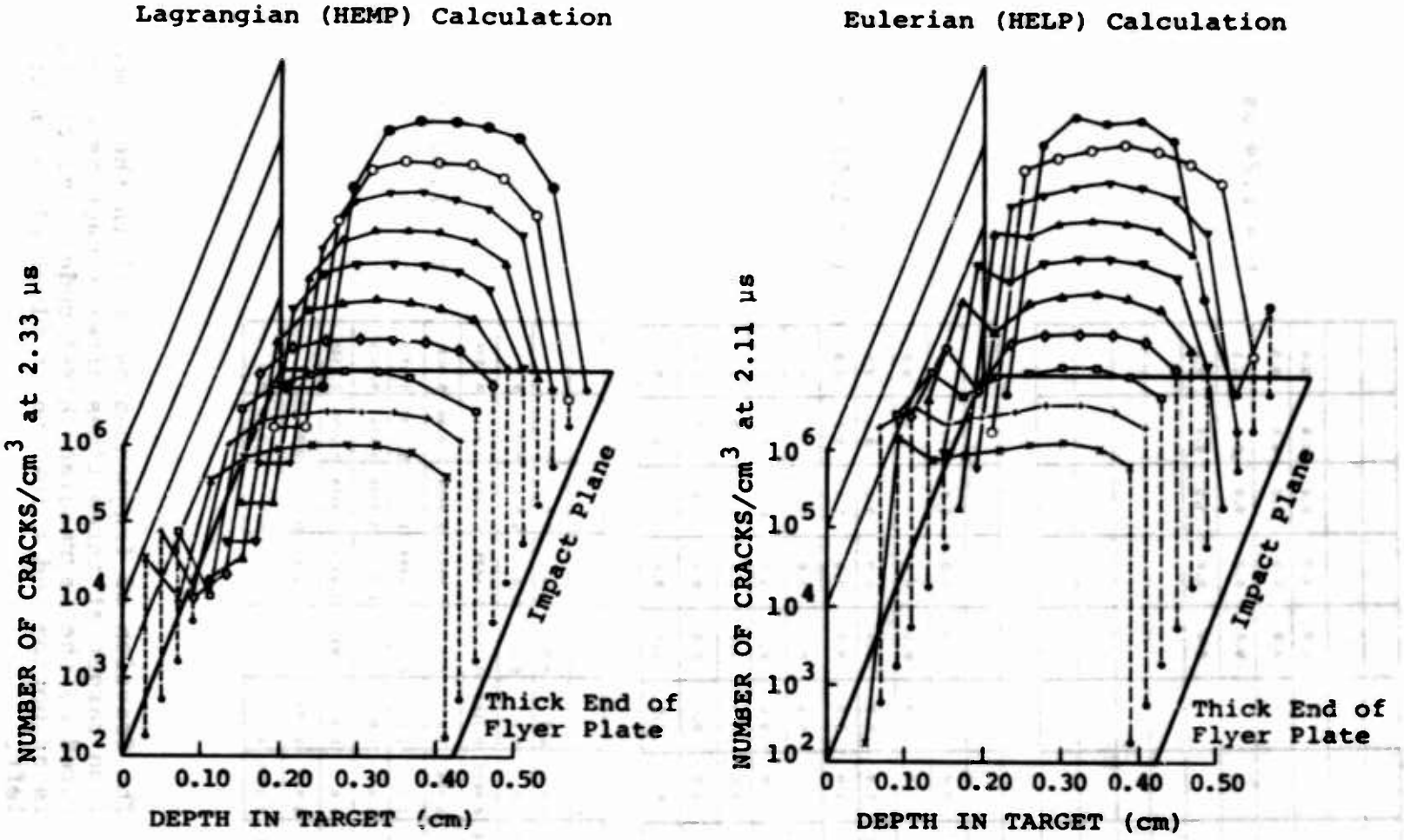

Figure 5.15. Number of cracks per cm^3 in the Armco iron target as computed by the Lagrangian (HEMP) code at 2.33 µs and by the Eulerian (HELP) code at 2.11 µs. (Dashed lines show the projection of the nonzero values of the leftmost and rightmost positions onto the reference plane.)

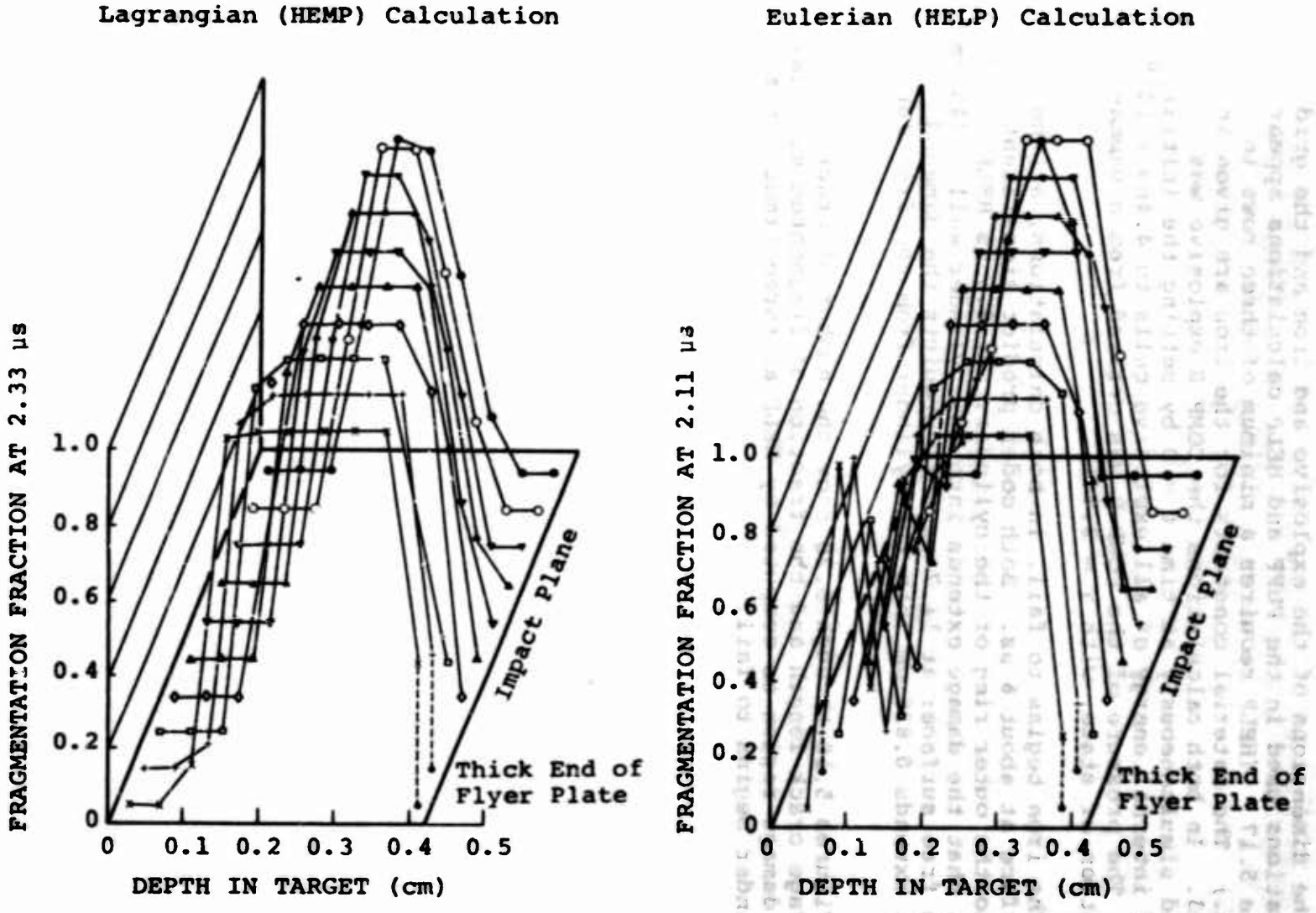

Figure 5.16. Fraction of fragmented material in the Armco iron target as computed by the Lagrangian (HEMP) code at 2.33 μs and by the Eulerian (HELP) code at 2.11 μs. (Dashed lines show the projection of the nonzero values of the leftmost and rightmost positions onto the reference plane.)

The dimensions of the explosive and iron and the grid configurations used in the PUFF and HELP calculations appear in Figure 5.17 (HELP requires a minimum of three rows in the grid.) The material constants for the iron are given in Table 5.3. In both calculations the COMP B explosive was detonated simultaneously at time t = 0 by setting the initial specific internal energy of all explosive cells to 4.469×10^{10} ergs/g. The pressure of the COMP B was derived from a gamma-law equation of state, with $\gamma = 2.841$.

The iron begins to fail, in both calculations, at the free surface at about 6 μs. Both codes predict significant damage to the outer ring of the cylinder. At 9.6 μs HELP predicts that the damage extends into the cylinder wall 0.745 cm from the free surface; at 11.7 μs PUFF predicts the damaged material extends 0.826 cm into the cylinder from the free surface.

Figures 5.18 through 5.20 show the number of cracks, the average crack length and the fraction of fragmented material in each damage region as computed by HELP at three times after the cylinder begins to fail.

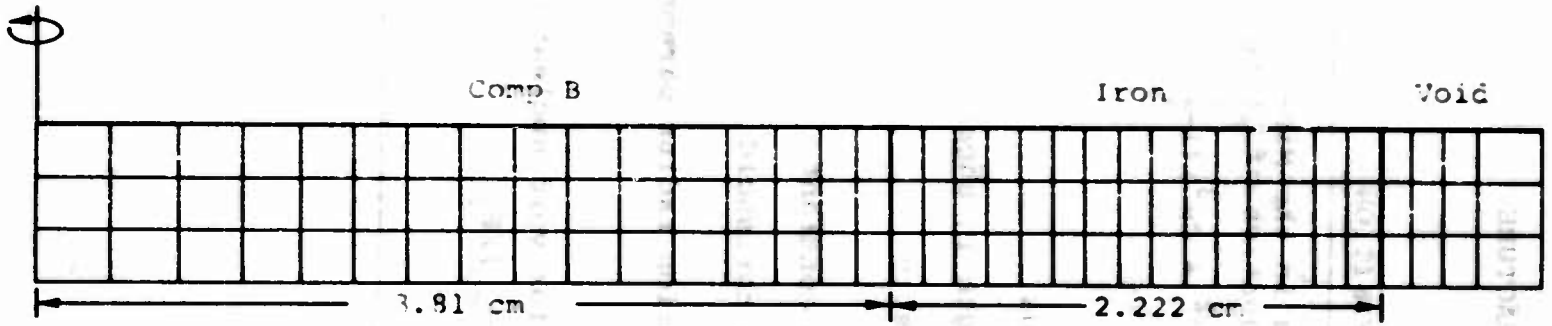

S Grid Configuration (HELP)

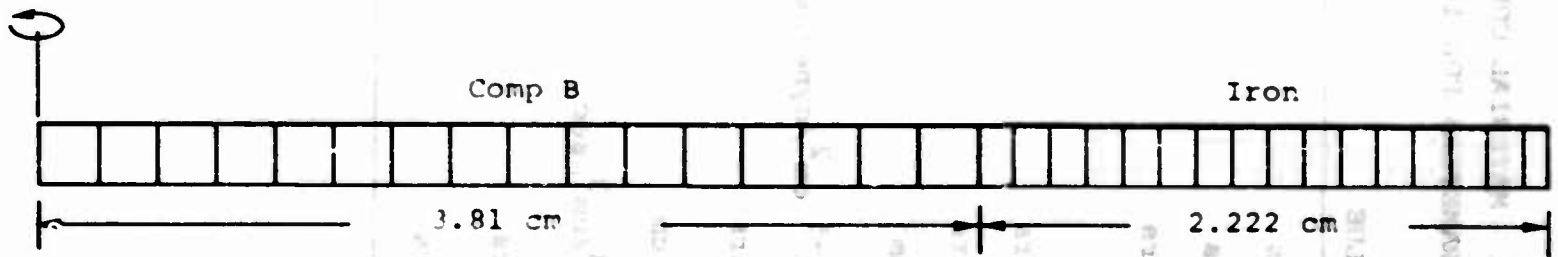

SRI Grid Configuration (PUFF)

Figure 5.17. Dimensions and grid configuration for the fragmenting round calculation.

TABLE 5.3. MATERIAL CONSTANTS AND FRACTURE PARAMETERS FOR IRON CYLINDER

SYMBOL	VALUE	DEFINITION
A	1589 kbars	Coefficients in the Mie-Gruneisen equation of state $P = (A\mu + B\mu^2 + C\mu^3)(1-\frac{\Gamma}{2}\mu)+\Gamma\rho E$ $\mu = (\rho/\rho_o - 1)$
B	5170 kbars	
C	51700 kbars	
Γ	1.69	
G	772.9 kbars	Shear modulus
Y	5.774 kbars	Yield strength in shear
ρ_o	7.85 gm/cm^3	Initial density
$\frac{3}{4\eta}$	-5.5×10^{-5} cm^2/dyne/sec	Void growth constant
P_{go}	-0.10 kbars	Void growth threshold
R_n	4×10^{-3} cm	Void nucleation radius parameter
$\dot{N}_o$	6.0×10^8/cm^3/sec	Parameters for void nucleation $\dot{N} = \dot{N}_o e^{(P-P_{no})/P_1}$
P_{no}	-9.0 kbars	
P_1	-1.3 kbars	

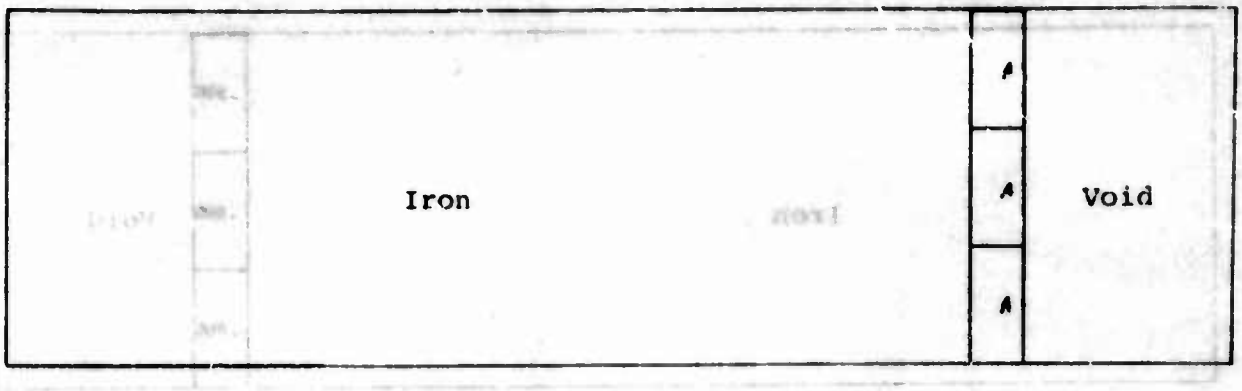

t = 6.2 μs

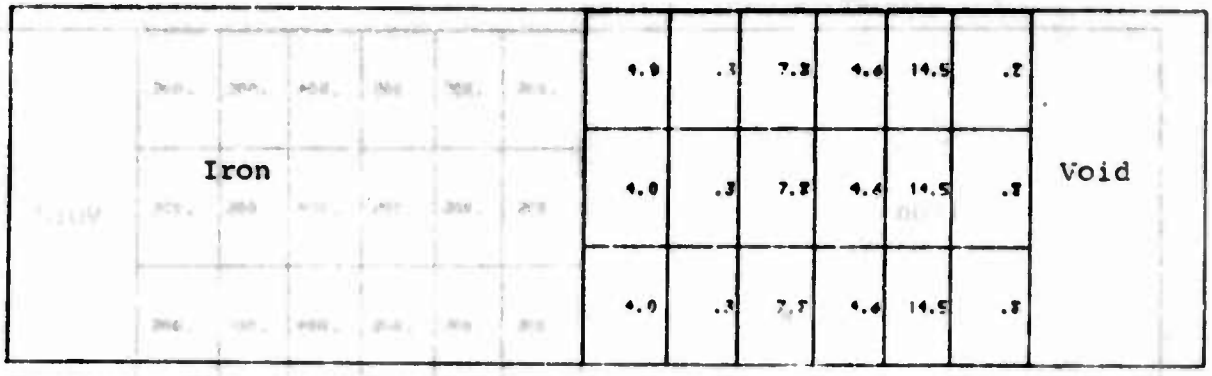

t = 7.9 μs

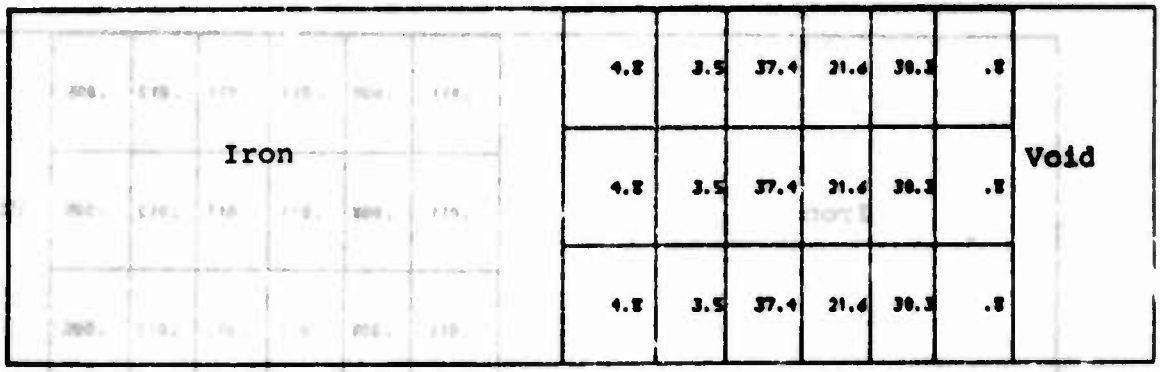

t = 9.6 μs

Figure 5.18. Number of cracks as computed by the HELP code at three different times after detonation in the 1-D fragmenting round calculation.

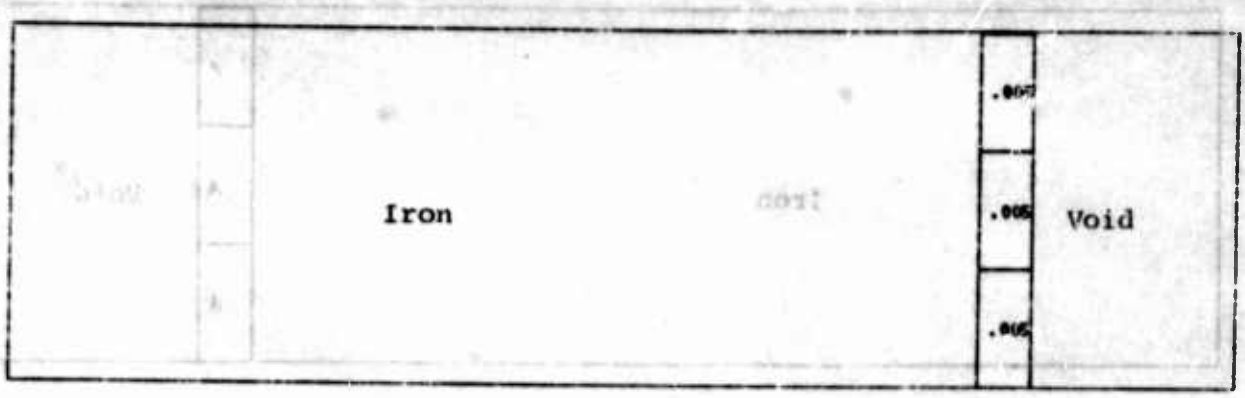

t = 6.2 μs

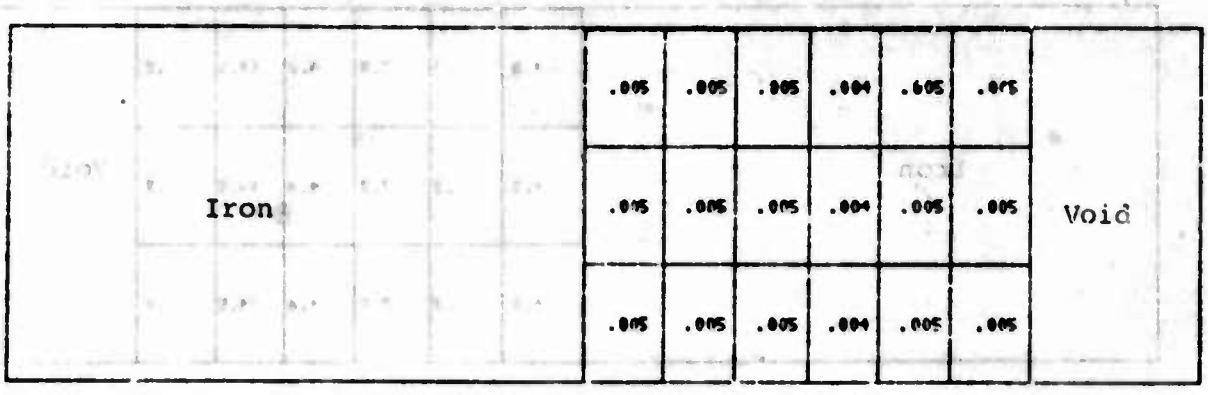

t = 7.9 μs

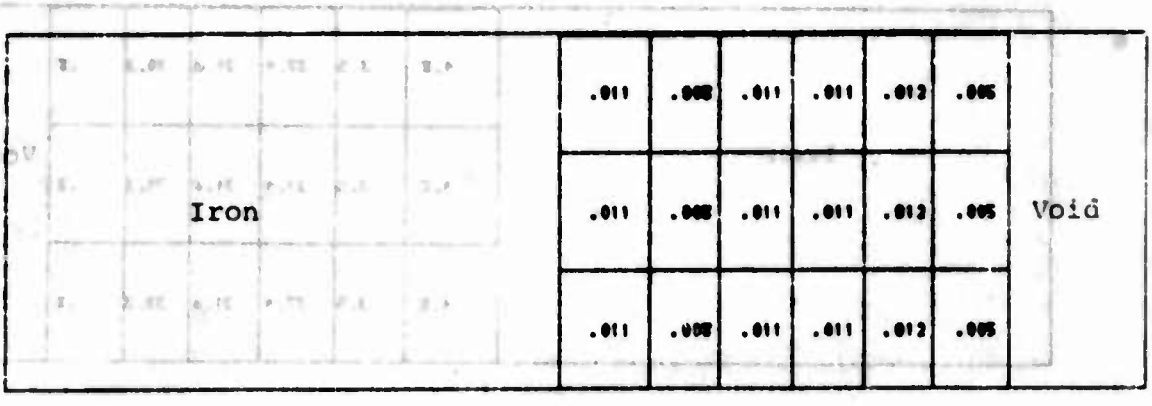

t = 9.6 μs

Figure 5.19. Average crack length as computed by the HELP code at three different times after detonation in the 1-D fragmenting round calculation.

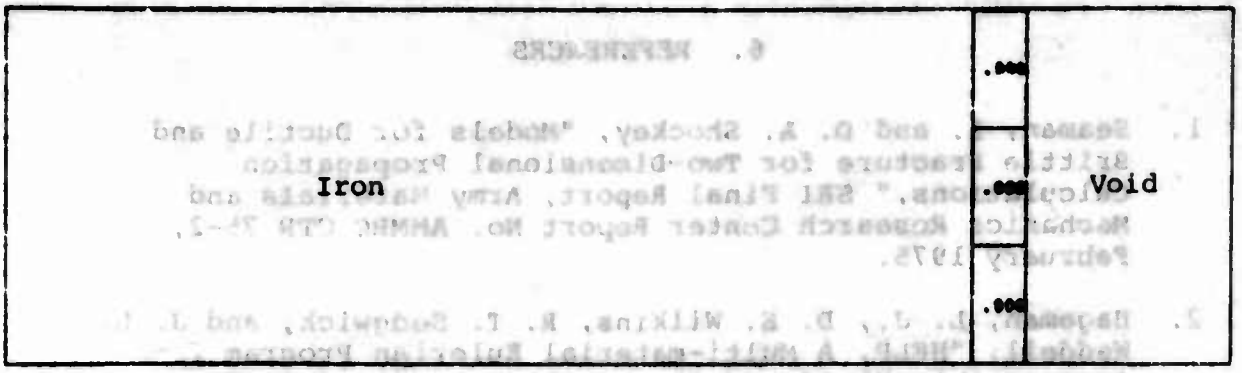

t = 6.2 μs

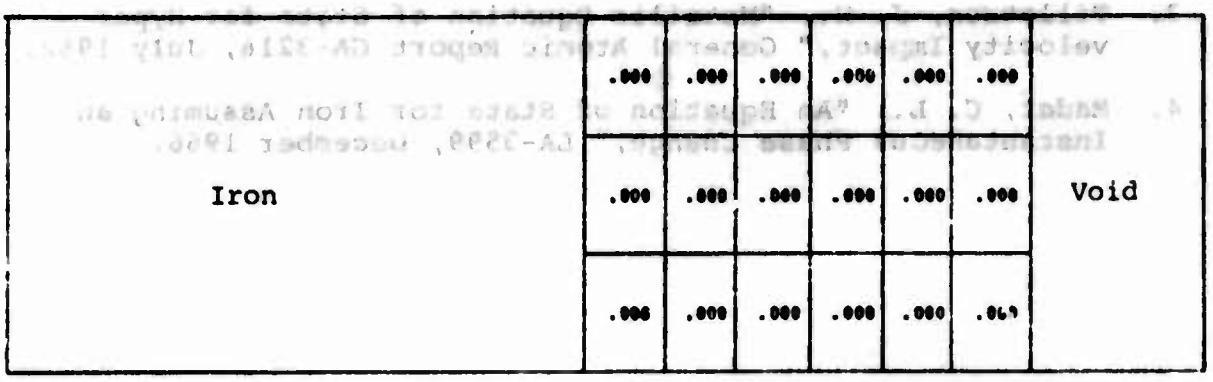

t = 7.9 μs

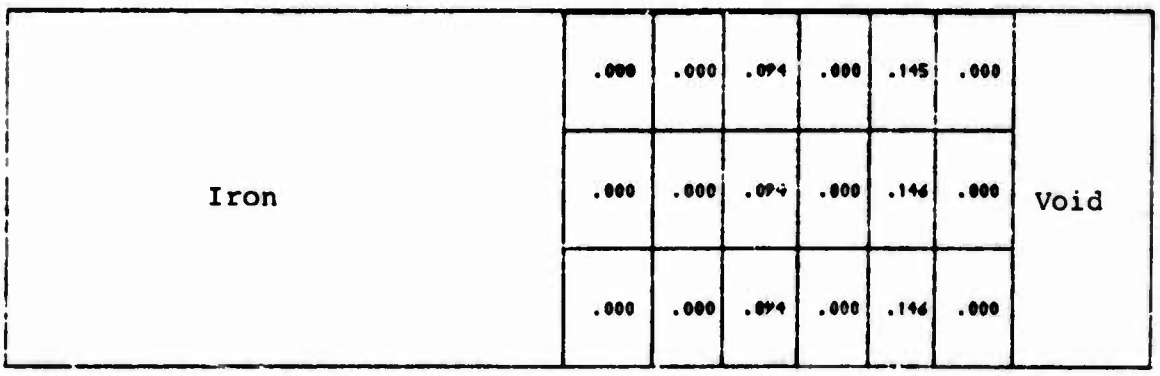

t = 9.6 μs

Figure 5.20. Fragmentation fraction as computed by the HELP code at three different times after detonation in the 1-D fragmenting round calculation.

6. REFERENCES

1. Seaman, L. and D. A. Shockey, "Models for Ductile and Brittle Fracture for Two-Dimensional Propagation Calculations," SRI Final Report, Army Materials and Mechanics Research Center Report No. AMMRC CTR 75-2, February 1975.

2. Hageman, L. J., D. E. Wilkins, R. T. Sedgwick, and J. L. Waddell, "HELP, A Multi-material Eulerian Program for Compressible Fluid and Elastic-Plastic Flows in Two Space Dimensions and Time," Systems, Science and Software, July 1975.

3. Tillotson, J. H., "Metallic Equation of State for Hypervelocity Impact," General Atomic Report GA-3216, July 1962.

4. Mader, C. L., "An Equation of State for Iron Assuming an Instantaneous Phase Change," LA-3599, December 1966.

APPENDIX A
USER'S GUIDE TO THE VERSION OF HELP WHICH EMPLOYS THE NAG-FRAG FAILURE MODEL

The documentation presented in this Appendix serves as a supplement to the 1975 documentation of the HELP code (Reference 2). Diagrams representing the organizational modifications as well as descriptions of new subroutines and new input variables are presented in the sections that follow. Additionally, this writeup provides an algorithm for estimating the core storage requirements of a given configuration.

A.1 ORGANIZATION MODIFICATIONS TO THE HELP CODE

The motivation for reorganizing parts of the HELP code has been given in Section 3 of this report. As indicated there, the division into three phases, a hydrodynamic phase, a strength phase, and a transport phase has been reduced to two phases by combining the effects of t cell pressures and the cell deviator stresses. Also, the Eulerian cell stresses are modified to reflect the existence of damaged materials by a procedure which maps the stresses of the Lagrangian damage regions into the Eulerian grid. Finally, the transport phase, including the motion of the tracer particles, is executed in two directional passes. These modifications can be seen in Figure A.1 by comparing the flow diagram of the 1975 documented HELP code with the flow diagram of the present NAG-FRAG version.

A.2 NEW SUBROUTINES

In addition to the BFRACT and DFRACT subroutines provided by SRI, several additional subroutines were created to accomplish the modifications mentioned above as well as to generate and update Lagrangian damage regions. These added subroutines are listed in alphabetical order and briefly described in the paragraphs below. Detailed flow diagrams of SCALC, MIXDMR and PURDMR, the major routines which process the damage regions, appear in Figures A.2, A.3, and A.4.

ADJ1D (called from MIXDMR)

Subroutine ADJ1D is called in place of CALFRC, VOLFND and INTSAV in 1-D calculations (JMAX=3) to enlarge and reduce existing damage regions.

BFRACT (called from DAMAGE)

Subroutine BFRACT was provided by SRI to compute the pressure, deviatoric stresses and damage parameters of brittle materials that have satisfied the BFRACT failure condition. Chapter 2 of this report describes the BFRACT failure conditions as well as the algorithms for crack nucleation and growth.

1975 DOCUMENTED HELP

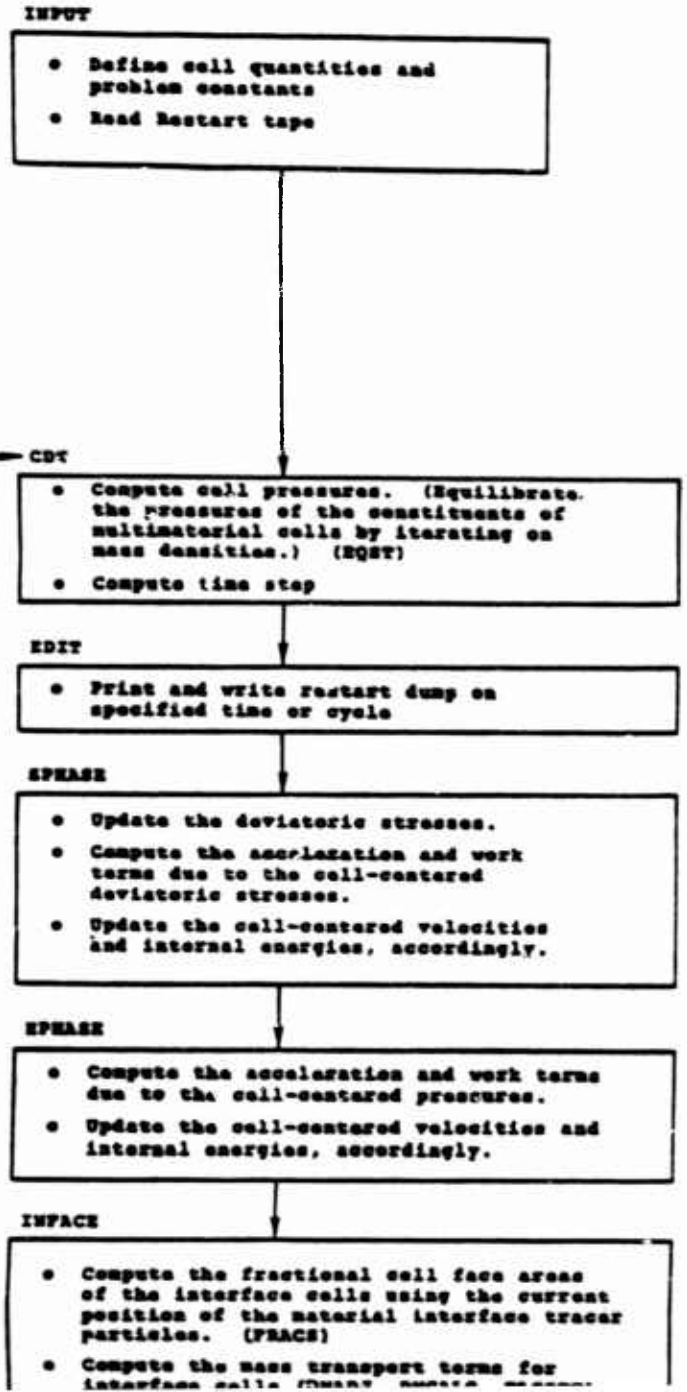

HELP WITH NAG-FRAG FAILURE MODEL

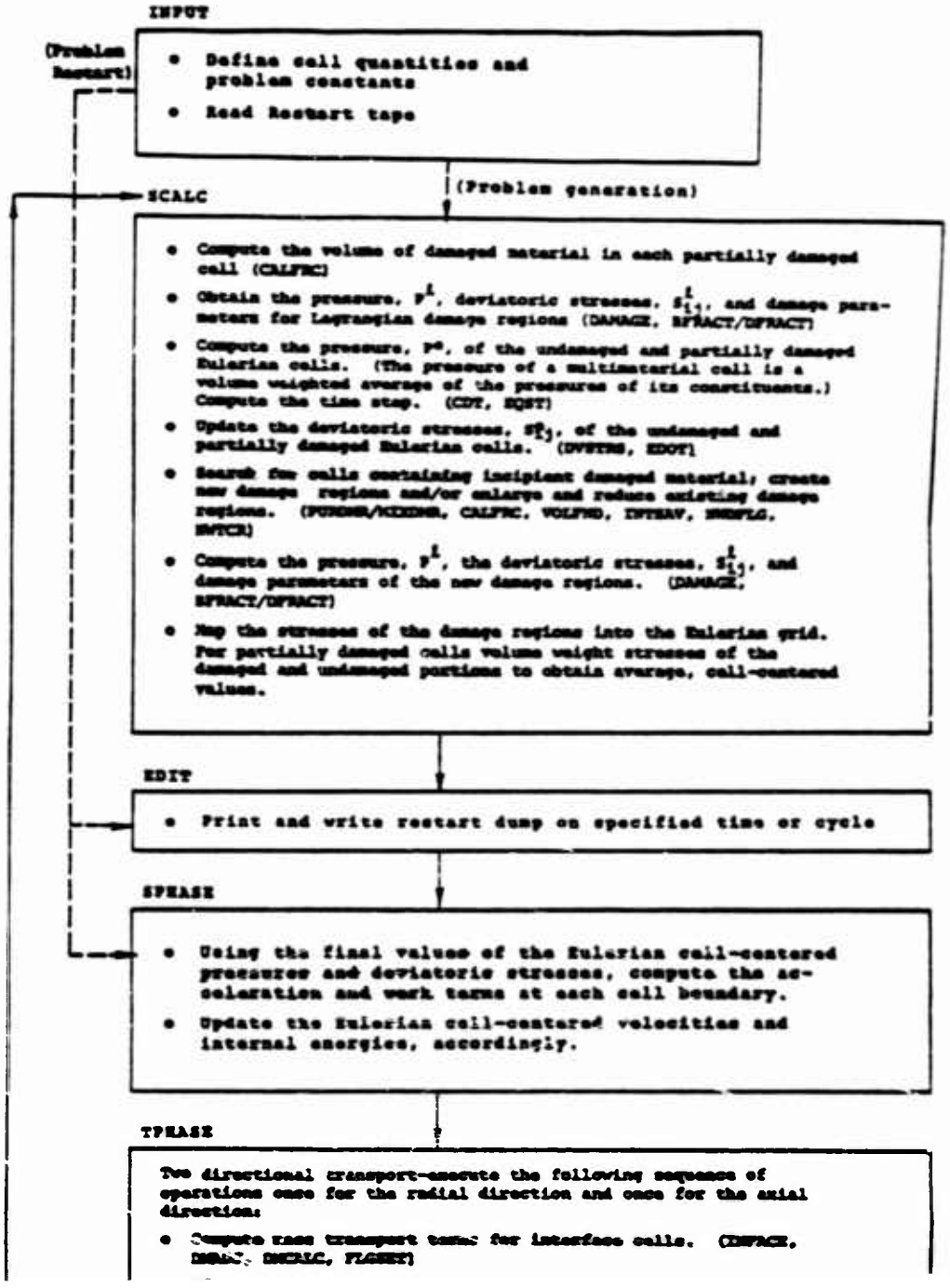

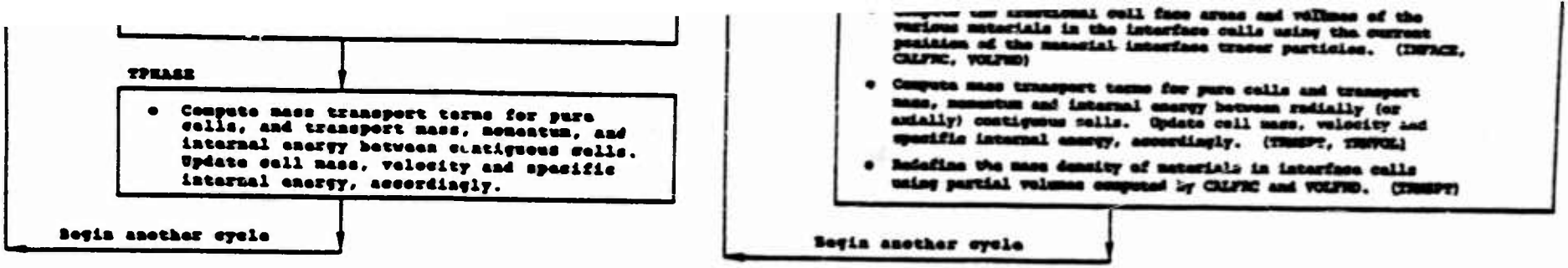

Figure A.1. Flow diagrams of the unmodified HELP code and the version of HELP in which the NAG-FRAG failure models have been incorporated.

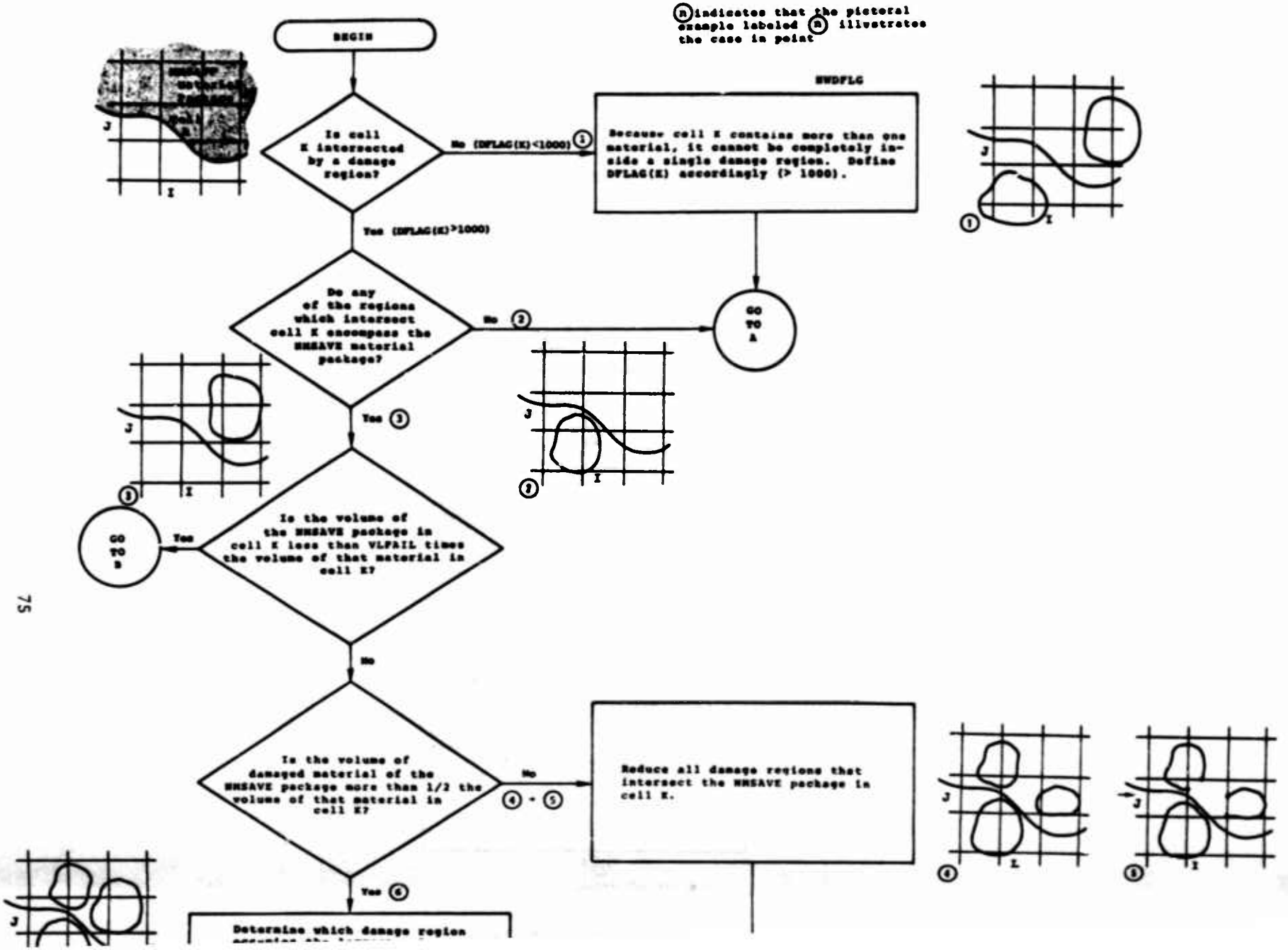
(n) indicates that the pictoral example labeled (n) illustrates the case in point
BEGIN
Is cell K intersected by a damage region?
No (DFLAG(K)<1000) (1)
Because cell K contains more than one material, it cannot be completely inside a single damage region. Define DFLAG(K) accordingly (> 1000).
NWDFLG
Yes (DFLAG(K)>1000)
Do any of the regions which intersect cell K encompass the NMSAVE material package?
No (2)
GO TO A
Yes (3)
Is the volume of the NMSAVE package in cell K less than VLFAIL times the volume of that material in cell K?
Yes
GO TO B
No
Is the volume of damaged material of the NMSAVE package more than 1/2 the volume of that material in cell K?
No (4) - (5)
Reduce all damage regions that intersect the NMSAVE package in cell K.
Yes (6)
Determine which damage region

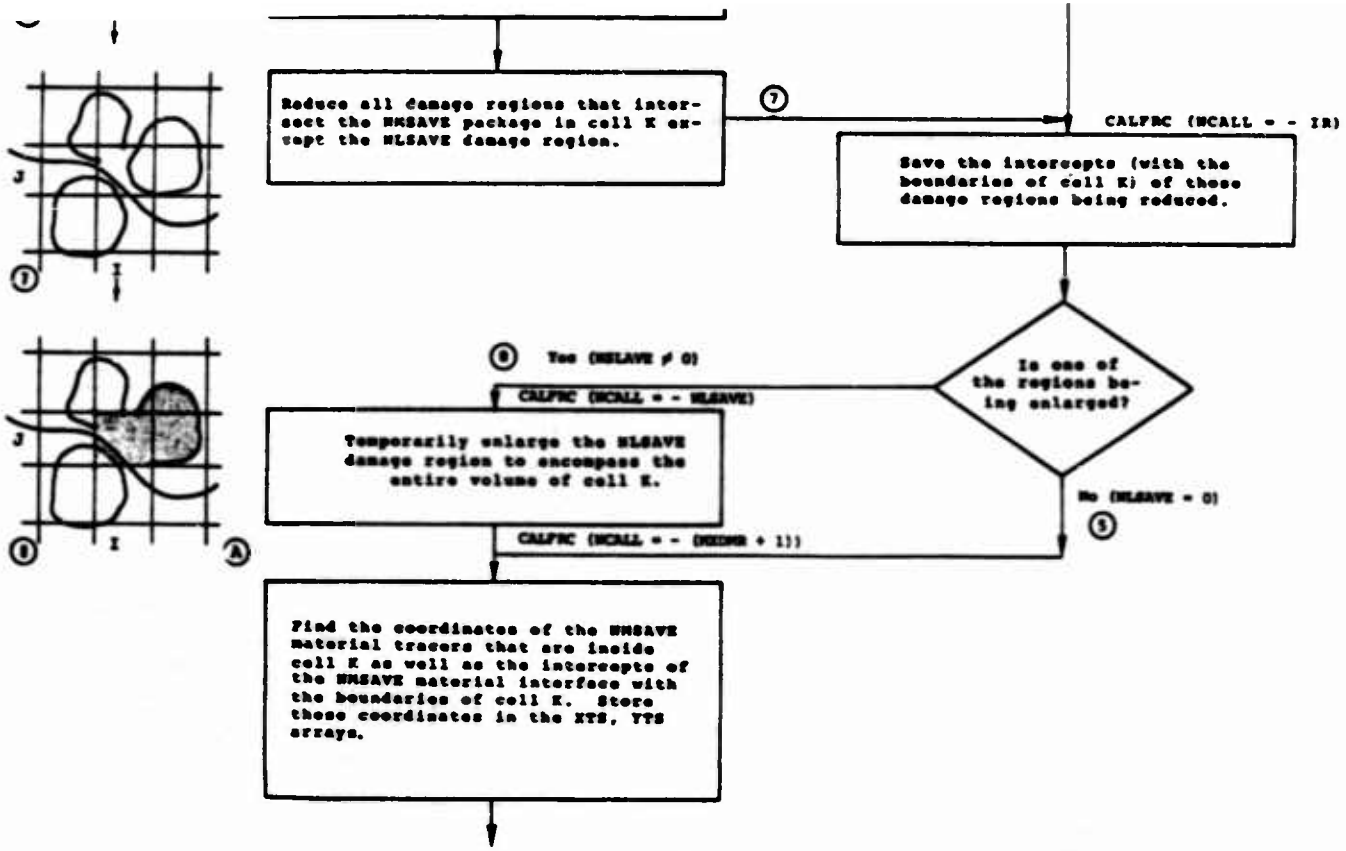

Figure A.2. Block diagram of subroutine MIXDMR. (NOTE: I, J, K, NMSAVE are blank common variables defined in SCALC.)

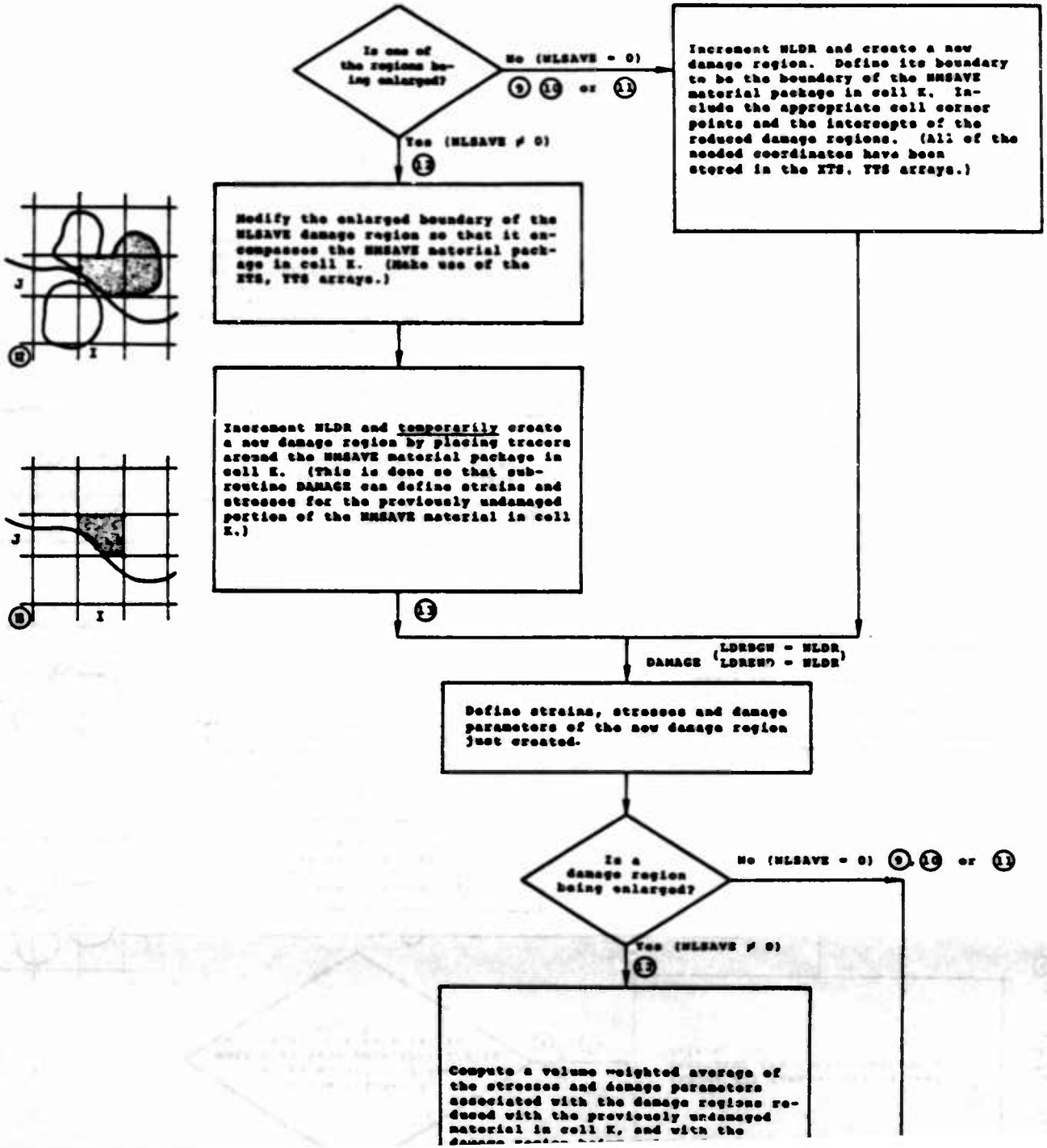
Is one of the regions being enlarged?
No (NLSAVE = 0)
9 10 or 11
Yes (NLSAVE ≠ 0)
12
Increment NLDR and create a new damage region. Define its boundary to be the boundary of the NMSAVE material package in cell K. Include the appropriate cell corner points and the intercepts of the reduced damage regions. (All of the needed coordinates have been stored in the XTS, YTS arrays.)
Modify the enlarged boundary of the NLSAVE damage region so that it encompasses the NMSAVE material package in cell K. (Make use of the XTS, YTS arrays.)
Increment NLDR and temporarily create a new damage region by placing tracers around the NMSAVE material package in cell K. (This is done so that subroutine DAMAGE can define strains and stresses for the previously undamaged portion of the NMSAVE material in cell K.)
13
DAMAGE (LDRBGN = NLDR, LDREND = NLDR)
Define strains, stresses and damage parameters of the new damage region just created.
Is a damage region being enlarged?
No (NLSAVE = 0) 9 10 or 11
Yes (NLSAVE ≠ 0)
12
Compute a volume weighted average of the stresses and damage parameters associated with the damage regions reduced with the previously undamaged material in cell K, and with the
J
I
or

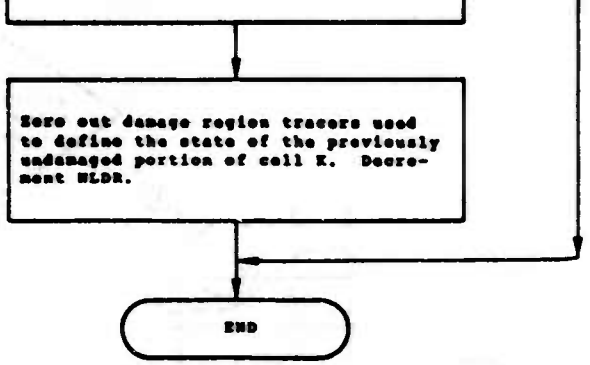

Figure A.2 (continued)

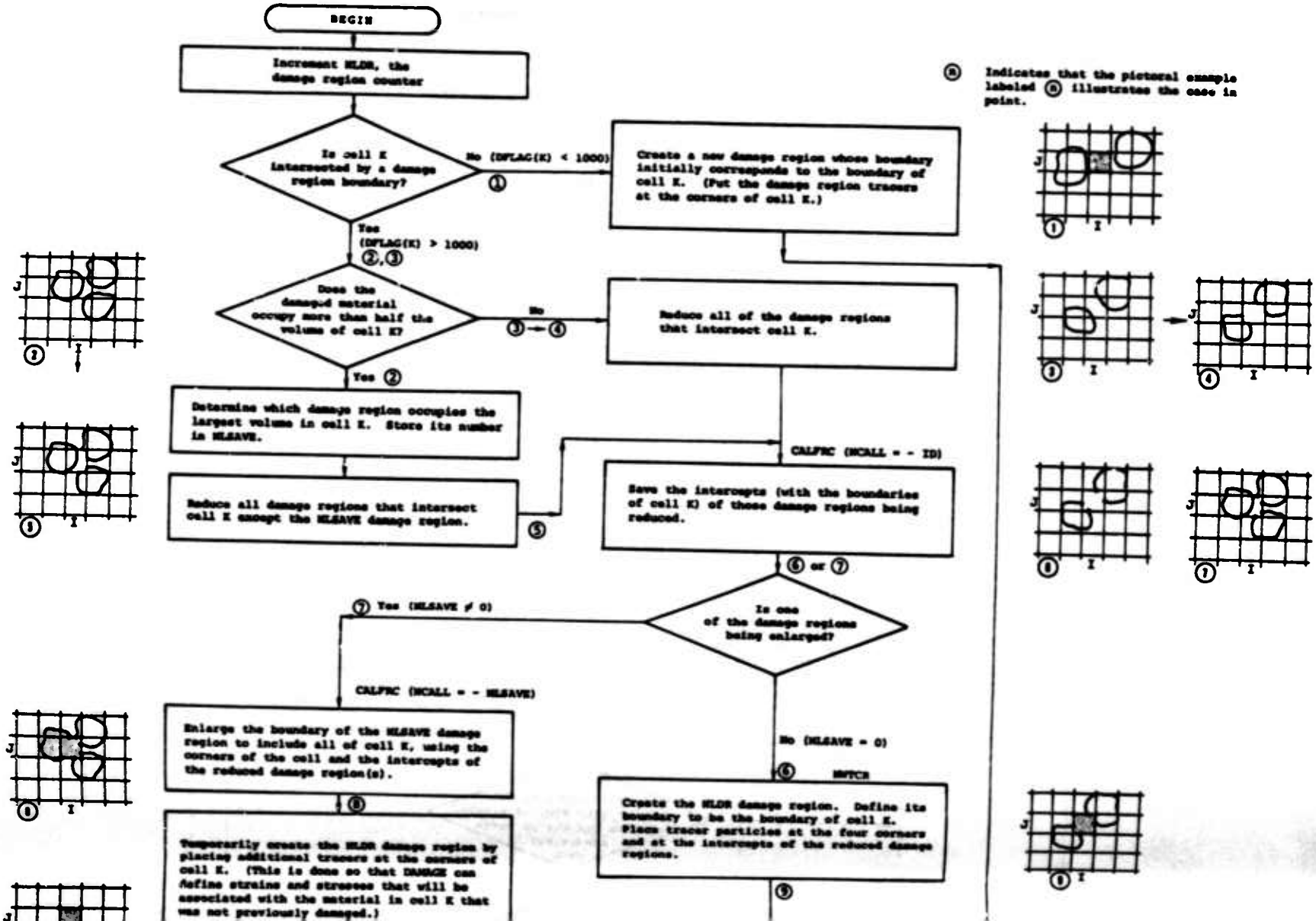
BEGIN
Increment NLDR, the damage region counter
Is cell K intersected by a damage region boundary?
No (DFLAG(K) < 1000) ①
Yes (DFLAG(K) > 1000) ②,③
Create a new damage region whose boundary initially corresponds to the boundary of cell K. (Put the damage region tracers at the corners of cell K.)
Does the damaged material occupy more than half the volume of cell K?
No ③→④
Yes ②
Reduce all of the damage regions that intersect cell K.
Determine which damage region occupies the largest volume in cell K. Store its number in NLSAVE.
Reduce all damage regions that intersect cell K except the NLSAVE damage region. ⑤
CALFRC (NCALL = - ID)
Save the intercepts (with the boundaries of cell K) of those damage regions being reduced.
⑥ or ⑦
Is one of the damage regions being enlarged?
⑦ Yes (NLSAVE ≠ 0)
CALFRC (NCALL = - NLSAVE)
Enlarge the boundary of the NLSAVE damage region to include all of cell K, using the corners of the cell and the intercepts of the reduced damage region(s).
⑧
Temporarily create the NLDR damage region by placing additional tracers at the corners of cell K. (This is done so that DAMAGE can define strains and stresses that will be associated with the material in cell K that was not previously damaged.)
No (NLSAVE = 0) ⑥
NWTCR
Create the NLDR damage region. Define its boundary to be the boundary of cell K. Place tracer particles at the four corners and at the intercepts of the reduced damage regions.
⑨
Ⓡ Indicates that the pictorial example labeled Ⓡ illustrates the case in point.

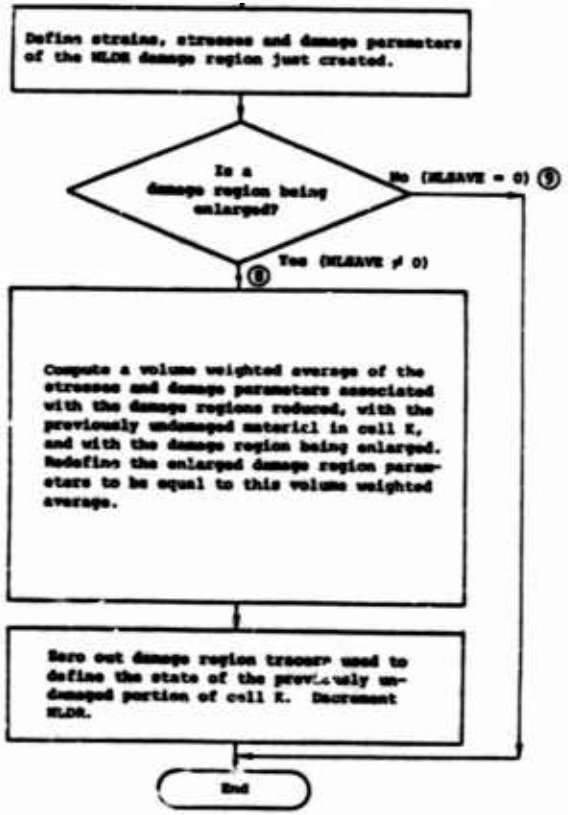

Figure A.3. Block diagram of subroutine PURDMR. (NOTE: I, J, K are blank common variables defined in SCALC.)

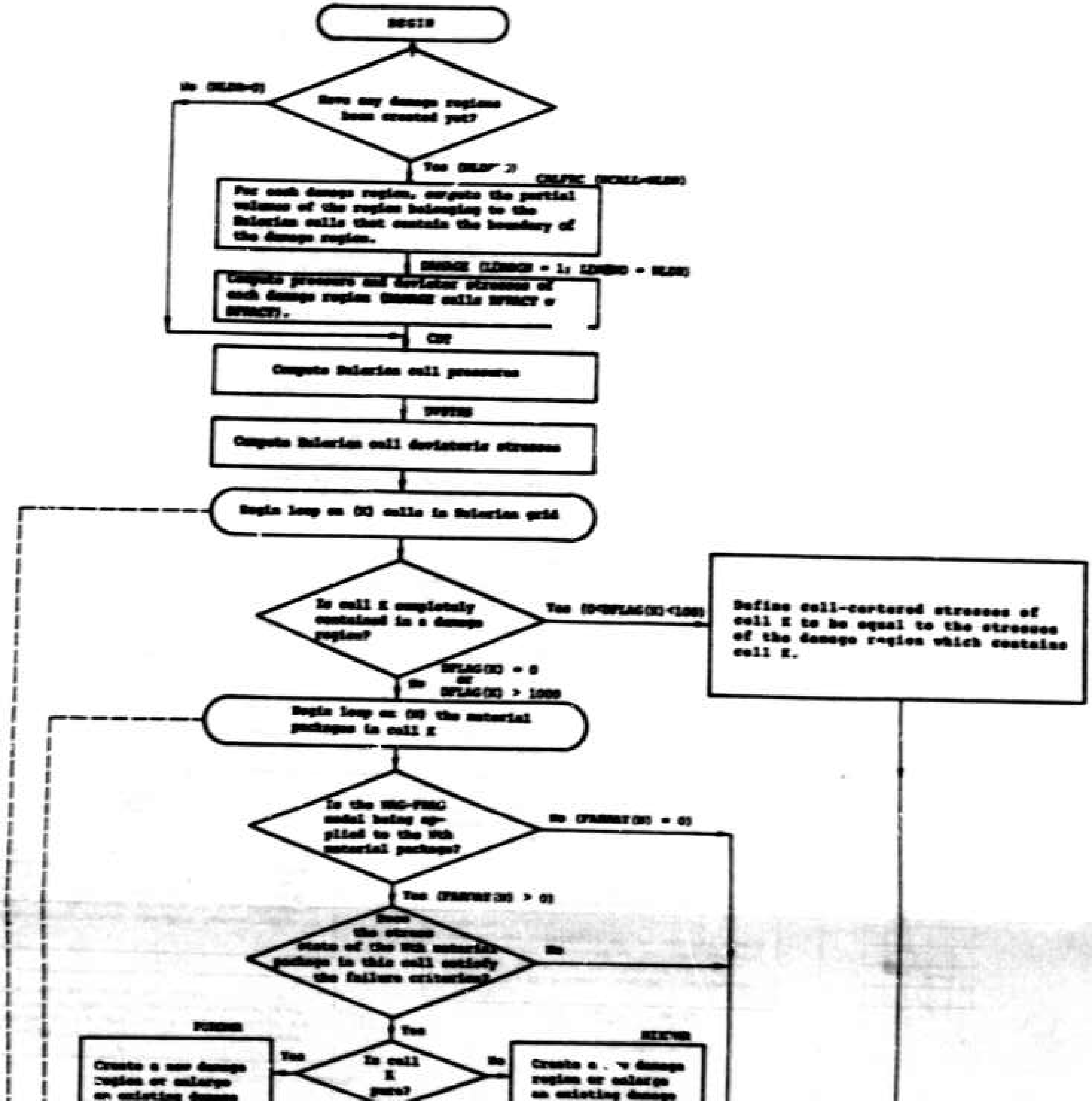
BEGIN
Have any damage regions been created yet?
For each damage region, compute the partial volumes of the region belonging to the Eulerian cells that contain the boundary of the damage region.
Compute Eulerian cell pressures
Compute Eulerian cell deviatoric stresses
Begin loop on (K) cells in Eulerian grid
Is cell K completely contained in a damage region?
Define cell-centered stresses of cell K to be equal to the stresses of the damage region which contains cell K.
Begin loop on (N) the material packages in cell K
Does the stress state of the Nth material package in this cell satisfy the failure criterion?
Is cell K pure?

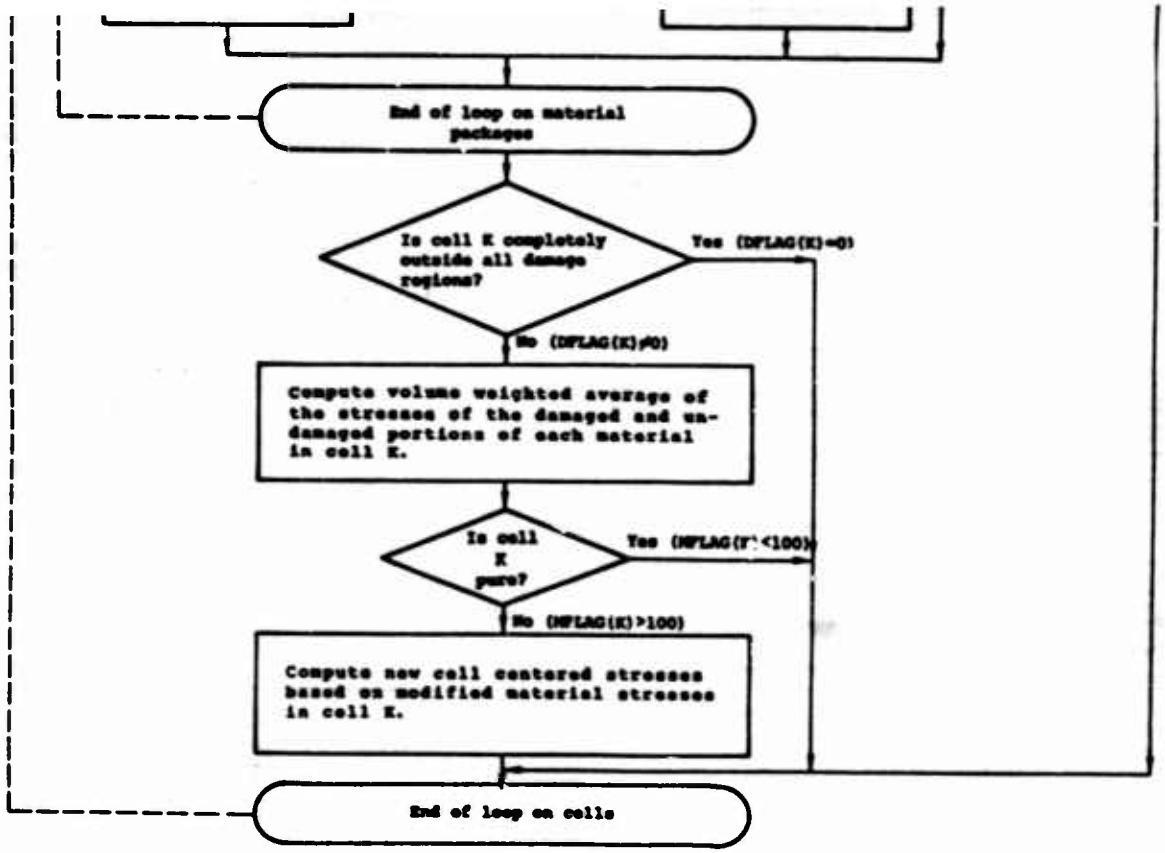

Figure A.4. Block diagram of subroutine SCALC.

DAMAGE (called from MIXDMR, PURDMR and SCALC)

This subroutine is called from SCALC each computational cycle (provided at least one damage region has been generated) to update the properties of all damaged material. It is also called from MIXDMR and PURDMR whenever a new damage region is created or an existing damage region is enlarged.

Subroutine DAMAGE computes the strain increments, a rotation increment, a new relative volume (or density) and an estimated new internal energy for the damage region(s). These quantities are used by the NAG-FRAG models to update the pressure, deviatoric stresses, number and size of voids or cracks and fragmentation data which are then mapped into the Eulerian grid.

DFRACT (called from DAMAGE)

Subroutine DFRACT was provided by SRI to compute the pressure, deviatoric stresses and damage parameters of ductile materials that have satisifed the DFRACT failure condition. Chapter 2 of this report describes the DFRACT failure condition as well as the algorithms for void nucleation and growth.

DVOL1D (called from CALFRC)

Subroutine DVOL1D is called instead of VOLFND in 1-D calculations (JMAX=3) to compute the volume of a cell that belongs to a given damage region.

DVSTRS (called from SCALC)

Subroutine DVSTRS updates the cell-centered deviatoric stresses of the pure Eulerian cells and the deviatoric stresses of each material in the multimaterial Eulerian cells. Basically, this subroutine replicates the first half of the SPHASE subroutine in the unmodified HELP code. However, unlike the earlier version of HELP, the deviatoric stresses of each constituent of a mixed cell are computed separately; (previously, the yield strengths and shear moduli of the constituents were averaged, and the same average stress state was associated with all of the materials in a mixed cell). A better definition of the stresses of the constituents in a mixed cell was necessitated by the separate application of the NAG-FRAG failure condition to each constituent of a mixed cell.

EDOT (called from DVSTRS)

Subroutine EDOT computes the spatial derivatives of the velocity field ($\frac{\partial u}{\partial x}$, $\frac{\partial v}{\partial y}$, $\frac{\partial u}{\partial y}$ and $\frac{\partial v}{\partial x}$) used in the computation of the deviatoric strain increments for a given pure cell or for one of the materials in a given multimaterial cell. Near the material interfaces, the difference equations are modified so that the derivatives are based only on the velocity field within the given material package, as illustrated below:

Pure cells:

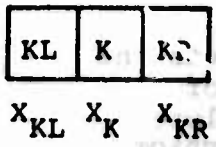

$$\left(\frac{\partial u}{\partial x}\right) = \frac{U_{KR}-U_{KL}}{X_{KR}-X_{KL}}$$

Interface cells:

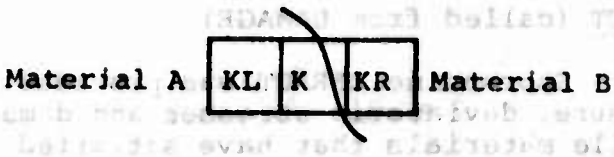

$$\left(\frac{\partial u}{\partial x}\right)_A = \frac{U_K^A-U_{KL}}{X_K-X_{KL}}$$

$$\left(\frac{\partial u}{\partial x}\right)_B = \frac{U_{KR}-U_K^B}{X_{KR}-X_K}$$

INTSAV (called from VOLFND and CALFRC)

Subroutine INTSAV is called when an existing damage region is being reduced or enlarged, i.e., when the undamaged material in a partially damaged cell has satisfied the failure criterion:

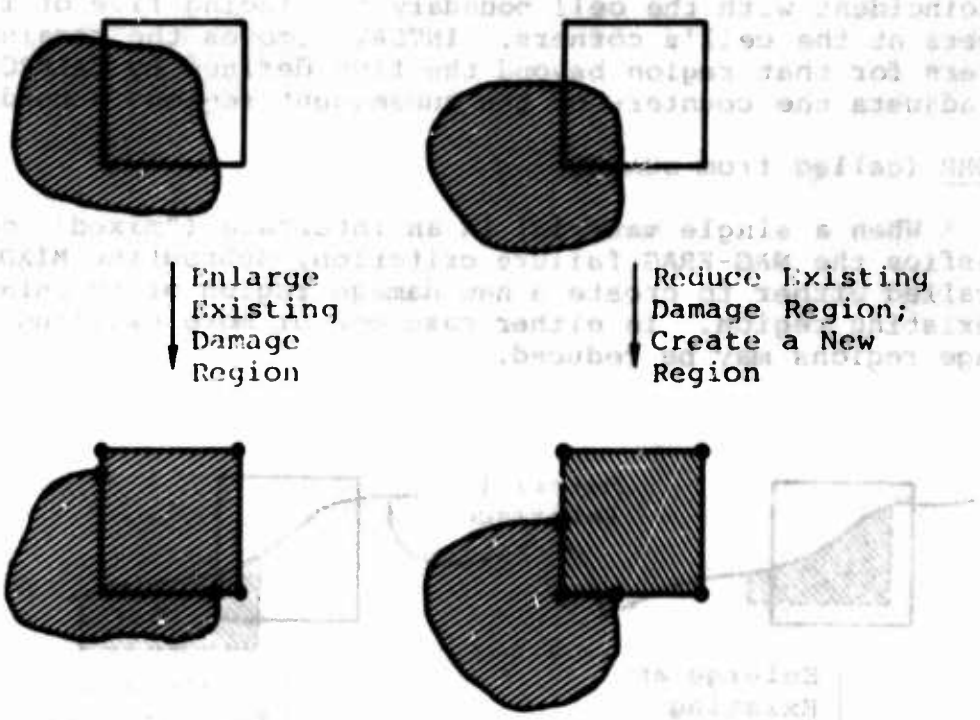

When a damage region is being either enlarged or reduced, INTSAV removes the damage tracers that are interior to the failed cell and adds the appropriate intercepts and corner points which have been defined by VOLFND and stored in the XT, YT arrays. The identification of the beginning and ending points (IBGN,IEND) of each subsequent damage region are adjusted to account for the tracers added and deleted in this process.

The intercepts of the reduced damage region with the failed cell are saved by subroutine INTSAV and added by subroutine NWTCR to the string of tracers defining the new damage region.

Finally, when a single material in an interface cell fails, subroutine INTSAV stores - in the XTS,YTS arrays - the material interface tracer coordinates and the included corner points as defined by VOLFND and CALFRC.

INTSAV is called from subroutine CALFRC only if the region being enlarged lies entirely inside the failed cell. In this case CALFRC defines the boundary of that region to

be coincident with the cell boundary by placing five of its tracers at the cell's corners. INTSAV removes the remaining tracers for that region beyond the five defined by CALFRC and adjusts the counters of the subsequent regions accordingly.

MIXDMR (called from SCALC)

When a single material in an interface ("mixed") cell satisfies the NAG-FRAG failure criterion, subroutine MIXDMR is called either to create a new damage region or to enlarge an existing region. In either case one or more existing damage regions may be reduced.

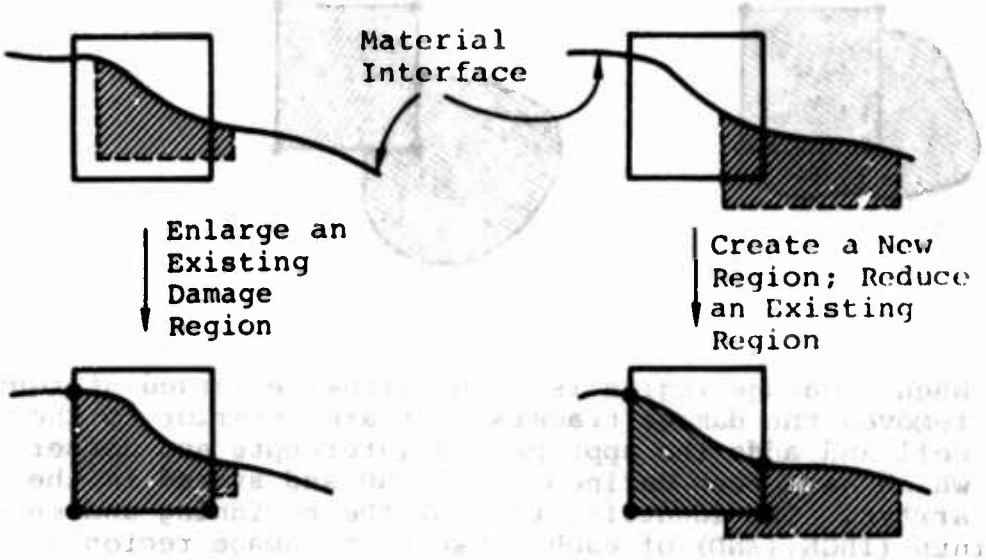

The enlargement or reduction of an existing damage region is accomplished by adding and/or deleting appropriate damage tracer particles, recomputing the region's volume and mass, and, in the case of enlargement, averaging the stresses and failure parameters of the added material with those of the region before it was enlarged.

The tracer strings of the modified regions are redefined by making use of the mechanisms of CALFRC and VOLFND to identify the intercepts of the damage region boundary with the boundaries of the cell and to identify which cell corners lie in the interior of the region. Subroutines CALFRC, VOLFND and INTSAV examine the value of the variable NCALL to discern whether the N^{th} region is being reduced or enlarged.

In MIXDMR a region is enlarged to encompass only a single material in a cell, i.e., not the whole cell. The procedure for doing so is broken down into two steps, each requiring a call to CALFRC and VOLFND. First, the damage tracers interior to the cell are removed and the cell corner points and intercepts, identified by CALFRC and VOLFND, are added by INTSAV as if the entire cell volume were being incorporated into the region. Next, a set of tracers which coincide with the interface tracers of the failed material that are interior to the cell and the intercepts of the material interface with the cell boundary are added to the tracer string and the exterior cell corner points are deleted. Again, the interior points, the intercepts and included corner points are defined by CALFRC and VOLFND.

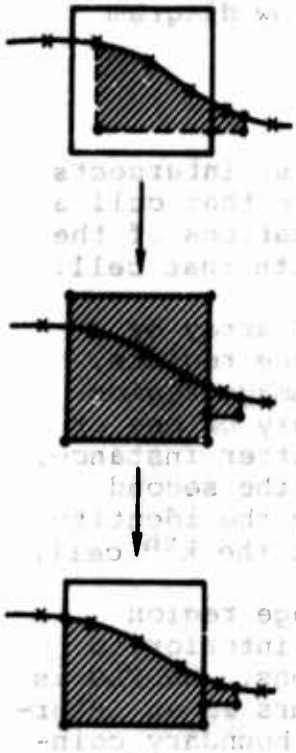

x Material Tracers

• Damage Tracers

STEP I

1. Interior damage tracers deleted.
2. Intercepts of damage region boundary and cell corner points added to encompass entire cell.

STEP II

1. Intercepts of material interface and duplicates of interior material tracers added.
2. Exterior cell corner points deleted.

The reduction of a damage region, on the other hand, is accomplished by a single call to CALFRC and VOLFND. The damage tracers interior to the failed cell are deleted and the intercepts and included corner points, as defined by CALFRC and VOLFND, are added.

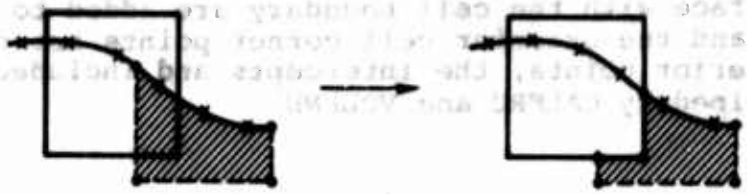

The steps outlined above are presented in greater detail in Figure A.2 which is an illustrated flow diagram of subroutine MIXDMR.

NWDFLG (called from VOLFND and MIXDMR)

When the boundary of a damage region first intersects a cell, subroutine NWDFLG is called to assign to that cell a unique value of DFLAG and to initialize the locations of the IDDR and DVOL arrays that will be associated with that cell.

The DFLAG array functions like the MFLAG array by identifying cells that are exterior to all damage regions, (DFLAG(k)=0), cells that are interior to N^{th} damage region (DFLAG(k)=N), and cells that contain the boundary of one or more damage regions (DFLAG(k)>1000). In the latter instance, the value of (DFLAG(k)-1000) is used to define the second index of the IDDR and DVOL arrays which specify the identity and volume of the damage regions that intersect the k^{th} cell.

NWDFLG is called from VOLFND when a damage region boundary moves into a cell that was previously interior to a single region or was outside all damage regions. NWDFLG is also called from MIXDMR when failure first occurs in an interface cell and a damage region is created whose boundary coincides with a material interface that intersects the cell.

NWTCR (called from PURDMR)

When a damage region is created from a pure cell that was partially contained in one or more damage regions that

are being reduced, the intercepts of those reduced regions with the cell's boundary are saved in the INTRCP array and added to the tracer string of the new region by subroutine NWTCR

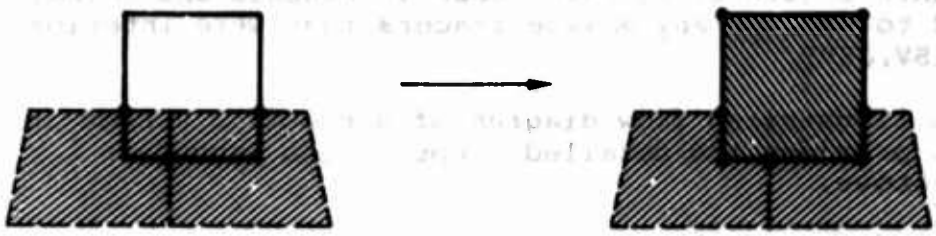

PURDMR (called from SCALC)

When the material in a pure cell that is not interior to an existing damage region satisfies the NAG-FRAG failure criterion, subroutine PURDMR is called either to create a new damage region or to enlarge an existing region. In either case one or more existing damage regions may be reduced.

If the cell is not already intersected by a damage region, PURDMR simply places tracers for the new region at the four corners of the cell and calls DAMAGE to define the stresses and damage parameters of the newly failed material.

If less than half of the cell is already contained in one or more damage regions, these regions are reduced and the tracer string which defines the new damage region contains the intercepts of the reduced regions as well as the four corner points of the cell (see NWTCR).

If more than half of the cell already belongs to one or more existing damage regions, then the region which encompasses the largest part of the cell is enlarged to include all of the cell and the other regions, if there are any, are reduced.

Region N is reduced by CALFRC, VOLFND and INTSAV when NCALL = -N and N ≠ NLSAVE (NLSAVE is the number of the region being enlarged). CALFRC and VOLFND compute the intercepts of the N^{th} region with the cell boundary and determine which, if any, corner points lie between the entering and existing sides. INTSAV adds these intercepts and corner points to the string of tracers of the reduced region while it deletes the damage tracers that were interior to the cell. PURDMR redefines the mass of the reduced region.

To enlarge a region, PURDMR sets NCALL = -NLSAVE and calls CALFRC. The intercepts of the NLSAVE damage region with cell (ISV,JSV) are computed by CALFRC; VOLFND identified the included corner points. INTSAV redefines the tracer string of the NLSAVE region to include these intercepts and corner points and to exclude any damage tracers that were interior to cell (ISV,JSV).

The illustrated flow diagram of subroutine PURDMR in Figure A.3 provides the detailed steps in the procedure described above.

SCALC (called from HELP)

Subroutine SCALC first calls DAMAGE to update the stresses of the Lagrangian damage region. Thereafter SCALC is concerned with the computation of the Eulerian cell pressures and deviatoric stresses. Once the cell stresses are updated by CDT and DVSTRS, the NAG-FRAG failure criterion is applied to those cells containing undamaged material. When the stresses of one of these cells satisfies the failure criterion, SCALC calls either PURDMR or MIXDMR, depending on whether the newly failed material is in a pure or interface ("mixed") cell. PURDMR and MIXDMR in turn either create new damage regions or enlarge existing ones to encompass the newly damaged material.

After the new damage regions have been created and, in some cases, the existing ones modified, the stresses of the damage regions are mapped back into the Eulerian grid as described in Chapter 3.

A flow diagram of SCALC appears as Figure A.4.

TPHASE (called from HELP)

As part of the changes resulting from transporting material in two passes: first radial then axial, or vice versa, subroutine TPHASE was created to call the transport routines, INFACE and TRNSPT for each pass and to set the flag which indicates the direction of the pass. TPHASE alternates the order of the passes each cycle: on odd numbered cycles the first pass is in the axial direction; whereas, on even numbered cycles the first pass is in the radial direction.

(NOTE: the TPHASE subroutine in the documented code was renamed TRNSPT in the NAG-FRAG version.)

TRNVOL (called from TRNSPT)

The volume of material to be transported in one direction (radial or axial) across the boundary between two pure

cells is computed by subroutine TRNVOL. As described in Section 3.2.1 the volume is based on the velocity at three positions, two on the cell edges parallel to the direction of the transport, and one at the cell center. (See Section 3.2.1.)

TRVOLI (called from DMCALC)

Subroutine TRVOLI performs the same function a subroutine TRNVOL, except one or both of the two cells is an interface cell. (See Section 3.2.1.)

A.3 MODIFICATION OF EXISTING HELP SUBROUTINES

Major modifications were made to several of the existing HELP subroutines in order to make available information required by the NAG-FRAG failure model and also to improve the synchronization of mass and tracer motion, the latter being necessitated by the mapping of the Lagrangian damage region stresses into the Eulerian grid. The modified subroutines are discussed below in alphabetical order.

CALFRC (called from INFACE, MIXDMR, PURDMR, SCALC, SETUPA)

In the documented version of HELP subroutine CALFRC is called only from SETUPA to generate the interface cells. (CALFRC together with VOLFND computes the volume of a given material in an interface cell as well as the fractional area of the right and top faces of the cell belonging to that material.)

In the present version CALFRC and VOLFND are used extensively during the calculation as well as in the problem generation. CALFRC is called at least once each cycle from INFACE to compute the partial volumes and fractional cell face areas of materials in interface (multimaterial and free surface) cells. The partial volumes are based on the position of the interface at the end of the time step. Thus these volumes, together with the mass of each material at the end of the time step (post-transport phase), determine the new densities of the materials in interface cells. (Previously, the new densities of materials in a multimaterial cell were determined in an iteration which equilibrated the materials' pressures; the densities of materials in a free surface cell were not changed from the original donor cell value unless the volume so defined exceeded the cell volume.)

Once at least one Lagrangian damage region has been created, CALFRC is called from SCALC, MIXDMR and/or PURDMR

to compute the volume of damaged material in cells containing the boundary of one or more damage regions and to compute appropriate intercepts and corner points for creating, reducing and enlarging the boundaries of existing damage regions. The desired function to be performed by CALFRC is indicated by the value of the blank common variable, NCALL, as discussed below.

NCALL = 0	Compute the partial volumes and fractional areas of materials in multimaterial cells (INFACE, SETUPA).
NCALL = NLDR	Compute the partial volumes of damage regions in cells containing damage region boundaries. (NLDR is the number of damage regions that have been created.) (SCALC).
NCALL = N (N≤MXDMR)	Compute the intercepts of the N^{th} damage region with cell ISV,JSV; the N^{th} damage region is being either reduced or enlarged. (MXDMR is the maximum number of damage regions that can be generated.) (MIXDMR, PURDMR).
NCALL = -(MXDMR+1)	Compute the intercepts of the NMSAVE material package boundary with cell ISV,JSV. Store the intercepts and included corner points in the XTS,YTS arrays. (NMSAVE is defined in SCALC)(MIXDMR)

When processing the damage region boundaries CALFRC examines the damage region tracer arrays, XP, YP, instead of the material interface tracer arrays, TX, TY. As indicated above, the value of NCALL instructs CALFRC as to which arrays to reference.

NCALL = 0 NCALL = -(MXDMR+1)	TX,TY	Material interface tracer arrays are referenced.
NCALL = ±N (0<N≤MXDMR)	XP,YP	Damage region tracer arrays are referenced.

When CALFRC is called to compute the volume of damaged material in the Eulerian cells intersected by damage region boundaries (NCALL = NLDR), the DFLAG array is redefined to reflect the new position of the damage region boundaries. For example, the DFLAG of those cells no longer intersected

by a damage region boundary is set to zero or to an integer, N,(≤NLDR) depending on whether the cell is currently outside all damage regions, or inside the N^{th} region.

CALFRC defines NTST and NTND which are passed to VOLFND, then INTSAV through an argument list when intercepts are added to the tracer string of a damage region. NTST and NTND identify the damage tracers after and before which the intercepts are to be added to the string.

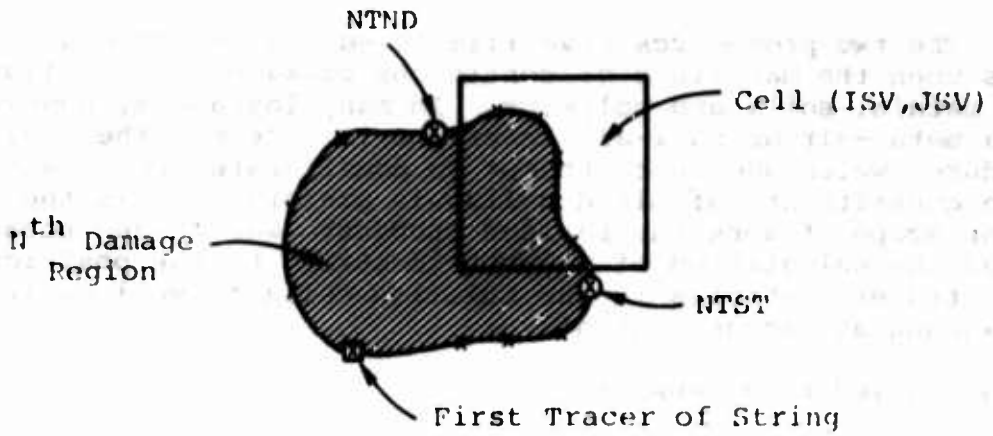

Before the string is altered, however, CALFRC insures that the beginning tracer of the string lies outside of cell(ISV, JSV) which is either being added to or subtracted from the N^{th} damage region.

CDT (called from SCALC)

In both versions of HELP subroutine CDT computes the pressures of the Eulerian cells, using the Tillotson equation of state (see subroutine EQST), and the time step for the current computational cycle using a Courant stability condition wherein the sound speed is estimated from the updated cell pressures. The difference in subroutine CDT in the two versions lies in its treatment of multimaterial and free surface cells.

In the NAG-FRAG version a pressure for each constituent of an interface cell is computed independently. The mass density of each constituent is derived from its current mass, M_i, and from the location of its interface in the cell. The interface, together with the boundaries of the cell, specifies the volume of the material V_i, and the density, ρ_i is simply

M_i/V_i. The pressure associated with the center of an interface cell is a volume weighted average of the pressures of the cell's constituents.

This procedure is very different from that employed in the documented version of HELP in which the position of the interface has no influence on the density assigned to the materials in a mixed cell. Instead the material densities as well as the cell pressure are uniquely determined in an iteration which adjusts the densities of the cell's constituents until the pressures of the materials are equilibrated.

The two procedures give rise to equivalent stress fields when the materials of contiguous packages are similar, e.g., metals, soils and polymers. In many instances, however, when a metal-air or soil-air interface is modeled, the revised procedure, which does not attempt to equilibrate the pressures of the constituents of mixed cells, is preferable. In the present scope of work the revised procedure was chosen because it tied the calculation of volumetric strain to the position of the tracer particles in the Eulerian cells as well as in the Lagrangian damage regions.

CMPRSN (called from SPHASE)

Subroutine CMPRSN calculates weighting factors that are applied to cell-centered stresses when the stresses at cell boundaries are being determined (in SPHASE). The weighting factors prevent cells having relatively small masses from being overaccelerated by more massive neighbor cells. If this situation occurs primarily at the free surface, it sufficies for the weighting factors to be "compression," i.e., the gross density of the cell divided by the reference density of the material. However, when a calculation involves large density discontinuities between material packages (e.g., metal-air interfaces) the "compression" weighting of cell stresses does not adequately prevent overacceleration of the less massive cells which contain normal density air.

CMPRSN has been modified so that the user can specify the gross density of a cell instead of its "compression" to be the weighting factor in the calculation of cell boundary stresses. An input variable, DENSWT, has been added to the Z-block. When DENSWT = 1.0, CMPRSN returns the gross density of the cell instead of its "compression."

DMADJ (called from INFACE)

The mass transport terms computed by DMCALC for interface cells are adjusted by subroutine DMADJ to prevent a cell

from being "overemptied" of a material and to exactly evacuate a material whose interface has just left a cell.

Because the mass transport is executed in two passes, the adjustment of the mass transport terms on the second pass must only affect the terms associated with the direction (axial or radial) of the second pass. Tests have been added to DMCALC to perform the appropriate adjustments depending on the pass number (NPS) and the direction of the pass (ID).

FLGSET (called from INFACE)

Subroutine FLGSET, which senses when a material interface leaves a cell and sets the appropriate flags for that material to be evacuated by DMADJ and in some cases for the cell to be again classified as "pure," has been rewritten so as to use the VOLM array to sense the presence or absence of a material interface in a given interface cell. The VOLM array, which stores the partial cell volume occupied by each material in an interface cell, was not computed in the documented version of the code, and FLGSET relied on values in the FRACRT and FRACTP arrays to determine whether or not an interface still cut across a given cell. By using the VOLM array, FLGSET has become a simpler and shorter subroutine.

FRACS

Subroutine FRACS has been removed. (See CALFRC, INFACE).

HELP (main driver of the HELP program)

The main driver routine of the HELP code has been modified as indicated in Figure A.1. Briefly, the changes reflect: (1) HPHASE has been combined with SPHASE; (2) a new subroutine, SCALC, controls the computation of the pressures, deviator stresses of the Eulerian cells as well as of the damage regions; and (3) the pressures are no longer recomputed when the calculation is restarted.

HPHASE

Subroutine HPHASE has been removed. The effects of cell pressures on cell energy and momentum are no longer accounted for in a separate computational phase of the cycle. The pressures are added to the normal deviator stresses in SPHASE and the effects of the total stress components are computed there. This change arose from the need to consider and modify both the pressures and the stress deviators of damaged material before either was used in the momentum and energy equations.

INFACE (called from TPHASE)

Subroutine INFACE is called twice each cycle from TPHASE, once for the radial pass and once for the axial pass. Because the transport phase has been split into two directional passes, it is less necessary to subcycle INFACE. Furthermore, it is no longer possible to subcycle INFACE without subcycling the entire transport phase of the cycle. Thus the subcycling loop has been removed from INFACE although the subcycling counters and flags have been retained.

The fractional volumes and cell face areas associated with the materials in interface cells are computed by CALFRC and VOLFND instead of by FRACS (subroutine FRACS has been removed from the program). INFACE calls CALFRC after the transport terms have been computed (DMCALC) and after the tracers have been moved (MOVTCR). Thus the fractional areas used to compute the transport terms are computed on the previous call to INFACE. On cycle zero the fractional areas and volumes are computed as the mixed cells are generated, i.e., when CALFRC is called from subroutine SETUPA.

INPUT (called from HELP)

The print statements and tape read statements in subroutine INPUT have been extended to include the damage parameters of the materials being modeled as well as the characteristics of the Lagrangian damage regions that have been created.

The mechanisms for sliplines and automatic grid rezoning have temporarily been deactivated by statements in INPUT which override the input values of the Z-block variables, NOSLIP, REZ, NUMREZ, IEXTX, and JEXTY.

MOVTCR (called from INFACE)

To better synchronize the tracer particle motion with the mass transport, the density weighting of cell velocities to arrive at tracer particle velocities was removed from subroutine MOVTCR. In addition, the logic of MOVTCR was altered slightly to accommodate the two directional subphases of the transport phase: MOVTCR is called twice each cycle and moves the tracers in only one direction.

SETUP (called from INPUT)

Subroutine SETUP reads input cards that define the TSR array for each material in the problem to which the NAG-FRAG failure model is to be applied. The parameters which govern the nucleation and growth of cracks (or voids) are stored in the TSR array. Only those materials whose code

numbers are 1 through 6 can utilize the NAG-FRAG routines because the first index of the TSR array, which identifies the material, is dimensioned six.

SPHASE (called from HELP)

The modified SPHASE subroutine is essentially the second half of the same routine in the documented version of HELP. The first half has been replaced by subroutine DVSTRS.

Two additional options have been added to SPHASE. First, the user can specify through a Z-block variable, DENSWT, whether the cell boundary stresses will be a density-weighted or "compression"-weighted average of the cell-centered stresses. Second, the user can activate the use of a linear and/or quadratic artificial viscosity when it is necessary to stabilize the stress field. The artificial viscosity terms are added to the cell boundary stresses.

In the present version, SPHASE computes the effects of the total stresses (pressure plus stress deviators) on cell momentum and energy; whereas, in the documented version SPHASE accounted only for the effects of the deviator stresses.

STRNG (called from DVSTRS)

Subroutine STRNG is called from DVSTRS to compute the shear yield strength of a given pure cell or of a given material in a mixed cell. Formerly, STRNG computed a volume weighted average yield strength for mixed cells, but this is no longer necessary in the current version, since the deviator stresses of each material in a mixed cell are computed independently. Similarly, STRNG no longer sets to zero the yield strength of materials in free surface cells. The void is accounted for in defining the cell-centered stress by volume weighting the stress deviators of the constituents, including the void.

TPHASE (called from HELP)

The subroutine called TPHASE in the documented version of HELP has been renamed TRNSPT. The new TPHASE routine is simply a driver routine which controls the two directional passes of the transport phase.

VOLFND (called from CALFRC)

Normally VOLFND computes the fractional cell face areas and fractional volume of a given material in a given interface cell. VOLFND takes the tracer particles that are

interior to the cell and the intercepts of the interface with the cell's boundaries (these are stored in the XT, YT arrays by CALFRC) and determines which corners of the cell are interior to the specified material package, thus creating a set of points which circumscribe the part of the material package that lies inside the cell in question.

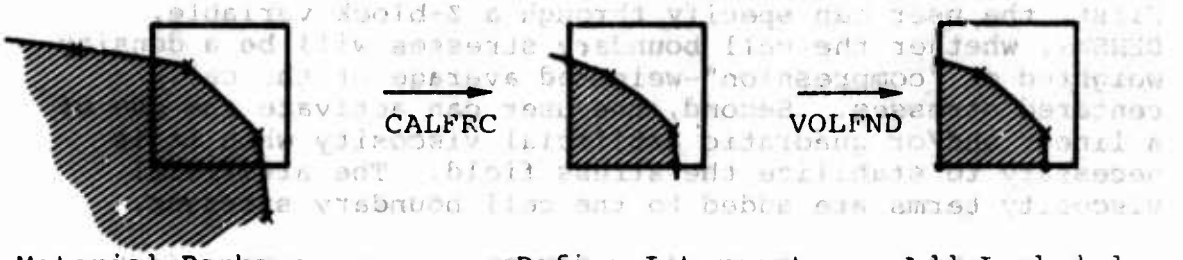

Material Package | Define Intercepts, Interior Points | Add Included Corners. Compute fractional cell face areas and volumes.

In the revised version of HELP these mechanisms are utilized by MIXDMR and PURDMR to modify existing damage regions to include or exclude portions of cells that have failed. They are also used to compute the volume of damaged material in those cells containing the boundary of one or more damage regions.

When VOLFND (which is always called from CALFRC) is being used to enlarge or reduce an existing damage region, it bypasses the calculation of fractional areas and volumes. After identifying the appropriate cell corner points and adding them to the XT, YT arrays, VOLFND calls subroutine INTSAV. Which corner points are chosen in these cases depends upon whether a region is being reduced or enlarged. When the damage region is being reduced the array of interior points and intercepts provided by CALFRC is unaltered and the same corner points are chosen by VOLFND as would be chosen if the points belonged to a materia interface rather than to a damage region boundary. On the other hand, when a region is being enlarged VOLFND reverses the order of the points provided by CALFRC and thereby chooses the other set of corner points.

The intercepts defined by CALFRC and the corner points defined by VOLFND are added to the damage region tracer strings by subroutine INTSAV.

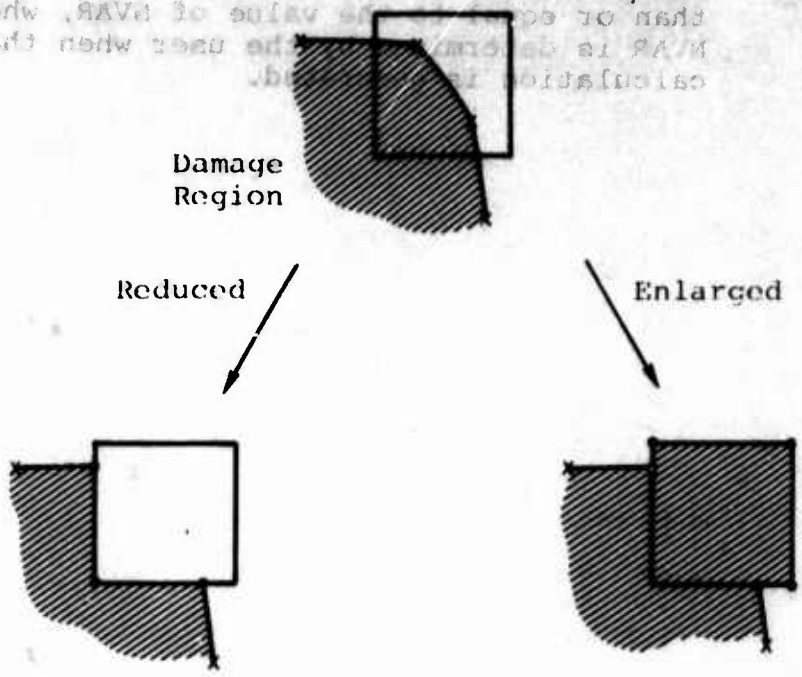

A.4 DICTIONARY OF NEW VARIABLES

A number of new blank common variables and new arrays have been added to HELP in the process of incorporating the NAG-FRAG subroutines for brittle and ductile failure. These new variables and arrays are defined below. The conventions used in describing the storage location of the variables is as follows:

(NAME)	The variable is local to subroutine NAME.
NAME	The variable is in common block NAME.
B.C.	The variable is in Blank Common or equivalenced to a variable in Blank Common.
=Z(N)	The variable is equivalenced to a member of the Z-array, the first array in Blank Common. Most of these variables are used in generating and restarting problems.
---	The variable is used as a calling argument.

In describing the dimensions of the variables the following conventions are used:

---	The variable is not dimensioned.
(30)	The array is always dimensioned 30.
(NVAR)	The dimension of the array must be greater than or equal to the value of NVAR, where NVAR is determined by the user when the calculation is generated.

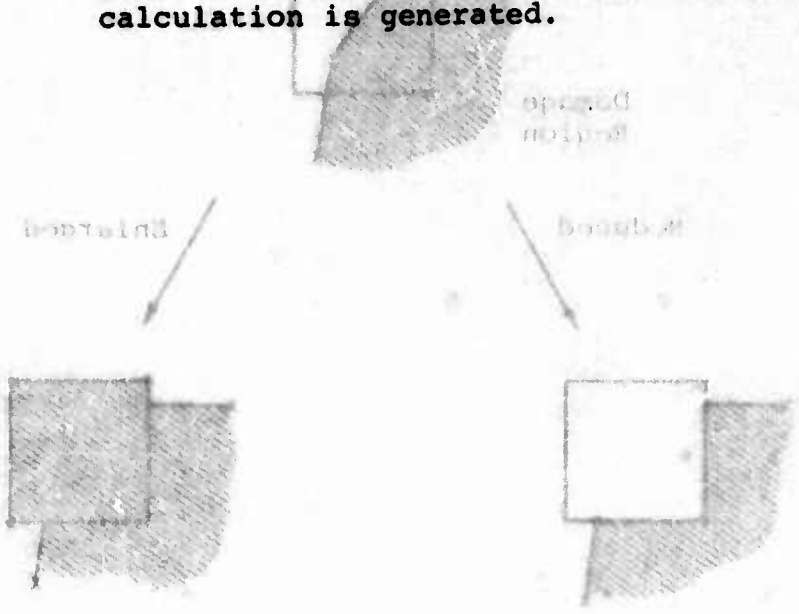

Variable Name	Location	Dimension of Array	Units	Definition
CL	PDMGE	(5,MXDMR)	cm^3	Cube of crack radius parameter for each of 5 bin angles.
CN	PDMGE	(5,MXDMR)	cm^3	Number of cracks per cm^3 for each of 5 bin angles.
CVISR	Z(126)	---	---	Flags for generating reflective-grid boundaries at right and top, respectively.
CVIST	Z(127)	---	---	
DENSWT	Z(60)	---	---	Flag for using density weighting rather than "compression" weighting when defining averaging cell boundary stresses.
DFLAG	B.C.	(KMAX)	---	Flag associated with each Eulerian cell which indicates whether the cell is undamaged (DFLAG(K)=0), is interior to a single damage region (DFLAG(K)≤NLDR), or contains the boundary of one or more damaged regions (NLDR>DFLAG>1000).
DRENG	PDMGE	(MXDMR)	ergs/g	The specific internal energy of the material in each damage region is stored in the DRENG array.
DRMASS	PDMGE	(MXDMR)	g	The mass of each damage region is stored in the DRMASS array.
DS	B.C.	(IJDX1,2) IJDX1= MAX(IMAX, JMAX)+1	cm	Equivalenced to DX and DY. Used in the double pass transport phase.
DSTLDR	PDMGE	(3,MXDMR)	dynes/cm^2	The stress deviators of the damage regions are stored in the DSTLDR array.

Variable Name	Location	Dimension of Array	Units	Definition
DVOL	PDMGE	(NLRMX, NPDCLS)	cm^3	The volume of material in an Eulerian cell belonging to a given damage region is stored in the DVOL array. (See IDDR.)
FARRAY	PDMGE	(NMAT)	---	The failure model to be applied to each material package in the problem is specified by the user-assigned value of the FARRAY for each package; e.g., for package N: FARRAY(N) = 0. Use simple volumetric failure criterion and zero out stresses in failed cells. FARRAY(N) = 1. Use DFRACT (ductile material). FARRAY(N) = 2. Use BFRACT (brittle material).
FMODEL	Z(128)	---	---	An input flag; when non-zero it indicates that one of the NAG-FRAG failure models is to be applied to at least one material package.
FRACBT	MXCELL	(NVOID, IMAX)	cm	The fractional area subtended by each material package interface on the bottom boundary of each cell in the bottom row of the grid.
IBGN	PDMGE	(MXDMR)	---	The beginning and ending index of the tracer coordinates (XP,YP) associated with a given damage region are stored in IBGN and IEND, respectively.
IEND	PDMGE	(MXDMR)	---	

Variable Name	Location	Dimension of Array	Units	Definition
ID	B.C.	---	---	The variable that indicates which direction the mass is being transported: ID = 1 radial ID = 2 axial
ID1	B.C.	---	---	The units on the DO-loops in TRNSPT which reflect the direction the mass is being transported.
ID2	B.C.	---	---	
ID3	B.C.	---	---	The complement of ID. When ID=1, then ID3=2 and vice versa.
IDDR	PDMGE	(NLRMX, NPDCLS)	---	The IDDR array identifies which damage regions intersect those cells that contain one or more damage region boundaries, e.g., if MD = DFLAG(K)-1000, then IDD = IDDR(N,MD) N=1,2..., and VL = DVOL(N,MD) NLRMX, where VL is the volume of cell K that is inside the damage region numbered IDD.
IGRP	B.C.	---	---	When a given material interface crosses a cell more than once, two or more non-contiguous regions inside the cell belong to that material. The number of such regions is determined by INTSAV when a given material in an interface cell fails. When IGRP>1 more than one damage region must be created to encompass the failed material.
INTRCP	PDMGE	(4,10)	cm	The intercepts of a damage region with the boundaries of a cell are stored by INTSAV when the region is being reduced.

Variable Name	Location	Dimension of Array	Units	Definition
LBG	Z(106)	---	---	The indices of the tracers of a given damage region that just precede (LBG) and just follow (LND) those tracers that are inside cell (ISV,JSV). When a damage region boundary is being enlarged or reduced, LBG and LND identify where, in the XP, YP arrays, tracers should be added or deleted.
LND	Z(107)	---	---	
LDRBGN	B.C.	---	---	Subroutine DAMAGE is called either to update all of the damage regions, in which case LDRBGN=1 and LDREND=NLDR, or to establish the stresses, etc., of a new damage region, in which case LDRBGN=LDREND.
LDREND	B.C.	---	---	
LSLDR	B.C.	---	---	The initialization of the arrays used by BFRACT occurs when LSLDR=0, i.e., when a calculation is generated or restarted. LSLDR is set to zero in INPUT and reset to one in BFRACT.
NBSAVE	B.C.	---	---	These are the indices of the entering and exiting intercepts of a given damage region with cell (ISV,JSV) after the region boundary has been enlarged or reduced to include or exclude cell (ISV,JSV) and after the appropriate intercepts and corner points have been added by INTSAV.
NESAVE	B.C.	---	---	
NCALL	B.C.	---	---	A flag defined by SETUP, MIXDMR, PURDMR and SCALC which establishes what function CALFRC is to perform (see discussions of CALFRC in A.2).

Variable Name	Location	Dimension of Array	Units	Definition
NEXIT	B.C.	---	---	Next is the index of the exiting intercept in the XTS,YTS arrays of a given material interface with cell (ISV,JSV). (Equals the number of points (NTEMP) transferred by CALFRA to VOLFND. Used in INTSAV to define the NEXT array.
NEXT	PDMGE	5	---	The index of the exiting intercept of each region of the NMSAVE material in cell (ISV, JSV) is stored in the NEXT array. (See NEXIT.)
NLDR	Z(147)	---	---	The number of existing damage regions. Incremented in MIXDMR and PURDMR (initially zero).
NLSAVE	B.C.	---	---	The number of the damage region being enlarged to encompass all of cell (ISV, JSV)(PURDMR) or all of the NMSAVE material package in cell (ISV,JSV) (MIXDMR).
NMPDR	(MXDMR)	---	---	The material package number of each damage region is stored in the NMPDR array. From this variable the code number of the material of a damage region is found, e.g., N = NMPDR(I) MN = MAT(N) MN is the code number of the material in the I^{th} damage region.
NMSAVE	B.C.	---	---	The material package number of the material in a mixed cell that has satisfied the NAG-FRAG failure criterion. Defined in SCALC; used in MIXDMR.

Variable Name	Location	Dimension of Array	Units	Definition
NPDCLS	Z(130)	---	---	The maximum number of cells containing one or more damage region boundaries on any one cycle. NPDCLS should correspond to the second dimension of the DVOL and IDDR arrays.
NTS	5	---	---	The number of material tracers, intercepts and corner points (defined by VOLFND and stored in the XTS, YTS arrays by INTSAV) which circumscribe each of at most five regions of the NMSAVE material package in cell (ISV, JSV).
PRS	MXCELL	(NMAT, NMXCLS)	dynes/ cm^2	The pressure of each material in an interface cell is stored in the PRS array.
PRSLDR	PDMGE	(MXDMR)	dynes/ cm^2	The pressure of each damage region (as defined by BFRACT or DFRACT) is stored in the PRSLDR array.
QLIN	Z(93)	---	---	The coefficients of the linear and quadratic artificial viscosity terms, respectively, added to the cell boundary stresses in SPHASE (see Section 4.2).
QQUAD	Z(94)	---	---	
RLVSAV	PDMGE	(MXDMR)	---	The relative volume of each damage region before the BFRACT or DFRACT are called.
ROT	PDMGE	(MXDMR)	radians	The cumulative rotation of each damage region is stored in the ROT array.
RVOL	PDMGE	(MXDMR)	---	The relative volume of each damage region (updated in DAMAGE) based on the region's gross density.

Variable Name	Location	Dimension of Array	Units	Definition
RVVLDR	PDMGE	(MXDMR)	---	The relative void or crack volume in each damage region (updated in BFRACT and DFRACT).
S	B.C.	Maximum of (IMAX, JMAX)+1	cm	Equivalenced to X and Y. Used in double pass transport phase.
SAMMXY SAMPXY	MXCELL by equivalence	(NMAT, NMXCLS, 2)	g	The mass of each material to be transported across the left and right boundaries, respectively, of a mixed cell on the radial pass of the transport phase, and across the bottom and top boundaries, respectively, on the axial pass. Equivalenced to SAMMY, SGAMC and to SAMPY, SAMMP, respectively.
SAMMUV SAMUVT	MXCELL by equivalence	(NMAT, NMXCLS, 2)	g-cm/ sec	The momentum of each material to be transported across the boundaries of a mixed cell. Equivalenced to SAMMU, SAMMV and to SAMUT, SAMVT, respectively.
STRR STRZ STZZ	MXCELL	(NMAT, NMXCLS)	dynes/ cm^2	The stress deviators (S_{rr}, S_{rz}, S_{zz}) associated with each material in a mixed cell.
TSR(N,1)	PDMGE	(6,30) Storage available for at most six materials in a calculation.	cm^2/ dynes-sec	Void (or crack) growth constant = 4/3η; η is material viscosity.

Variable Name	Location	Dimension of Array	Units	Definition
TSR(N,2)	PDMGE	All 30 locations for each material are not currently used.	dyne/ cm^2	Void (or crack) growth threshold.
TSR(N,3)	PDMGE		cm	Void (or crack) nucleation radius parameter.
TSR(N,4) through TSR(N,6)	PDMGE		no_3/ cm^3-sec dynes/ cm^2 dynes/ cm^2	N_o $P_{no}(\sigma_{no})$ $P_1(\sigma_1)$ $N=N_o e^{(P-P_{no})/P_1}$ (DFRACT) $N=N_o e^{(\sigma_{\phi\psi}-\sigma_{no})/P_1}$ (BFRACT) where $\sigma_{\phi\psi}$ is the stress normal to the plane of the cracks. Used in void nucleation rate equation.
TSR(N,9) through TSR(N,13)	PDMGE			Fragmentation parameters provided by SRI.
TVSAVE	B.C.	Maximum of (IMAX,JMAX) +1	cm^3	The transport volume computed between pure cells is based on the velocity at three positions. The velocity at the top (ID=1) or left (ID=2) is saved in TVSAVE for use when the next row (ID=1) or column (ID=2) of the grid is processed.
UNFRAG	PDMGE	(MXDMR)	---	The fraction of unfragmented material in each damage region of a brittle material.
UV	B.C.	(KMAX,2)	cm/sec	Equivalenced to U and V. Used in the double pass transport phase.

Variable Name	Location	Dimension of Array	Units	Definition
VLFAIL	Z(98)	---	---	The volume of unfailed material must be greater than VLFAIL times the volume of that material in the cell before a new damaged region is created or an existing region is enlarged. (Default value = 0.03.)
VOLM	MXCELL	(NVOID, NMXCLS)	cm^3	The volume of each material in an interface cell, as computed from the positions of the tracer particles in CALFRC and VOLFND, is stored in the VOLM array.
VOLMIN	Z(117)	---	---	When computing the cell-centered pressure of a multimaterial cell, the pressure of any material, whose volume is less than VOLMIN times the cell volume, is omitted from the average. (Default value = 0.01.)
XTS YTS	PDMGE	(5,50)	cm	These arrays store the x and y coordinates of the material tracers interior to cell (ISV, JSV) plus the intercepts and cell corner points; used by MIXDMR when creating or enlarging a damage region in an interface cell.

A.5 MODIFICATIONS TO THE HELP INPUT

A minimum number of changes were made to the HELP input. Some Z-block variables were added, some were deleted and some were relocated. A set of cards defining the NAG-FRAG nucleation and growth parameters for each material being modeled by either BFRACT or DFRACT was added to the input, and the input cards defining the shear strength and tensile strength of each material package were altered to define another array specifying the failure model to be employed.

The Z-block variables that were added are listed below. They are defined in the preceding dictionary and in the input form of Appendix B.

DENSWT	CVISR
MXDMR	CVIST
QLIN	FMODEL
QQUAD	NPDCLS
VLFAIL	NLRMX
VOLMIN	

The deleted Z-block variables were related either to the removal of the plugging option and the subcycling of INFACE, or to the modified artificial viscosity:

IPLGRT, PLWMIN, IPLGBT, IPLGTP, PLGOPT	plugging failure removed
CYCMX	INFACE not subcycled
LVISC	use of artificial viscosity now specified by QLIN and QQUAD.

The variables that were relocated in the Z-block so as to be next to closely related parameters were:

CVIS	(moved from Z(27) to Z(125) to be near CVISR (Z(126)) and CVIST (Z(127))
CRATIO	(moved from Z(148) to Z(61) to be near DENSWT (Z(60))

The cards that define the shear yield and tensile strength of each material package now define an additional array, FARRAY, which specifies which failure model is to be applied to each package. (See the input form in Appendix B.)

The TSR variables that store the NAG-FRAG nucleation and growth parameters are defined by the fourth set of input cards following the Z-block data. They are defined in the dictionary as well as in Appendix B.

This version of HELP can be run without utilizing either BFRACT or DFRACT. When those models are employed, however, the grid cannot, at this time, be automatically rezoned. Thus when FMODEL = 1., the rezone parameters are turned off in subroutine INPUT.

The subroutine which approximated the slippage between materials separated by a slip line (UVCALC) was removed because it depended upon momentum terms resulting only from the pressure field as computed by HPHASE. Because the effects of the pressure and stress deviators have been combined in SPHASE, the simple algorithm employed by UVCALC must be replaced by one which considers the components of the total stress normal and tangential to the slip line in the cell. Until this modification is made and a subroutine added which replaces UVCALC, slip lines cannot be used. Thus subroutine INPUT overrides all parameters which attempt to generate and use slip lines.

A.6 STORAGE REQUIREMENTS OF HELP WITH NAG-FRAG FAILURE MODELS

When segmented, as shown in Figure A.5, and executed on the UNIVAC 1108, the version of the HELP code with the NAG-FRAG failure models and the associated systems routines require approximately 17,800 words of core storage for the instruction bank. This represents an increase of about 6800 words over the 1975 documented version of HELP.

In the figure, the subroutines in the first column, which is labeled LEVEL 1, are loaded into core and remain in core for the duration of the calculation. The blocks of subroutines, or segments, under LEVEL 2 and LEVEL 3 are then rolled in and out of core as needed by the various stages of the computational cycle. The INPUT-GENERATOR segment is executed only once per run, either in generating or restarting a calculation. In most of the cycles only three LEVEL 2 segments (the SCALC segment, the SPHASE segment, and the TPHASE segment) and four LEVEL 3 segments are rolled in and out of core. (At the present time the REZONE routine is deactivated and so the REZONE segment is never loaded.)

The amount of storage required for the data bank, in this new version of the code, is, of course, highly dependent on the dimensions of the grid, the number of materials and

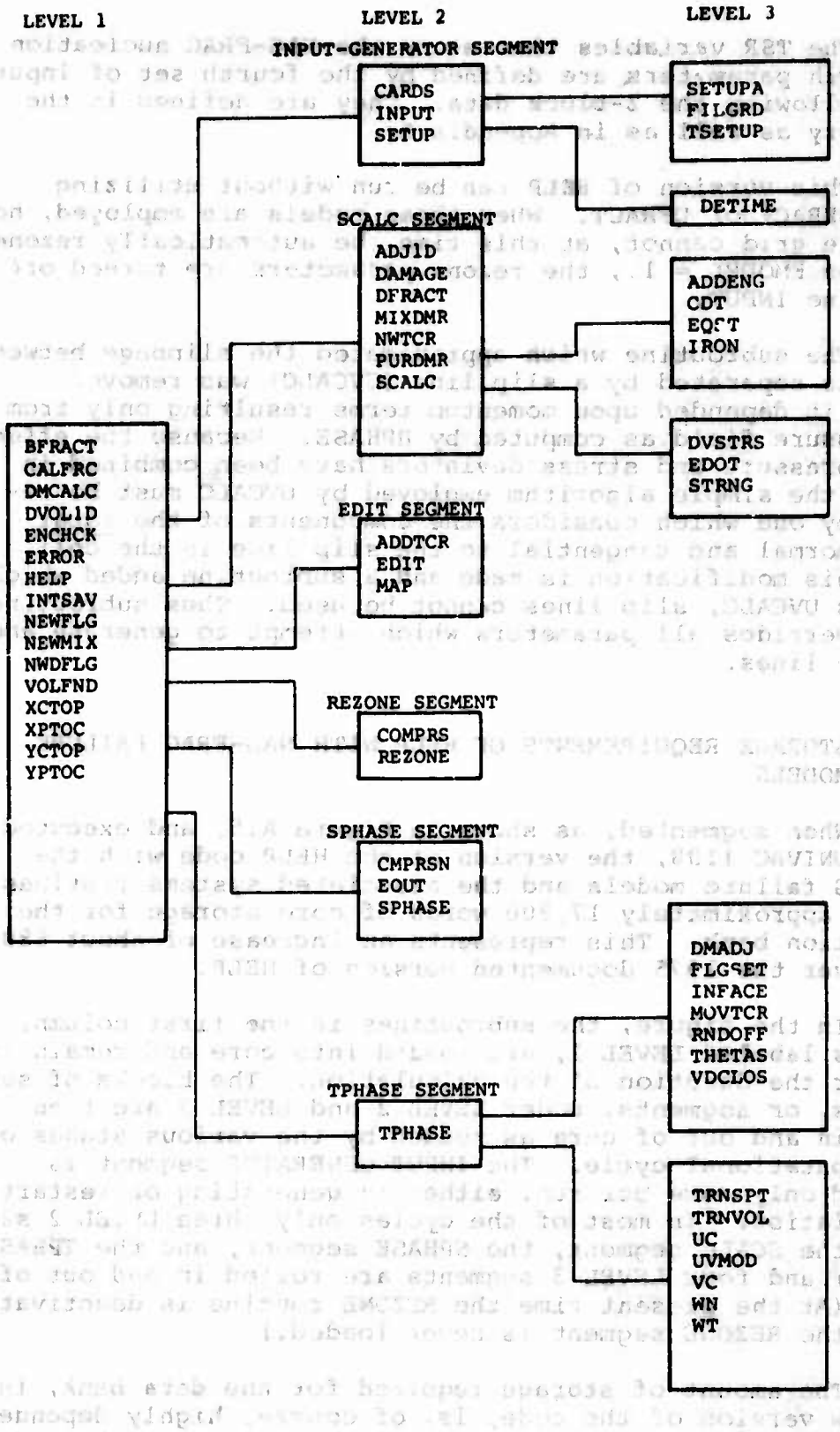

Figure A.5. A schematic representation of an efficient method of segmenting HELP which minimizes core storage requirements.

the extent of the damage incurred in the course of the calculation. The number of cells that at one time or another will satisfy the NAG-FRAG failure condition will determine the number of damage regions that will be created (MXDMR) and the maximum number of Eulerian cells that will contain damage region boundaries on any one cycle (NPDCLS).

Twelve arrays which store information on the damage regions have been added to the data storage requirement of HELP. If the user estimates that at most 100 damage regions will be created then these arrays would add 22 x 100 or 2,200 words to the data bank. In addition to these twelve arrays, two more arrays, DVOL and IDDR, which store information on cells containing damage region boundaries, require core storage. Since one can expect that no more than nine different damage region boundaries will cross a given cell on the same cycle, the first index of DVOL and IDDR can safely be nine. Therefore, if one expects at most 100 cells to contain damage region boundaries, then another 2 x 9 x 100 or 1,800 words would be added to the data bank.

In addition to these arrays whose dimensions depend upon the volume of damaged material, there are five arrays (INTRCP, NEXT, TSR, XTS, YTS) whose dimensions are fixed; these arrays require an additional 520 words of core storage.

The DFLAG array was added to blank common in order to identify those cells containing damaged material, those containing both damaged and undamaged material, and those containing only undamaged material. The DFLAG array is dimensioned by the total number of cells in the grid. In addition, four arrays (PRS, VOLM, FRACTP, FRACBT) were added to the named common block, MXCELL. Their dimensions depend upon the number of materials and the maximum number of interface cells that exist on a single cycle of the calculation. The PRS and VOLM arrays store the pressure and volume of each material in each interface cell. The fractional cell area arrays, FRACBT and FRACTP were previously equivalenced to the P array, but since they must now be saved between cycles, they too have been added to MXCELL.

To summarize the effects on the storage requirements of the revised HELP code, brought about by the additional arrays described above, assume the following problem parameters:

1500	cells
2	material packages
300	interface cells
100	damage regions
100	cells containing damage region boundaries.

A calculation with these parameters, using the version of HELP with the NAG-FRAG models, would require (2200 + 1800 + 520 + 1500 + 11 x 300) = 9320 more words in the data bank than would the same calculation using the 1975 documented HELP code.

APPENDIX B

INPUT FORM FOR HELP WITH NAG-FRAG FAILURE MODELS

The input form included here reflects the modifications discussed in the previous section. The default values of most Z-block variables appear in parentheses after the definition; if no value is specified, the default value is zero as blank common is initialized before the input cards are read.

Heading Card

(Numbers in Parentheses are Non-Zero Default Values)

1	2	3	4	5	6	7	8	9	10	11	12	13	14	15	16		
1			1	5	1	1										PK(1)	Problem number. (Range: 00.0001 to 99.9999)
					1	1										PROB	Problem number, same as PK(1).
2					5	1										NFRELP	Every "NFRELP" EDIT prints is a long print.
2					6	1										NDUMP7	Every "NDUMP7" EDIT prints, a restart dump is written.
2					7	1										ICSTOP	Cycle on which calculation stops if stopping on cycles.
2				1	2	1										NUMREZ	Number of times grid is to be automatically rezoned. (Cannot be activated if FMODEL ≠0.)
2				1	4	1										KUNITR	Number-name of file INPUT reads from. (7)
2				1	5	1										IPR	Maximum number of iterations to equilibrate pressures in multimaterial cells. (35)
				1	6	1										PRCNT	Convergence limit for pressure iteration (10^{-3}).
2				1	7	1										KUNITW	Number-name of file SETUP and EDIT write on. (7)
2				2	1	1										IGM	When IGM=1, code uses plane rather than cylindrical coordinates.
				2	4	1										DMIN	Maximum relative error in energy sum.
2				3	3	1										IMAX	Number of columns in grid. (Must be at least 3.)
2				3	5	1										JMAX	Number of rows in grid. (Must be at least 3.)

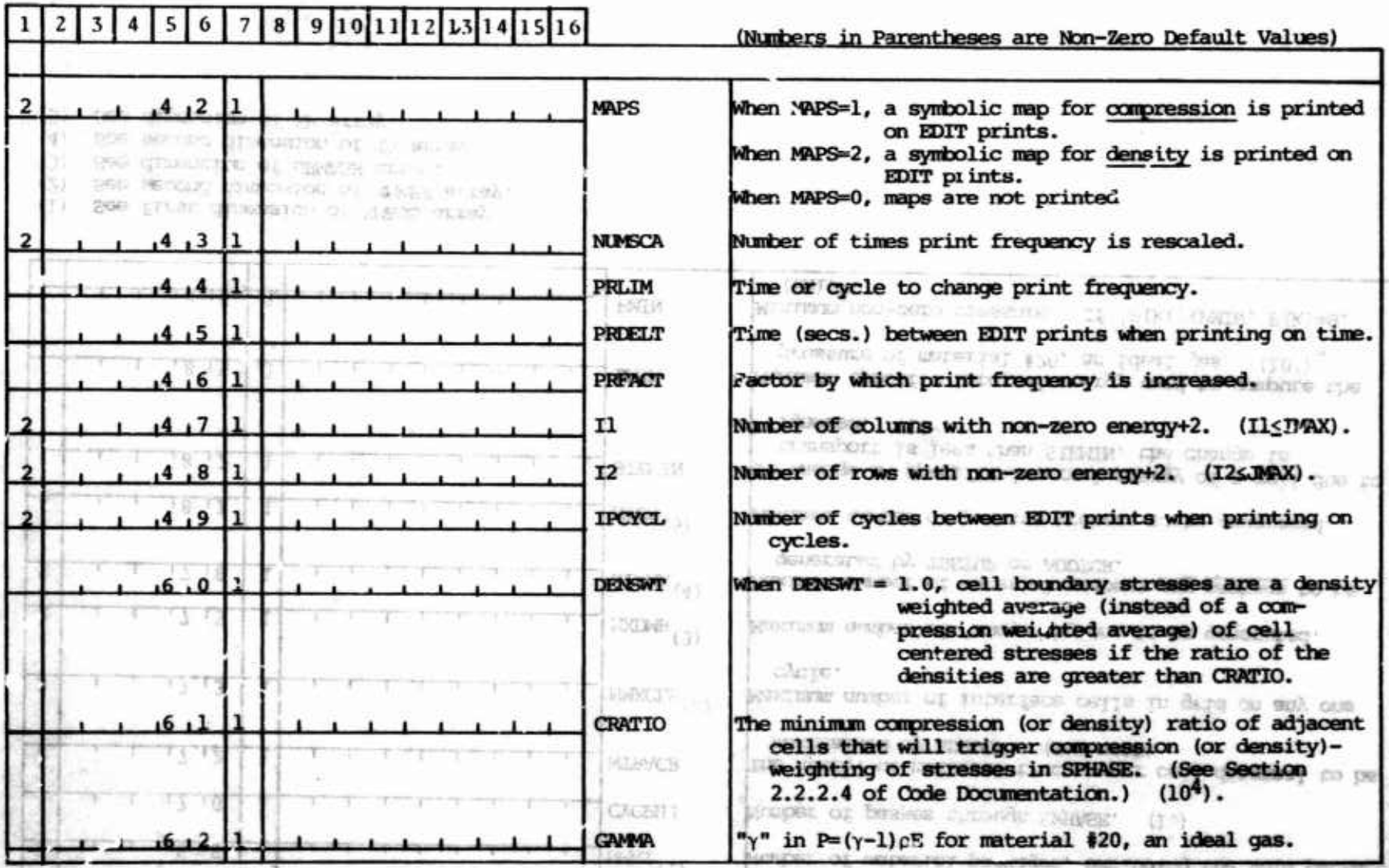

(Numbers in Parentheses are Non-Zero Default Values)

2	MAPS	When MAPS=1, a symbolic map for compression is printed on EDIT prints. When MAPS=2, a symbolic map for density is printed on EDIT prints. When MAPS=0, maps are not printed.
2	NUMSCA	Number of times print frequency is rescaled.
	PRLIM	Time or cycle to change print frequency.
	PRDELT	Time (secs.) between EDIT prints when printing on time.
	PRFACT	Factor by which print frequency is increased.
2	I1	Number of columns with non-zero energy+2. (I1≤IMAX).
2	I2	Number of rows with non-zero energy+2. (I2≤JMAX).
2	IPCYCL	Number of cycles between EDIT prints when printing on cycles.
	DENSWT	When DENSWT = 1.0, cell boundary stresses are a density weighted average (instead of a compression weighted average) of cell centered stresses if the ratio of the densities are greater than CRATIO.
	CRATIO	The minimum compression (or density) ratio of adjacent cells that will trigger compression (or density)-weighting of stresses in SPHASE. (See Section 2.2.2.4 of Code Documentation.) (10^4).
	GAMMA	"γ" in $P=(\gamma-1)\rho E$ for material #20, an ideal gas.

1	2	3	4	5	6	7	8	9	10	11	12	13	14	15	16		
																	(Numbers in Parentheses are Non-Zero Default Values)
2				6	8	1										NMAT(1)	Number of material packages, excluding the void package.
				7	0	1										CYCPH3	Number of passes through SPHASE. (1.)
2				7	2	1										NTRACR	The number of material tracers per cell diagonal to be maintained by ADDTCR. (See NADD)
2				7	3	1										NMXCLS(2)	Maximum number of interface cells in grid on any one cycle.
2				7	5	1										MXDMR(3)	Maximum number of damage regions to be generated.
2				7	8	1										NTPMX(4)	Maximum number of material tracers per package to be generated by TSETUP or ADDTCR.
2				8	1	1										NTCC(5)	Maximum number of passive tracers to be generated.
				8	2	1										SIEMIN	If change in specific internal energy of a cell due to transport is less than SIEMIN, the change is ignored. (10^5)
				8	5	1										EMIN	Minimum specific internal energy used to compute the pressure of material #20, an ideal gas. (10^7)
				8	6	1										PMIN	Minimum non-zero pressure. If $\|P(k)\|<$PMIN, P(k)=0. (5×10^6)

(1) See first dimension of XMASS array.
(2) See second dimension of XMASS array.
(3) See dimension of DRMASS array.
(4) See second dimension of TX array.
(5) See dimension of XP array.

1	2	3	4	5	6	7	8	9	10	11	12	13	14	15	16		
																	(Numbers in Parentheses are Non-Zero Default Values)
2				8	7	1										INTER	When non-zero, INTER generates certain diagnostic prints. (See Section 9.2 of Code Documentation.)
				9	3	1										QLIN	Linear artificial viscosity coefficient.
				9	4	1										QQUAD	Quadratic artificial viscosity coefficient.
				9	5	1										REZ	When REZ=1.0 on a restart cycle, the grid is rezoned. (See Section 8.1 and IEXTX, JEXTY of Code Documentation.) (Not activated when FMODEL ≠0.)
				9	6	1										NODUMP	When NODUMP=1, EDIT does not write any restart dumps.
				9	8	1										VLFAIL	Minimum volume fraction of material to be added to an existing damage region. (.03)
2			1	0	5	1										NLINER	The package number of the liner material that forms the jet. Define only when calculating the collapse of a shaped charge liner.
2			1	0	9	1										NVRTEX	The second index of the void tracer that is at the vertex of the void closing region. Define only if using the automatic void closing routine, VDCLOS.
			1	1	0	1										ROEPS	Round-off epsilon. (10^{-5})
2			1	1	2	1										NSLD(6)	Maximum number of slipline cells in grid during any one cycle.
			1	1	3	1										FINAL	Final value of stability fraction. (.4)
2			1	1	5	1										NOSLIP	NOSLIP should be set to 1 when sliplines are not used. (Automatically set to 1 when FMODEL ≠0.)
			1	1	7	1										VOLMIN	Minimum volume fraction of a material in an interface cell for which a pressure is computed. (.01)

(6) See dimension of MSLD array.

1	2	3	4	5	6	7	8	9	10	11	12	13	14	15	16		(Numbers in Parentheses are Non-Zero Default Values)
2			1	1	8	1										NADD	Every cycle that is a multiple of NADD, ADDTCR checks the spacing of the material tracers in the region specified by MINX, MAXX, MINY, MAXY. (Define NTRACR also.)
2			1	1	9	1										MINX	Leftmost column of region in which tracers will be added.
2			1	2	0	1										MAXX	Rightmost column of region in which tracers will be added.
2			1	2	1	1										MINY	Bottom row of region in which tracers will be added.
2			1	2	2	1										MAXY	Top row of region in which tracers will be added.
2			1	2	3	1										IEXTX	If IEXTX=1, the grid will be rezoned in the X-direction, unless FMODEL=1.
2			1	2	4	1										JEXTY	If JEXTY=1, the grid will be rezoned in the Y-direction, unless FMODEL=1.
			1	2	5	1										CVIS	Boundary condition for bottom grid boundary.
			1	2	6	1										CVISR	Boundary condition for right grid boundary.
			1	2	7	1										CVIST	Boundary condition for top grid boundary.
			1	2	8	1										FMODEL	The NAG-FRAG failure model is employed only if FMODEL=1.
2			1	3	0	1										NPDCLS (7)	Maximum number of cells that are partially contained in one or more damage regions.

transmittive = 0.

reflective = -1.

(7) See second dimension of DVOL array.

1	2	3	4	5	6	7	8	9	10	11	12	13	14	15	16		(Numbers in Parentheses are Non-Zero Default Values)
			1	3	9	1										STAB	Initial value of stability fraction. (10^{-3})
			1	4	4	1										DTMIN	Minimum allowable value of time step. If DT < DTMIN, the calculation stops (10^{-11})
2			1	4	5	1										NLRMX(8)	Maximum number of damage regions in any one cell.
			1	4	9	1										BBAR	Constant in approximation of local speed: $C=C_o+BBAR\cdot\sqrt{P}$. Used to determine Δt. (.5)
1				5	0	1										TSTOP	Time (secs.) calculation will stop if stopping on time. (Must be included even when stopping on cycles in which case TSTOP=0.)

(8) See first dimension of DVOL array.

CARDS DEFINING DX AND DY ARRAYS

Define DX first.
NNT(I) is the number of zones that have dimension TEMP (I).
Set NNT(I) = 999 after all DX are defined and after all DY are defined.

1-10					11-20	21-30	31-40	41-50	51-60	61-70	71-80
1 2 3 4 5 6 7 8 9 0					1 2 3 4 5 6 7 8 9 0	1 2 3 4 5 6 7 8 9 0	1 2 3 4 5 6 7 8 9 0	1 2 3 4 5 6 7 8 9 0	1 2 3 4 5 6 7 8 9 0	1 2 3 4 5 6 7 8 9 0	1 2 3 4 5 6 7 8 9 0
NNT(1)	NNT(2)	NNT(3)	NNT(4)			TEMP(1)	TEMP(2)	TEMP(3)	TEMP(4)	(4I4,4X,4E10.2)	

Before the dummy end card (Z(150)), insert the following sets of data cards. (The formats for these sets of cards are specified in the pages that follow.)

1. Cards defining cell dimensions.
2. Cards defining initial conditions of each material package.
3. Cards defining strength properties of each material package.
4. Cards defining NAG-FRAG parameters. If FMODEL = 0., these cards are omitted.
5. Cards defining material tracer particles of each material package and the void.
6. Cards defining slipline endpoints. If NOSLIP = 1, these cards are omitted.
7. Cards defining HE initiation points. If no HE, insert <u>one</u> blank card.

CARDS DEFINING INITIAL CONDITIONS OF EACH MATERIAL PACKAGE

1-10	11-20	21-30	31-40	41-50	51-60	61-70	71-80
1 2 3 4 5 6 7 8 9 0	1 2 3 4 5 6 7 8 9 0	1 2 3 4 5 6 7 8 9 0	1 2 3 4 5 6 7 8 9 0	1 2 3 4 5 6 7 8 9 0	1 2 3 4 5 6 7 8 9 0	1 2 3 4 5 6 7 8 9 0	1 2 3 4 5 6 7 8 9 0
MFLAG(2)							

(I5) Card defining the MFLAG of cell k = 2.
MFLAG(2) = - 1 if cell k = 2 contains an interface.
MFLAG(2) = N if cell k = 2 is a pure cell in material package N.
MFLAG(2) = 0 if cell k = 2 is a pure void cell.

Cards defining initial ρ, u, v, E_I of each material package. One card for each material package.

Material Code #		Density	Specific Internal Energy	Radial Velocity	Axial Velocity	(I5, 5X, 4E10.2)

CARDS DEFINING STRENGTH PROPERTIES OF EACH MATERIAL PACKAGE

Yield strength of material = $(Y_o + Y_1\mu + Y_2\mu^2)(1 - \frac{E}{E_m})$, E ≡ specific internal energy.

Failure Models:

Volumetric Criterion for Limiting Tensile Pressures: $0.001 \leq AMDM \leq 1.0$, FARRAY = 0.

NAG-FRAG Model for Ductile Materials: AMDM = 0., FARRAY = 1.

NAG-FRAG Model for Brittle Materials: AMDM = 0., FARRAY = 2.

Include one card for each material package.

1-10	11-20	21-30	31-40	41-50	51-60	61-70	71-80
1 2 3 4 5 6 7 8 9 0	1 2 3 4 5 6 7 8 9 0	1 2 3 4 5 6 7 8 9 0	1 2 3 4 5 6 7 8 9 0	1 2 3 4 5 6 7 8 9 0	1 2 3 4 5 6 7 8 9 0	1 2 3 4 5 6 7 8 9 0	1 2 3 4 5 6 7 8 9 0
Y_o	Y_1	Y_2	E_m	Rigidity Modulus G	Failure Threshold AMDM	NAG-FRAG Model Type Array	

CARDS DEFINING NAG-FRAG PARAMETERS OF EACH MATERIAL PACKAGE

If FMODEL [≡Z(128)] is input as 0, these cards must be omitted; otherwise, three cards must be included for each material package, M, for which FARRAY(M) ≠ 0.

N = MAT(M), N ≤ 6.

TSR(N,1) = Void growth constant, $T_1 = 4/3\eta$ (cm^2/dynes-sec)

TSR(N,2) = Void growth threshold stress, σ_{go} or P_{go} (dynes/cm^2)

TSR(N,3) = Void nucleation radius parameter, R_n (cm)

TSR(N,4) = $\dot{N}_o$ (no./cm^3-sec)

TSR(N,5) = P_{no}(DFRACT) or σ_{no}(BFRACT) (dynes/cm^2)

TSR(N,6) = P_1(DFRACT) or σ_1(BFRACT) (dynes/cm^2)

As used in the void nucleation rate equation.

$N = N_o \exp [(P-P_{no})/P_1]$(DFRACT)

$N = N_o \exp [(\sigma_{\phi\psi}-\sigma_{no}/\sigma_1)$(BFRACT)

TSR(N,7) = Not used

TSR(N,8) = Not used

TSR(N,9)
TSR(N,10)
TSR(N,11)
TSR(N,12)
TSR(N,13)

Fragmentation parameters; used by BFRACT only. These are normally provided by SRI.

TSR(N,14)= Not used

	1-10	11-20	21-30	31-40	41-50	51-60	61-70	71-80
	1 2 3 4 5 6 7 8 9 0	1 2 3 4 5 6 7 8 9 0	1 2 3 4 5 6 7 8 9 0	1 2 3 4 5 6 7 8 9 0	1 2 3 4 5 6 7 8 9 0	1 2 3 4 5 6 7 8 9 0	1 2 3 4 5 6 7 8 9 0	1 2 3 4 5 6 7 8 9 0
Card 1	N=MAT(M)							
Card 2	TSR(N,1)	TSR(N,2)	TSR(N,3)	TSR(N,4)	TSR(N,5)	TSR(N,6)	TSR(N,7)	(7E10.2)
Card 3	TSR(N,8)	TSR(N,9)	TSR(N,10)	TSR(N,11)	TSR(N,12)	TSR(N,13)	TSR(N,14)	(7E10.2)

(Form for NAG-FRAG parameters)

1-10	11-20	21-30	31-40	41-50	51-60	61-70	71-80
1 2 3 4 5 6 7 8 9 0	1 2 3 4 5 6 7 8 9 0	1 2 3 4 5 6 7 8 9 0	1 2 3 4 5 6 7 8 9 0	1 2 3 4 5 6 7 8 9 0	1 2 3 4 5 6 7 8 9 0	1 2 3 4 5 6 7 8 9 0	1 2 3 4 5 6 7 8 9 0

CARDS DEFINING TRACER PARTICLES OF EACH MATERIAL PACKAGE AND THE VOID

Repeat cards 1, 2 and (if required) 3 for each line segment or arc of each material and void package boundary (except package boundaries that are also grid boundaries).

Tracer particles for each package must be input in an order that will put the package to the left of any two consecutive particles. Refer to Section 7.2.5.

LTYPE = 1 straight horizontal line
2 straight vertical line
3 straight diagonal line
4 arc of circle
5 arc of ellipse

MPN = Material package number (void = NMAT + 1)

NPTS = Number of points to be placed along line or arc.

LTYPE must be negative on last segment of a package or subpackage.
LTYPE = 100 after all boundaries of all packages are defined.

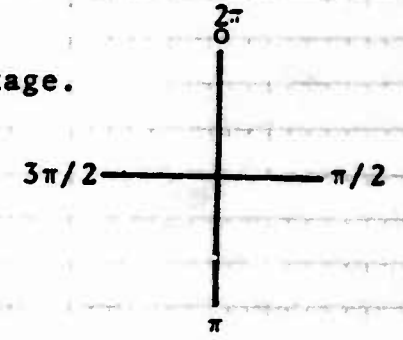

	1-10	11-20	21-30	31-40	41-50	51-60	61-70	71-80
1	LTYPE, MPN	NPTS			(3I5)			
2	starting x-coordinate Starting Angle of Arc	starting y-coordinate Terminal Angle of Arc	final x-coordinate	final y-coordinate	For line segment (cm) (4E10.4) For arc of circle or ellipse (radians) (2E10.4)			
3	x-coordinate of center of circle	y-coordinate of center of circle	Radius of circle		For arc of circle (cm) (3E10.4)			
	A	B	XC	YC	For arc of ellipse (cm) (4E10.4)	$\frac{(X-XC)^2}{A^2} + \frac{(Y-YC)^2}{B^2} = 1$		

(Form for tracer particle definitions)

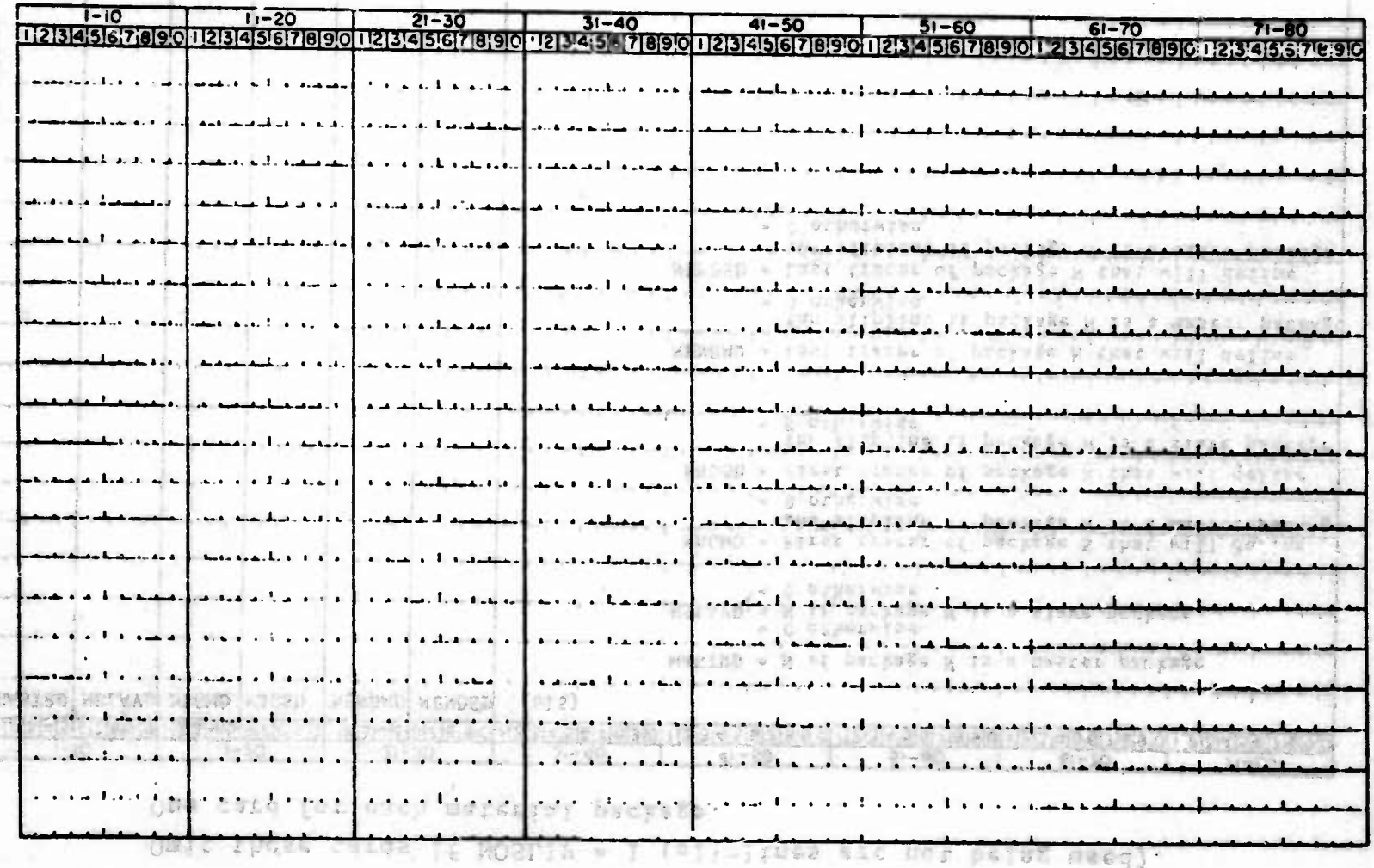

CARDS DEFINING SLIPLINE ENDPOINTS

Omit these cards if NOSLIP = 1 (sliplines are not being used).

One card for each material package.

1-10		11-20		21-30		31-40	41-50	51-60	61-70	71-80
1 2 3 4 5 6 7 8 9 0		1 2 3 4 5 6 7 8 9 0		1 2 3 4 5 6 7 8 9 0		1 2 3 4 5 6 7 8 9 0	1 2 3 4 5 6 7 8 9 0	1 2 3 4 5 6 7 8 9 0	1 2 3 4 5 6 7 8 9 0	1 2 3 4 5 6 7 8 9 0
MASTRD	NSLAVD	NBGMD	NBGSD	NENDMD	NENDSD	(6I5)				

MASTRD = N if package N is a master package
= 0 otherwise

NSLAVD = N if package N is a slave package
= 0 otherwise

NBGMD = First tracer of package N that will define the slipline if package N is a master package
= 0 otherwise

NBGSD = First tracer of package N that will define the slipline if package N is a slave package
= 0 otherwise

NENDMD = Last tracer of package N that will define the slipline if package N is a master package
= 0 otherwise

NENDSD = Last tracer of package N that will define the slipline if package N is a slave package
= 0 otherwise

CARDS DEFINING INITIATION POINTS OF HIGH EXPLOSIVES

The initiation points must be input in ascending order of probable detonation time. Insert one blank card if calculation does not involve detonation of a high explosive.

IDET = 1 for primary initiation point
IDET = 2 for secondary initiation point
IDET = 0 end of initiation point data

1-10	11-20	21-30	31-40	41-50	51-60	61-70	71-80
1 2 3 4 5 6 7 8 9 0	1 2 3 4 5 6 7 8 9 0	1 2 3 4 5 6 7 8 9 0	1 2 3 4 5 6 7 8 9 0	1 2 3 4 5 6 7 8 9 0	1 2 3 4 5 6 7 8 9 0	1 2 3 4 5 6 7 8 9 0	1 2 3 4 5 6 7 8 9 0
IDET	Material Package Number of HE	x-coordinate of Initiation Pt. (cm)	y-coordinate of Initiation Pt. (cm)	Time Delay (if any) (secs)	(2I10, 3E10.2)		

CARDS DEFINING AREA OF INITIATION FOR EACH INITIATION POINT

Specify areas in same order as points are specified above.

1-10	11-20	21-30	31-40	41-50	51-60	61-70	71-80
1 2 3 4 5 6 7 8 9 0	1 2 3 4 5 6 7 8 9 0	1 2 3 4 5 6 7 8 9 0	1 2 3 4 5 6 7 8 9 0	1 2 3 4 5 6 7 8 9 0	1 2 3 4 5 6 7 8 9 0	1 2 3 4 5 6 7 8 9 0	1 2 3 4 5 6 7 8 9 0
Left x-coordinate (cm)	Bottom y-coordinate (cm)	Right x-coordinate (cm)	Top y-coordinate (cm)	(4E10.2)			

1	2 3 4 5 6	7	8 9 10 11 12 13 14 15 16		
1	1 5 0	1	0		Dummy end of generation deck.

DISTRIBUTION LIST

No. of Copies	Organization
12	Commander Defense Documentation Center ATTN: DDC-TCA Cameron Station Alexandria, VA 22314
1	Director Defense Advanced Research Projects Agency ATTN: Tech Info 1400 Wilson Boulevard Arlington, VA 22209
1	Director Defense Nuclear Agency ATTN: MAJ Spangler Arlington, VA 22209
1	Commander US Army Materiel Development and Readiness Command ATTN: DRCDMD-ST, N. Klein 5001 Eisenhower Avenue Alexandria, VA 22333
1	Commander US Army Aviation Research and Development Command ATTN: DRSAV-E 12th and Spruce Streets St. Louis, MO 63166
1	Director US Army Air Mobility Research and Development Laboratory Ames Research Center Moffett Field, CA 94035
1	Commander US Army Electronics Research and Development Command Technical Support Activity ATTN: DELSD-L Fort Monmouth, NJ 07703
1	Commander US Army Communications Rsch and Development Command ATTN: DRDCO-SGS Fort Monmouth, NJ 07703
2	Commander US Army Missile Research and Development Command ATTN: DRDMI-R DRDMI-RBL Redstone Arsenal, AL 35809
1	Commander US Army Missile Materiel Readiness Command ATTN: DRSMI-AOM Redstone Arsenal, AL 35809
1	Commander US Army Tank Automotive Research & Development Cmd ATTN: DRDTA-UL Warren, MI 48090
2	Commander US Army Armament Research and Development Command ATTN: DRDAR-TSS (2 cys) Dover, NJ 07801
4	Commander US Army Armament Research and Development Command ATTN: Mr. V. Guadagno Mr. R. Davitt Dr. J. T. Frasier G. Demitrak Dover, NJ 07801
1	Commander US Army Armament Materiel Readiness Command ATTN: DRSAR-LEP-L, Tech Lib Rock Island, IL 61299

DISTRIBUTION LIST

No. of Copies	Organization
5	Commander US Army Materials and Mechanics Research Center ATTN: DRXMR-T, Mr. J. Bluhm Dr. D. Roylance Dr. A. F. Wilde Dr. J. Mescall DRXMR-ATL Watertown, MA 02172
1	Director US Army TRADOC Systems Analysis Activity ATTN: ATAA-SL, Tech Lib White Sands Missile Range NM 88002
1	Deputy Assistant Secretary of the Army (R&D) Department of the Army Washington, DC 20310
1	HQDA (DAMA-ARP) Washington, DC 20310
1	HQDA (DAMA-MS) Washington, DC 20310
1	Commander US Army Research Office ATTN: Dr. E. Saibel P. O. Box 12211 Research Triangle Park NC 27709
1	Commander US Army BMD Advanced Technology Center ATTN: BMDATC-M, Mr. P. Boyd P. O. Box 1500 Huntsville, AL 35807
1	Office of Naval Research ATTN: Code ONR 439, N.Perrone Department of the Navy 800 North Quincy Street Arlington, VA 22217
3	Commander Naval Air Systems Command ATTN: AIR-604 Washington, DC 20360
3	Commander Naval Ordnance Systems Command ATTN: ORD-9132 Washington, DC 20360
2	Commander Naval Air Development Center, Johnsville Warminster, PA 18974
1	Commander Naval Missile Center Point Mugu, CA 93041
1	Commander & Director David W. Taylor Naval Ship Research & Development Ctr Bethesda, MD 20084
1	Commander Naval Surface Weapons Center ATTN: Code TX, Dr. W.G. Soper Dahlgren, VA 22448
2	Commander Naval Surface Weapons Center Silver Spring, MD 20910
3	Commander Naval Weapons Center ATTN: Code 4057 Code 4011, Dr.E.Lundstrom Code 3813, Mr.M.Backman China Lake, CA 93555

DISTRIBUTION LIST

No. of Copies	Organization
4	Commander Naval Research Laboratory ATTN: Mr. W. J. Ferguson Dr. C. Sanday Dr. H. Pusey Dr. F. Rosenthal Washington, DC 20375
1	Superintendent Naval Postgraduate School ATTN: Dir of Lib Monterey, CA 93940
2	ADTC/DLJW (MAJ D. Matuska, LTC J. Osborn) Eglin AFB, FL 32542
1	AFFDL (FDT) Wright-Patterson AFB, OH 45433
1	AFML (Dr. T. Nicholas) Wright-Patterson AFB, OH 45433
2	ASD (XROT, Gerald Bennett; ENFTV, Martin Lentz) Wright-Patterson AFB, OH 45433
3	Director Lawrence Livermore Laboratory ATTN: Dr. R. H. Toland, L-424 Dr. M. L. Wilkins Dr. R. Werne Livermore, CA 94550
1	Headquarters National Aeronautics and Space Administration Washington, DC 20546
1	Director Jet Propulsion Laboratory ATTN: Lib (TD) 4800 Oak Grove Drive Pasadena, CA 91103
4	Director National Aeronautics and Space Administration Langley Research Center Langley Station Hampton, VA 23365
1	Director National Aeronautics and Space Administration Manned Spacecraft Center ATTN: Lib Houston, TX 77058
1	Aeronautical Research Associates of Princeton, Inc. 50 Washington Road Princeton, NJ 08540
2	Aerospace Corporation ATTN: Mr. L. Rubin Mr. L. G. King 2350 E. El Segundo Blvd El Segundo, CA 90009
1	Boeing Aerospace Company ATTN: Mr. R. G. Blaisdell (M.S. 40-25) Seattle, WA 98124
1	Effects Technology, Inc. 5383 Hollister Avenue P. O. Box 30400 Santa Barbara, CA 93105
1	Falcon R&D ATTN: Mr. R. Miller 1225 S. Huron Street Denver, CO 80223

DISTRIBUTION LIST

No. of Copies	Organization
1	FMC Corporation Ordnance Engineering Div. San Jose, CA 95114
1	General Electric Company Armament Systems Dept. Burlington, VT 05401
1	President General Research Corporation ATTN: Lib McLean, VA 22101
1	Goodier Aerospace Corp. 1210 Massillon Road Akron, OH 44315
3	Honeywell, Inc. Government & Aerospace Products Division ATTN: Mr. J. Blackburn Dr. G. Johnson Mr. R. Simpson 600 Second Street, NE Hopkins, MN 55343
1	H. P. White Laboratory Bel Air, MD 21014
1	Kaman Sciences Corporation ATTN: Dr. P. Snow 1500 Garden of the Gods Road Colorado Springs, CO 80933
1	Lockheed Corporation ATTN: Dr. C. E. Vivian Department 8114 Sunnyvale, CA 94087
1	Materials Research Laboratory, Inc. 1 Science Road Glenwood, IL 60427
1	McDonnell-Douglas Astronautics Company ATTN: Mail Station 21-2 Dr. J. Wall 5301 Bolsa Avenue Huntington Beach, CA 92647
1	New Mexico Institute of Mining and Technology Terra Group Socorro, NM 87801
1	Pacific Technical Corporation ATTN: Dr. F. K. Feldmann 460 Ward Drive Santa Barbara, CA 93105
2	Physics International Company ATTN: Dr. D. Orphal Dr. E. T. Moore 2700 Merced San Leandro, CA 94577
1	Rockwell International Autonetics Missile Sys Div ATTN: Dr. M. Chawla 4300 E. 5th Avenue Columbus, OH 43216
3	Sandia Laboratories ATTN: Dr. W. Herrmann Dr. L. Bertholf Dr. J. W. Nunziato Albuquerque, NM 87115
1	Science Applications, Inc. 101 Continental Boulevard Suite 310 El Segundo, CA 90245
1	Science Applications, Inc. 201 W. Dyer Road (Unit B) ATTN: G. Burghart Santa Ana, CA 92707

DISTRIBUTION LIST

No. of Copies	Organization
5	Systems, Science & Software ATTN: Dr. R. Sedgwick Ms. L. Hageman R. G. Herrmann D. Grine M. Rice P. O. Box 1620 La Jolla, CA 92038
1	US Steel Corporation Research Center 125 Jamison Lane Monroeville, PA 15146
1	Drexel University Dept of Mechanical Engineering ATTN: Dr. P. C. Chou 32d and Chestnut Streets Philadelphia, PA 19104
1	Forrestal Research Center Aeronautical Engineering Lab Princeton University ATTN: Dr. A. Eringen Princeton, NJ 08540
3	Southwest Research Institute Dept of Mechanical Sciences ATTN: Dr. U. Lindholm Dr. W. Baker Dr. P. H. Francis 8500 Culebra Road San Antonio, TX 78228
3	Stanford Research Institute ATTN: Dr. L. Seaman Dr. D. Curran Dr. D. Shockey 333 Ravenswood Avenue Menlo Park, CA 94025
2	University of Arizona Civil Engineering Dept ATTN: Dr. A. DaDeppo Dr. R. Richard Tucson, AZ 85721
4	University of California Los Alamos Scientific Lab ATTN: Dr. R. Karpp Dr. J. Dienes Dr. L. Germain Dr. B. Germain P. O. Box 808 Livermore, CA 94550
1	University of Dayton Univ of Dayton Research Inst. ATTN: Mr. H. F. Swift Dayton, OH 45405
2	University of Delaware Dept of Mechanical Engineering ATTN: Prof. J. Vinson Dean I. Greenfield Newark, DE 19711
1	University of Denver Denver Research Institute ATTN: Mr. R. F. Recht 2390 S. University Boulevard Denver, CO 80210
2	University of Florida Department of Engineering Science and Mechanics ATTN: Dr. C. A. Sciammarella Dr. L. Malvern Gainesville, FL 32601
	Aberdeen Proving Ground
	Cdr, USATECOM ATTN: Mr. W. Pless Mr. S. Keithley DRSTE-SG-H
	Dir, USAMSAA